FUNCTIONAL CHARACTERIZATION OF METALLOENZYMES IN LUMICHROME CATABOLISM AND CHUANGXINMYCIN BIOSYNTHESIS

A Dissertation

by

SAAD NASEEM

Submitted to the Graduate and Professional School of
Texas A&M University
in partial fulfillment of the requirements for the degree of

DOCTOR OF PHILOSOPHY

Chair of Committee,	Tadhg P. Begley
Committee Members,	Frank M. Raushel
	David P. Barondeau
	Paul D. Straight
Head of Department,	Simon W. North

May 2022

Major Subject: Chemistry

ABSTRACT

Cofactors play vital roles in augmenting the limited functionality available on proteins for catalysis. Little is known about cofactor breakdown in contrast to the extensive literature on cofactor biosynthesis and enzymology. Our lab discovered strains capable of degrading riboflavin and lumichrome. We identified the lumichrome catabolic gene cluster in *Pimelobacter simplex* and reconstituted most of the biodegradation reactions.

I report the reconstitution of 8 enzymes, including a cytochrome P450 monooxygenase, a molybdenum enzyme, a rieske dioxygenase, and a catechol dioxygenase, in the lumichrome catabolic pathway. Cytochrome P450 (quinoxaline monooxygenase) hydroxylates the C7 position of lumichrome. Nature does this to increase the solubility of lumichrome for biodegradation. The pyrimidine ring of 7-carboxylumichrome is then hydrolyzed by amidohydrolases. Rieske dioxygenase (quinoxaline dioxygenase) carries out cis-dihydroxylation of dihydroxyquinoxaline-carboxylic acid to open the quinoxaline heterocycle. Amidocatechol dioxygenase catalyzes ring cleavage with oxygen insertion to form as yet unidentified ring-opened product.

CxnD, cytochrome P450 monooxygenase, catalyzes carbon-sulfur bond formation to form demethyl-chuangxinmycin. It was recently biochemically and structurally characterized by Shi *et al.*, but the mechanism of C-S bond formation is poorly understood. We proposed two plausible mechanisms for the formation of aryl carbon and sulfur bond

via i) aryl radical anion intermediate ii) (2-3)-epoxyindole intermediate. We tested the proposal by feeding several substrate analogs to CxnD. Bromo-substituted substrate analogs ruled out the carbon-sulfur bond formation via aryl radical anion intermediate. Intriguingly, indole-3-propanoic acid, as a mechanistic probe, releases five products that support the mechanism involving (2-3)-epoxyindole intermediate for C-S bond formation.

DEDICATION

To my parents and brothers

ACKNOWLEDGEMENTS

I would like to thank my committee chair, Dr. Tadhg P. Begley, and my committee members, Dr. Frank Raushel, Dr. Paul Straight, and Dr. David Barondeau, for their guidance and support throughout this research.

Thanks also to my friends and colleagues and the department faculty and staff for making my time at Texas A&M University a great experience.

CONTRIBUTORS AND FUNDING SOURCES

This work was supervised by a dissertation committee consisting of Professor Tadhg P. Begley (advisor), Professor Frank M. Raushel, Professor David P. Barondeau from the Department of Chemistry, and Professor Paul D. Straight from the Department of Biochemistry and Biophysics.

Dr. Xiaohong Jian identified and isolated the strain capable of growing on lumichrome. Dr. Sanjoy Adak identified the lumichrome catabolic cluster and showed the initial activity of carboxy-lumichrome hydantoinase, Ureidoquinoxaline amidase, aminoquinoxaline amidinase, and carboxyquinoxaline decarboxylase. Sreyashi Sinha has done mechanistic studies on carboxyquinoxaline decarboxylase. All other work conducted for the dissertation was performed by the student independently.

Dr. Nitai Giri proposed chuangxinmycin biosynthetic cluster as a potential system to be studied in our lab.

Graduate study was supported by funding from the following:

1) Graduate Teaching Assistant in the First Year Chemistry Program (9 semesters)
2) Graduate Teaching Assistant in the Organic Chemistry Program (2 semesters)
3) Funding from Robert A. Welch Foundation grant A-0034

NOMENCLATURE

EIC	Extracted Ion Chromatogram
FMN	Flavin mononucleotide
FAD	Flavin adenine dinucleotide
LC-MS	Liquid Chromatography- Mass Spectrometry
HPLC	High Performance Liquid Chromatography
kDa	kilodalton
NAD^+	Nicotinamide adenine dinucleotide
NADH	Nicotinamide adenine dinucleotide, reduced
NCBI	National Center for Biotechnology Information
NMR	Nuclear Magnetic Resonance
OD_{600}	Optical density at 600 nm
DCM	Dichloromethane

TABLE OF CONTENTS

Page

LIST OF FIGURES

Page

LIST OF TABLES

Page

CHAPTER I

INTRODUCTION

Cofactors play an essential role in providing additional functionality to enzymes. Sometimes enzymes require an organic molecule, metal, or metal-organic complex to carry out its chemistry. Cofactor biosynthesis and enzymology have extensively been studied, yet cofactor catabolism remains an unwritten chapter in cofactor biochemistry. Only NAD, folate, pyridoxal, and heme catabolism have been studied in detail. Meanwhile, there are reports of thiamin, riboflavin (**2**), and biotin degrading strains, but the strains were not preserved.

Riboflavin

Riboflavin **2** (Vitamin B_2) plays an essential role in the metabolism of cells. Other biologically active forms of riboflavin are flavin mononucleotide (FMN, **3**) and flavin adenine dinucleotide (FAD, **4**). Riboflavin deficiency in humans leads to various skin disorders, edema, cracked lips, and hair loss.

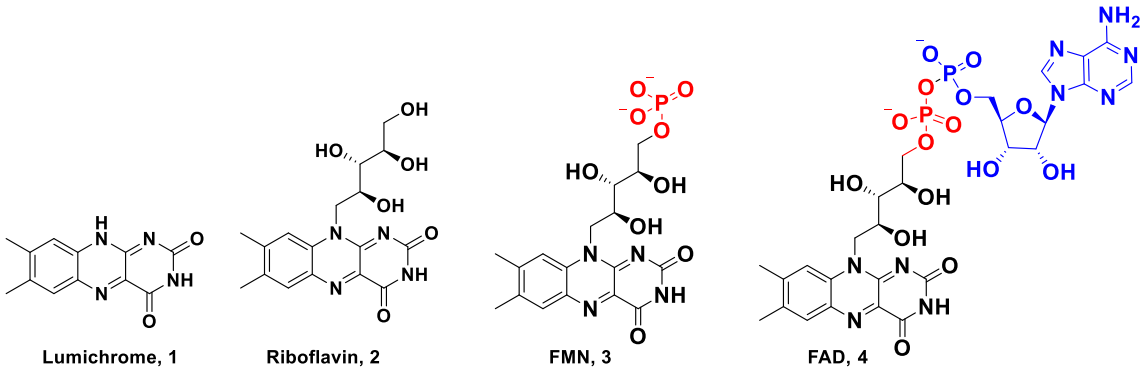

Figure I.1: Structure of lumichrome, riboflavin, FMN and FAD.

Riboflavin catabolism

Multiple riboflavin (**2**) catabolic strains have been reported, but the genes responsible for the breakdown of riboflavin have not been identified, and the strains have been lost. In 1944, the Foster group showed *Pseudomonas riboflavina* degrades riboflavin to lumichrome (**1**) and ribitol (**9**)[1-2]. The Stadtman group reported another riboflavin catabolic strain in 1965; they detected intermediates of riboflavin degradation[3-4]. Unfortunately, the strain was lost, and detailed enzymology could not be done (Figure I.2).

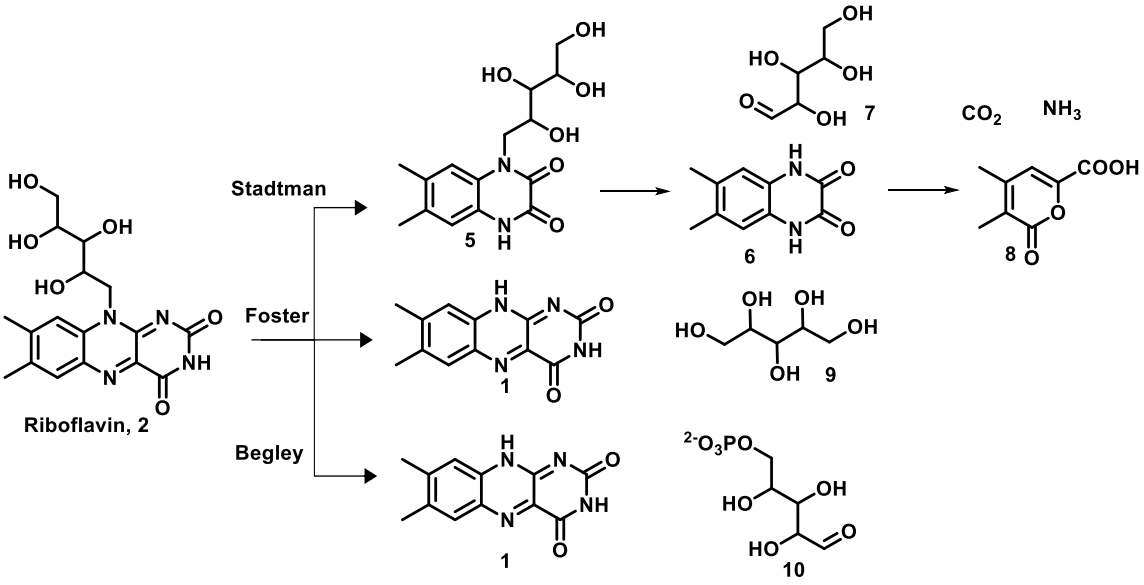

Figure I.2: Reported degradation pathways of riboflavin.

Our group has embarked on the challenge of discovering and studying cofactor catabolism pathways in nature. Usually, the cofactor catabolism pathways evolve at cofactor-rich environments; using this strategy, we discovered a riboflavin catabolizing strain, *Microbacterium maritypicum*, isolated from a riboflavin production facility. We were able to identify the riboflavin catabolizing operon and carried out detailed

mechanistic studies on riboflavin lyase, RcaE enzyme[5]. The strain grows on riboflavin to precipitate lumichrome and uses the ribose side chain as a carbon source for growth.

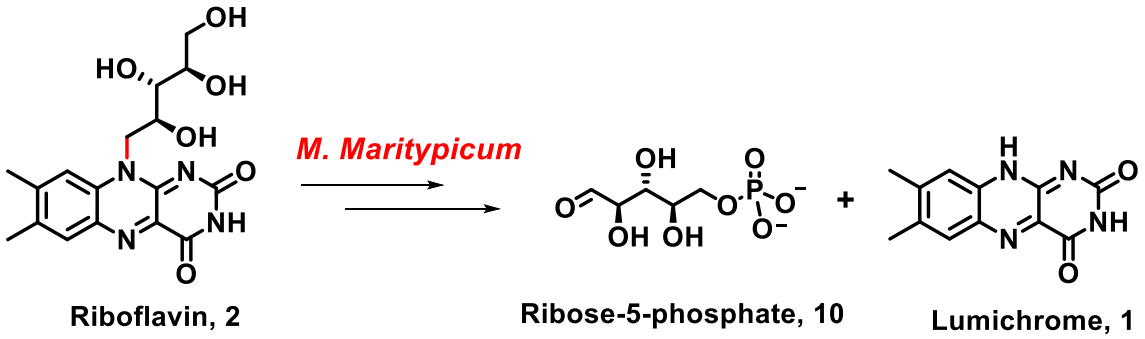

Figure I.3: Riboflavin catabolism in *Microbacterium maritypicum*.

Lumichrome catabolism

As chemists, we were interested in how nature would break down the stable isoalloxazine heterocycle of lumichrome and use it as a carbon and nitrogen source for growth. Dr. Xiaohong Jian isolated a strain, *Pimelobacter simplex*, that could grow on lumichrome as a carbon and nitrogen source. Based on isolated metabolites, Dr. Sanjoy Adak searched for hydrolases that can hydrolyze cyclic amides. Based on homologous cyclic amidases and their genome context in *P. simplex*, we were able to identify the lumichrome catabolic operon in *Pimelobacter simplex* (Figure I.4). Dr. Sanjoy Adak functionally characterized the first four enzymes in the catabolic operon (Figure I.5).

Table 1: Gene names and annotations belonging to lumichrome catabolic cluster in *P. simplex*

Gene annotation	**Gene name in Lumichrome catabolic pathway in *P. simplex***
Hydantoinase	Carboxy-lumichrome hydrolase
Nicotinamidase	Ureidoquinoxaline amidase
Amidohydrolase	Aminoquinoxaline amidinase
Decarboxylase	Carboxyquinoxaline decarboxylase
Xanthine oxidase	Quinoxaline oxidase
Rieske dioxygenase	Quinoxaline dioxygenase
Catechol dioxygenase	Amidocatechol dioxygenase
Cytochrome P450	Lumichrome monooxygenase
NDMA-alcohol dehydrogenase	Hydroxymethyl-lumichrome oxidase

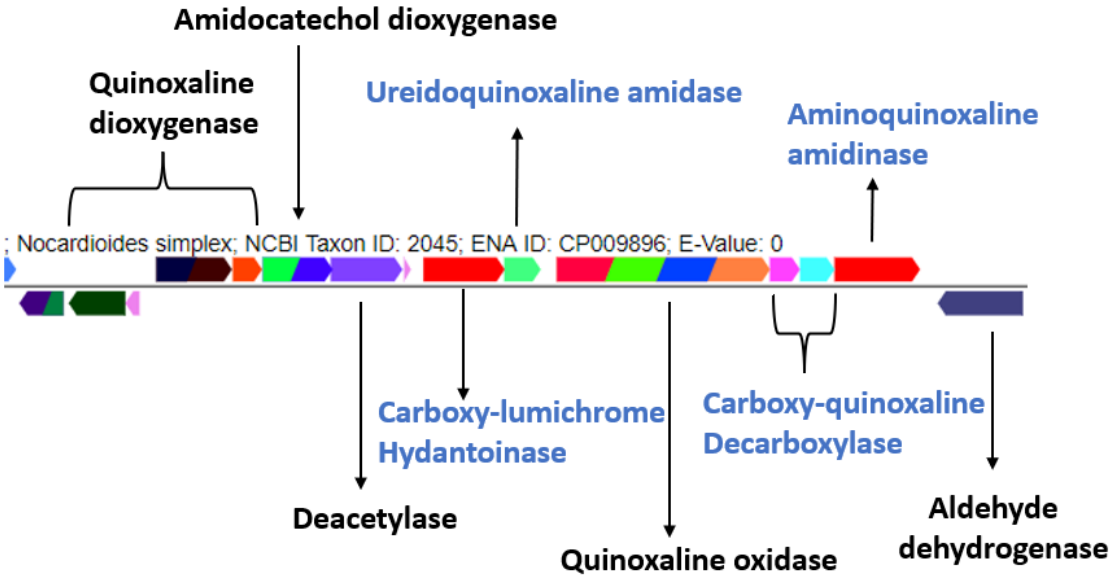

Figure I.4: The lumichrome catabolic operon in *Pimelobacter simplex*. Dr. Sanjoy Adak functionally characterized the genes in blue. Sreyashi Sinha has done mechanistic studies on carboxyquinoxaline decarboxylase.

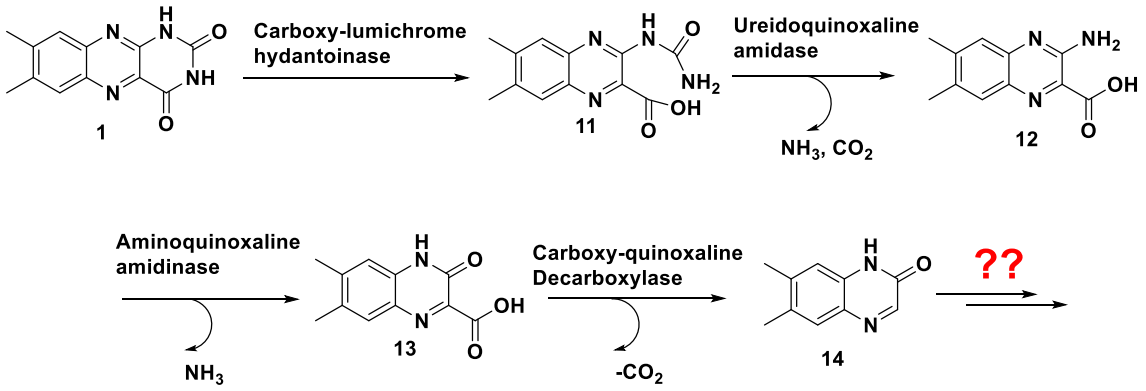

Figure I.5: The functional characterization of carboxy-lumichrome hydantoinase, Ureidoquinoxaline amidase, aminoquinoxaline amidinase, and carboxy-quinoxaline decarboxylase.

Despite many attempts, we were unable to show further degradation of compound **14** for many months. It turned out to be challenging to express the quinoxaline oxidase enzyme. No activity was observed with quinoxaline monooxygenase (rieske dioxygenase), aldehyde dehydrogenase, and deacetylase. In comparison, catechol dioxygenase (now will be referred to as amidocatechol dioxygenase) was consuming catechol type of compounds and giving intractable products.

I discovered that the Open Reading Frames (ORF) of xanthine oxidase (now will be referred to as quinoxaline oxidase) and rieske dioxygenase (now will be referred as quinoxaline dioxygenase) were incorrect in the Uniprot and NCBI database. It was this breakthrough that helped me advance this project. In the following chapters, I will provide a mechanistic hypothesis for the enzymes and demonstrate their role in the catabolism of lumichrome in *Pimelobacter simplex.*

CHAPTER II

QUINOXALINE DEGRADATION BY QUINOXALINE DIOXYGENASE

Introduction

Rieske non-heme iron-dependent oxygenases are well known for their role in the biodegradation of aromatic compounds[6]. Lately, many rieske oxygenases have been biochemically characterized to carry out a variety of reactions, including dihydroxylation, monooxygenation, desaturation, cyclization, and dealkylation reactions[7]. Rieske dioxygenases are the only enzymes known for the cis-dihydroxylations of aromatic compounds; this strategy activates the aromatic ring by making them electron-rich, followed by subsequent degradation.

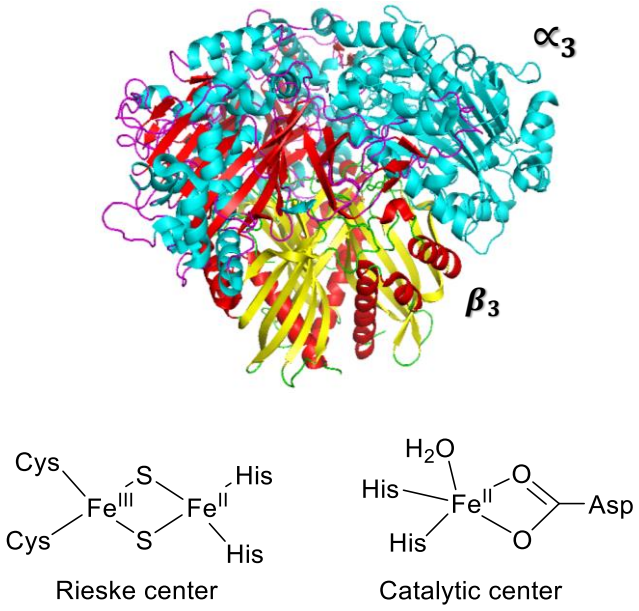

Figure II.1: The structure represents the $\alpha_3\beta_3$ complex of naphthalene-2,3-dioxygenase. The $\propto$ large subunit is in cyan, and the β complex is in yellow/orange. PDB 2B1X

Rieske oxygenases typically have multiple components consisting of a reducing system and a catalytic center. The active site has a non-heme iron and a [2Fe-2S] rieske cluster. Typically, NAD(P)H reduces the ferredoxin reductase, followed by single electron transfer to ferredoxin, and then the ferredoxin does single electron transfer two times to the $\propto_3\beta_3$ complex of rieske large $\propto$ and small subunit β (Figure II.2).

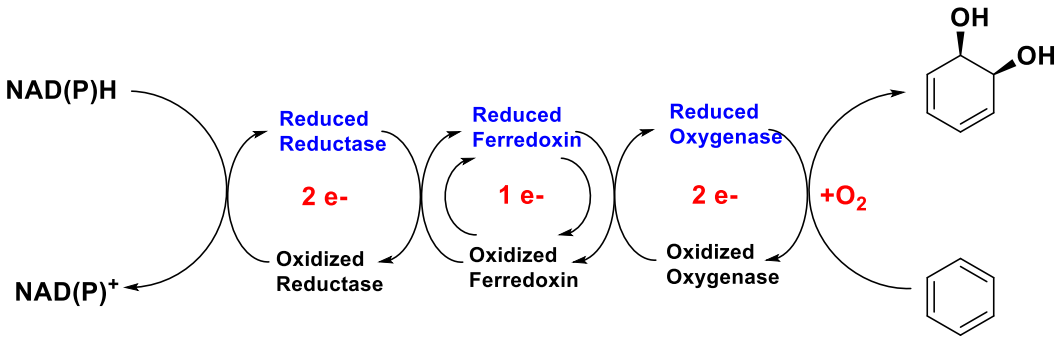

Figure II.2: The electron transfer sequence in rieske dioxygenase enzymes.

The dibenzofuran degradation pathway in Pseudomonas species strain (STDF1) is known to undergo angular dihydroxylation by rieske dioxygenase (Figure II.3)[8]. Besides the heteroatom of dibenzofuran (**15**), the dihydroxylation (**16**), followed by cleavage of the carbon-oxygen bridge, opens the heterocycle to form a catechol compound (**17**). The catechol compound is proposed to be the substrate of catechol dioxygenase in the pathway.

Similarly, I proposed the role of quinoxaline dioxygenase to dihydroxylate besides the heterocyclic nitrogen of compound **22**. Subsequent carbon-oxygen double bond formation and cleavage of the C-N bond will open the heterocycle, **23**. The catechol-type compound **24** will be further degraded by amidocatechol dioxygenase (Figure II.3).

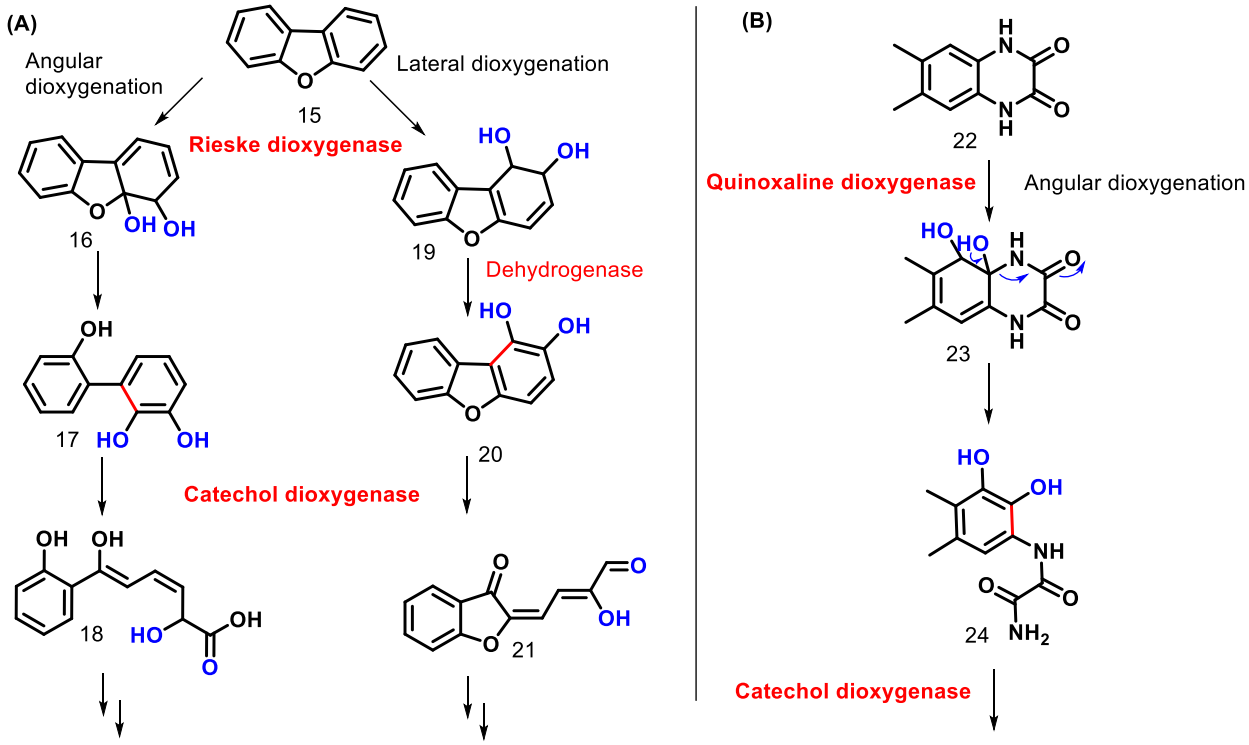

Figure II.3: The proposed degradation pathway of dibenzofuran **15** in Pseudomonas sp. Strain reported by Jaiswal et al.[9] (B) The proposed role of quinoxaline dioxygenase and amidocatechol dioxygenase in the degradation of quinoxaline-diamide (**22**) in *Pimelobacter simplex*.

Results and Discussion

Expression and purification of quinoxaline dioxygenase subunits and reducing system

The genes for the quinoxaline dioxygenase large ∝ subunit, small β subunit, ferredoxin, and ferredoxin reductase were cloned into separate vectors with N-terminal his-tag. The proteins were heterologously expressed in *E. coli* BL21(DE3) and purified by nickel-affinity chromatography (Figure II.4: SDS-PAGE of quinoxaline dioxygenase system.). The quinoxaline dioxygenase large ∝ subunit and ferredoxin are brown-red,

typical of [2Fe-2S] clusters. Ferredoxin reductase is yellow, typical for bound FMN or FAD. The quinoxaline dioxygenase small β subunit is colorless.

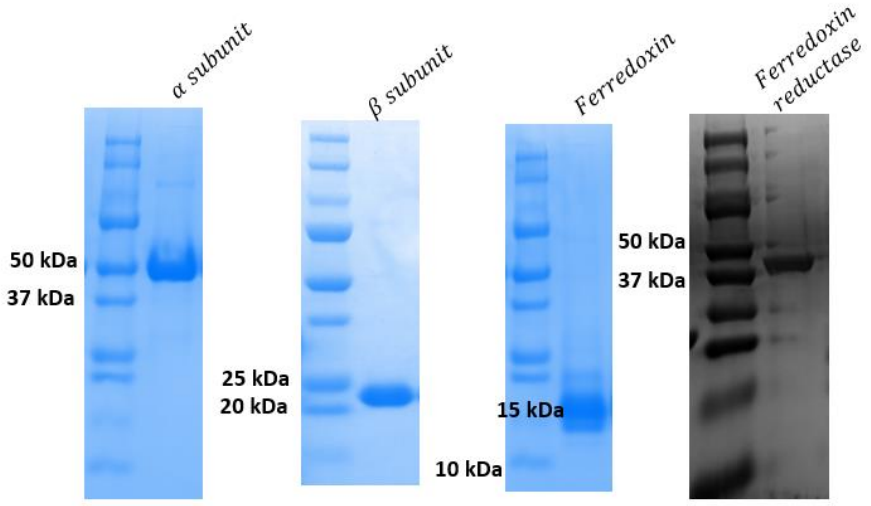

Figure II.4: SDS-PAGE of quinoxaline dioxygenase system.

Quaternary structure of quinoxaline dioxygenase

It is known that the quinoxaline dioxygenase large ∝ and small β subunits form a $\alpha_3\beta_3$ quaternary structure. The function of β subunit remains a mystery, yet activity is not observed in the absence of β subunit. The correct folding and interaction of the two subunits were tested with native-PAGE gel. In native-PAGE, the interactions between the enzymes are intact, and the complex formation can be observed.

The quinoxaline dioxygenase large ∝ and small β subunits were mixed at equimolar concentration and incubated on ice for 30 minutes. Then the samples were loaded onto the gel, and a protocol provided by the NuPAGE was followed. After staining, a band corresponding to 216 kDa ($\alpha_3\beta_3$) was observed; this provides evidence that the enzymes are folding properly and have a correct quaternary structure (Figure II.5).

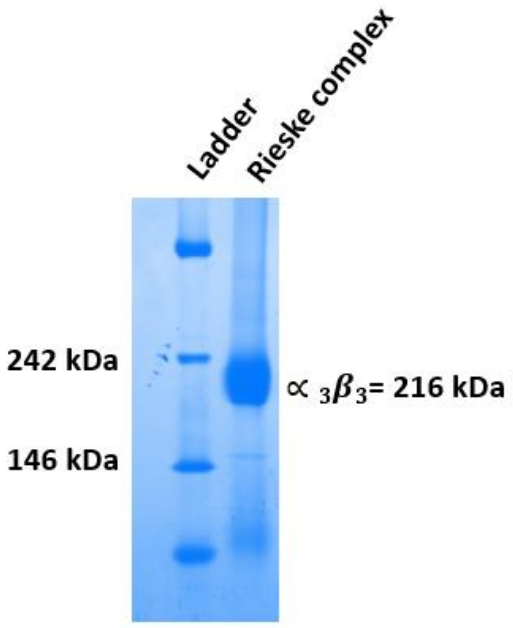

Figure II.5: Native-PAGE of quinoxaline dioxygenase large and small subunit.

Compounds tested for activity with quinoxaline dioxygenase

Based on the proposal in Figure II.3, the quinoxaline dioxygenase large $\propto$, small β subunit, ferredoxin, and ferredoxin reductase were incubated with the proposed substrate compound **22**, NADPH, glucose-6-phosphate, glucose dehydrogenase, and iron(II) ammonium sulfate. The reactions were filter quenched after 6 hours and analyzed by HPLC. Testing of compound **22** showed no substrate consumption and no product formation on the HPLC chromatogram. A library of compounds with quinoxaline core was prepared and tested with the quinoxaline dioxygenase enzymes (Figure II.6). Only compound **30**, carboxy-quinoxaline-diamide, was consumed by quinoxaline dioxygenase in the full reaction (Figure II.6).

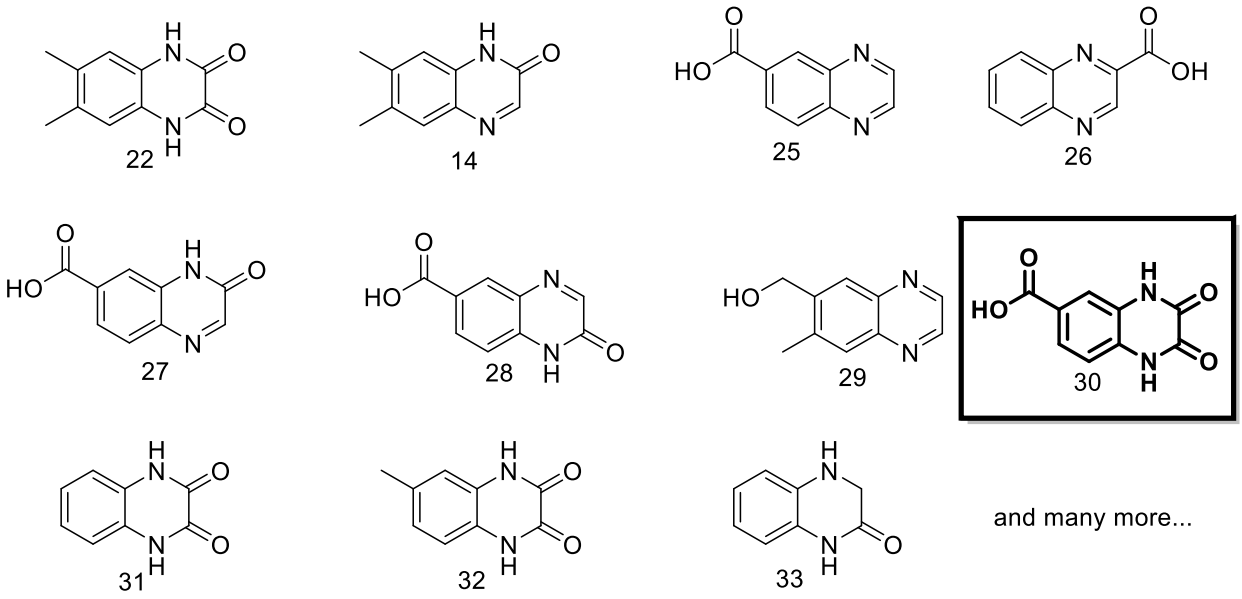

Figure II.6:The list of compounds that were tested with quinoxaline dioxygenase. Amongst them, consumption of compound **30** was observed.

The activity of quinoxaline dioxygenase with substrate analog, 30

Compound **30**, a substrate analog (missing a methyl), showed activity with quinoxaline dioxygenase. Consumption of substrate analog is observed at 7.2 minutes, and a new peak at 3.5 minutes was detected only in the full reaction on HPLC (Figure II.7). The product peak has a mass of [M-H] =240.0149. The mass corresponds to structure **34** or **35** based on MS/MS data; the proposed structure has three additional oxygens and one nitrogen loss (Figure II.8).

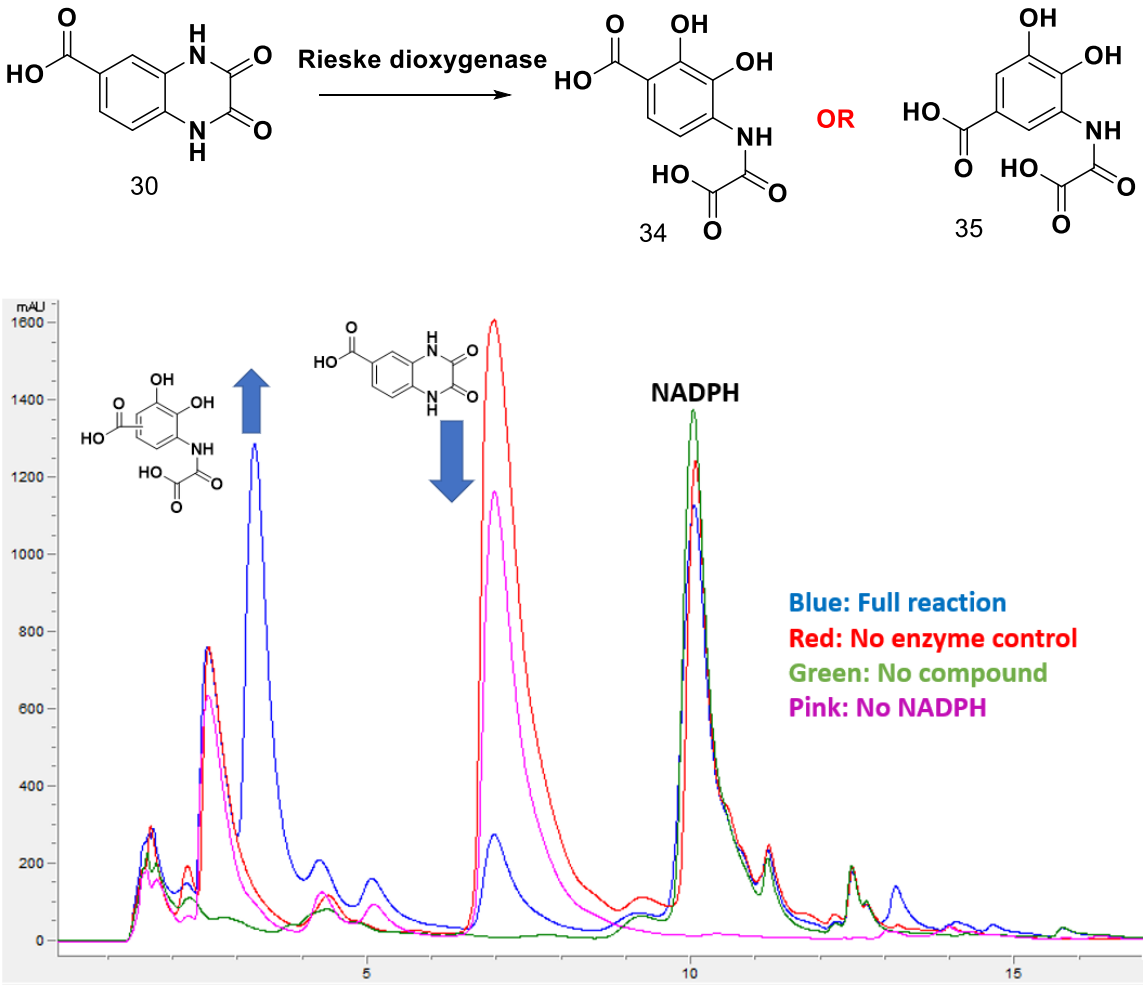

Figure II.7: Analysis of quinoxaline dioxygenase activity. The HPLC chromatogram at 254 nm for the assay of compound **30** with quinoxaline dioxygenase. The full reaction shows consumption of compound **30** and the formation of a new peak at 3.5 minutes. The product could be either of the two regioisomers (**34** or **35**).

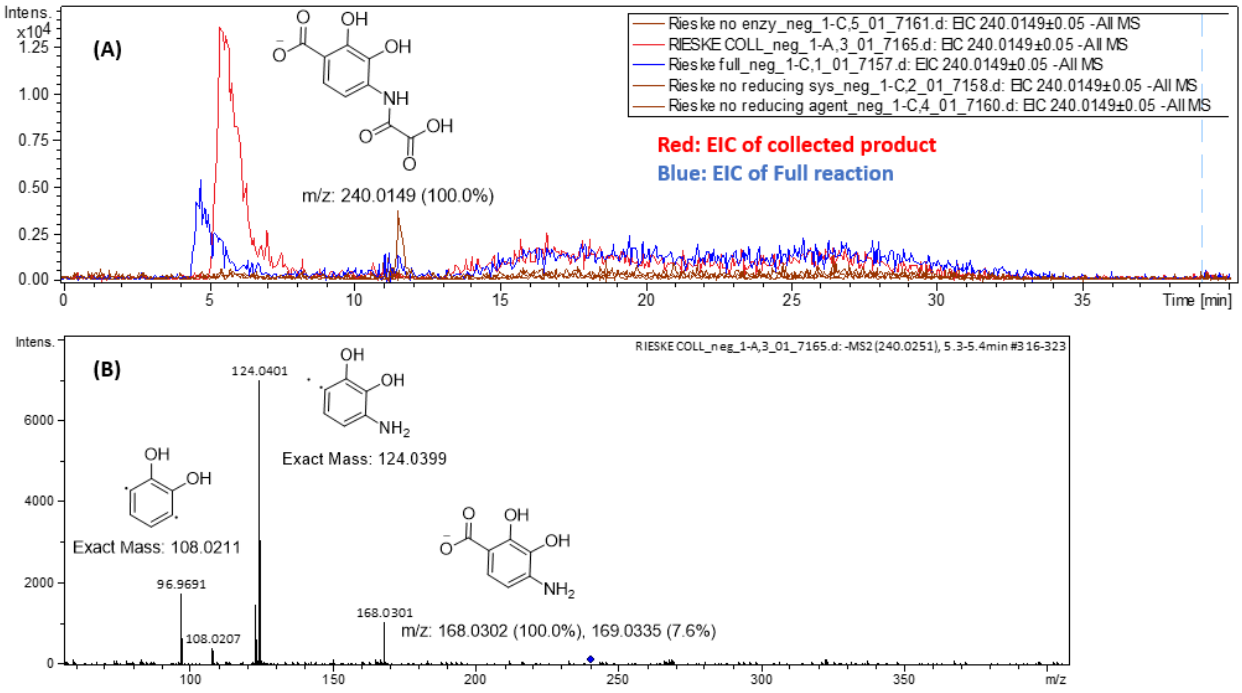

Figure II.8: LC-MS analysis of quinoxaline dioxygenase reaction. A) The EIC of 240.0149 m/z shows the product mass only in the full reaction (blue) and the collected product peak at 3.5 minutes on HPLC (red). B) The MS/MS data at [M-H]=240.0251 supports the proposed structure.

Mechanistic proposal of quinoxaline dioxygenase enzyme with demethy-quinoxaline-diamide-substrate analog, 30

We propose that quinoxaline dioxygenase carries out angular dihydroxylation besides the nitrogen of heterocycle (compound **36 or 38)** (Figure II.9). Cleavage of the carbon-nitrogen bond breaks open the heterocycle, and the acyl-amide (compound **37, 39**) could either be hydrolyzed enzymatically or non-enzymatically to give the final product (**34 or 35**).

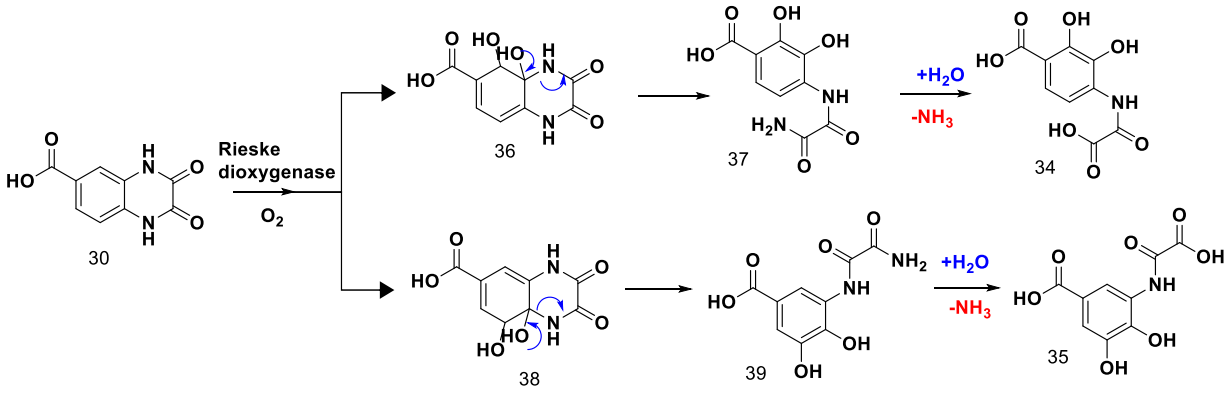

Figure II.9: The proposal of quinoxaline dioxygenase with the demethyl-quinoxaline-diamide substrate analog, **30**.

Labeling experiment with heavy water ($H_2{}^{18}O$)

Labeling experiments with 50% heavy water ($H_2{}^{18}O$) were carried out to determine the source of oxygens in the proposed product (**34** or **35**). The samples were analyzed using LC-MS, and an M and M+2 peak in 1:1 ratio for the product (**34**, **35**) was observed with 50% heavy water. There is one oxygen incorporation from water (H_2O), and the other two oxygens are from molecular oxygen (O_2).

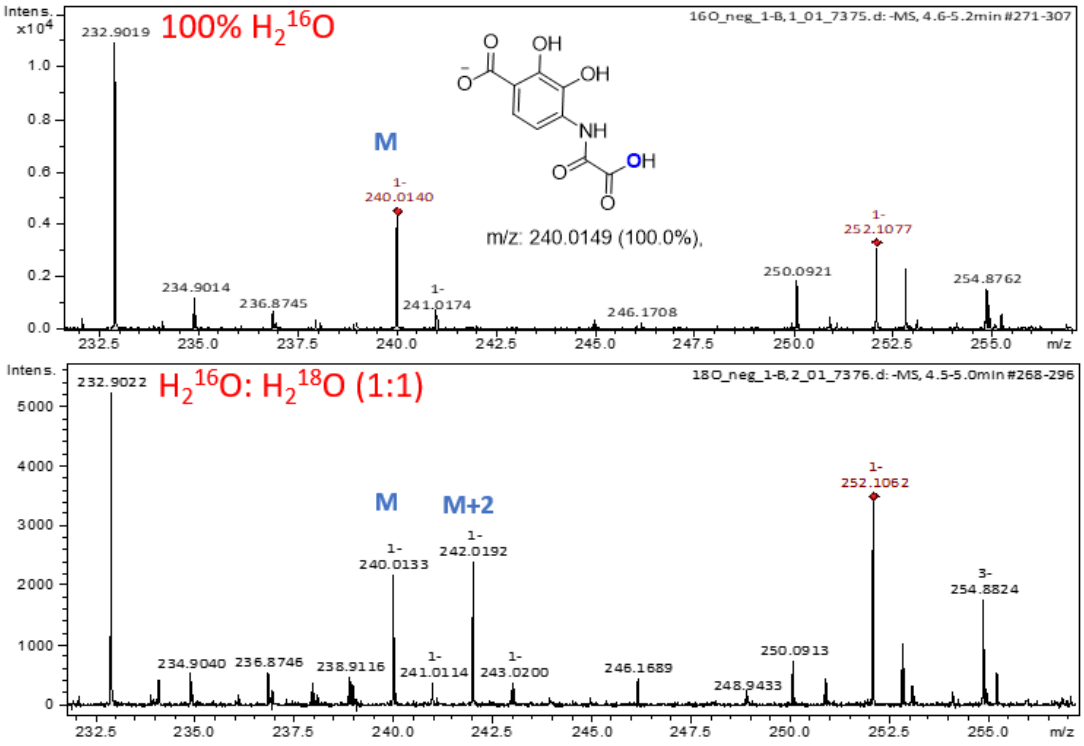

Figure II.10: The LC-MS analysis of the product peak in $H_2{}^{16}O$ and 50% heavy water $H_2{}^{18}O$. The M and M+2 product peaks are in a 1:1 ratio supporting one heavy oxygen incorporation.

Model studies of amide hydrolysis

Rieske dioxygenases are known to hydroxylate aromatic rings, yet the amide hydrolysis is not a typical rieske dioxygenase reaction. I designed an analog **40** with key functionalities of the proposed product (**34** or **35**) to investigate the role of quinoxaline dioxygenase in the amide hydrolysis after the opening of the heterocycle (Figure II.11). The stability of the amide can be assessed by incubating compound **40** in buffer and organic solvent (acetonitrile) and immediately analyzing the mixture by mass spectrometry. Compound **41** was the major compound when compound **40** was incubated in water. Whereas compound **40** was the major compound when it was incubated in acetonitrile (Figure II.12).

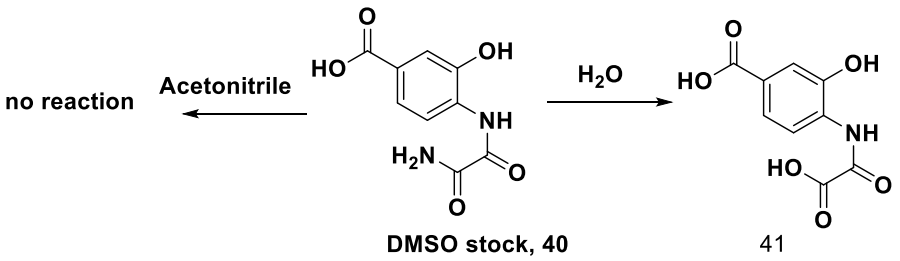

Figure II.11: Model study for hydrolysis of an amide of compound **40**. The compound **40** incubated in acetonitrile remained unreacted [M-H]=223.0360. In contrast, the compound **40** incubated in buffer reacted to form hydrolyzed compound **41** at [M-H]=224.0200.

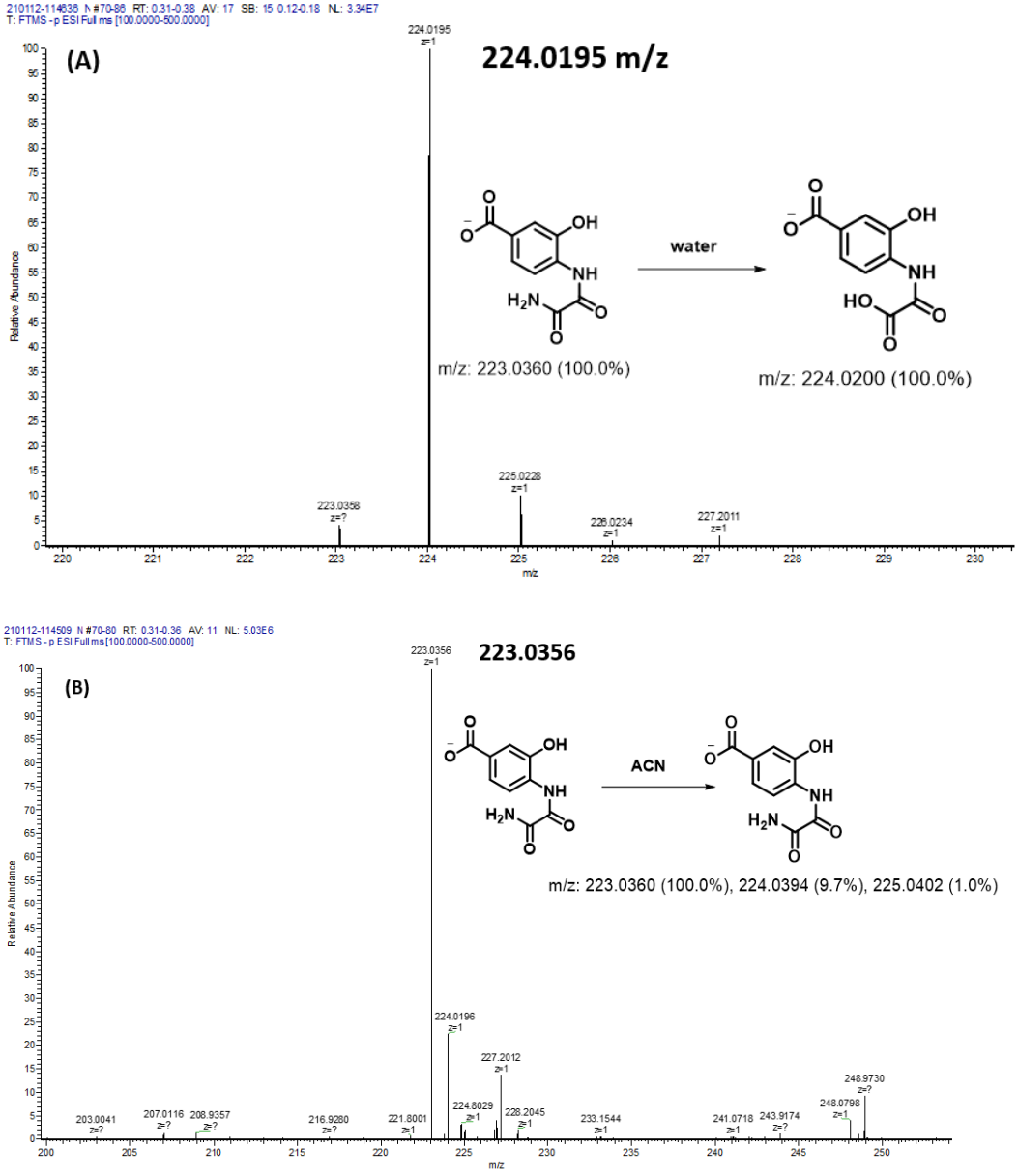

Figure II.12: Mass spectrometry of model study for the hydrolysis of amide compound. (A) The mass spectra of compound **40** incubated in water show conversion to the hydrolyzed compound **41**. (B) The incubation of compound **40** with acetonitrile shows compound **40** as the major compound.

Reconstitution of quinoxaline dioxygenase with proposed native substrate, 43:

The activity of quinoxaline dioxygenase is demonstrated with a substrate analog **30** (missing a methyl group). The proposed native substrate **43** was synthesized and tested with quinoxaline dioxygenase. The compound **43** was consumed in the full reaction (6 minutes). A peak corresponding to the polar product is not observed on the reverse-phase C18 HPLC column (Figure II.13). The reaction analyzed on LC-MS shows an EIC of product **44** [M-H]= 254.0306 only in the full reaction (Figure II.14).

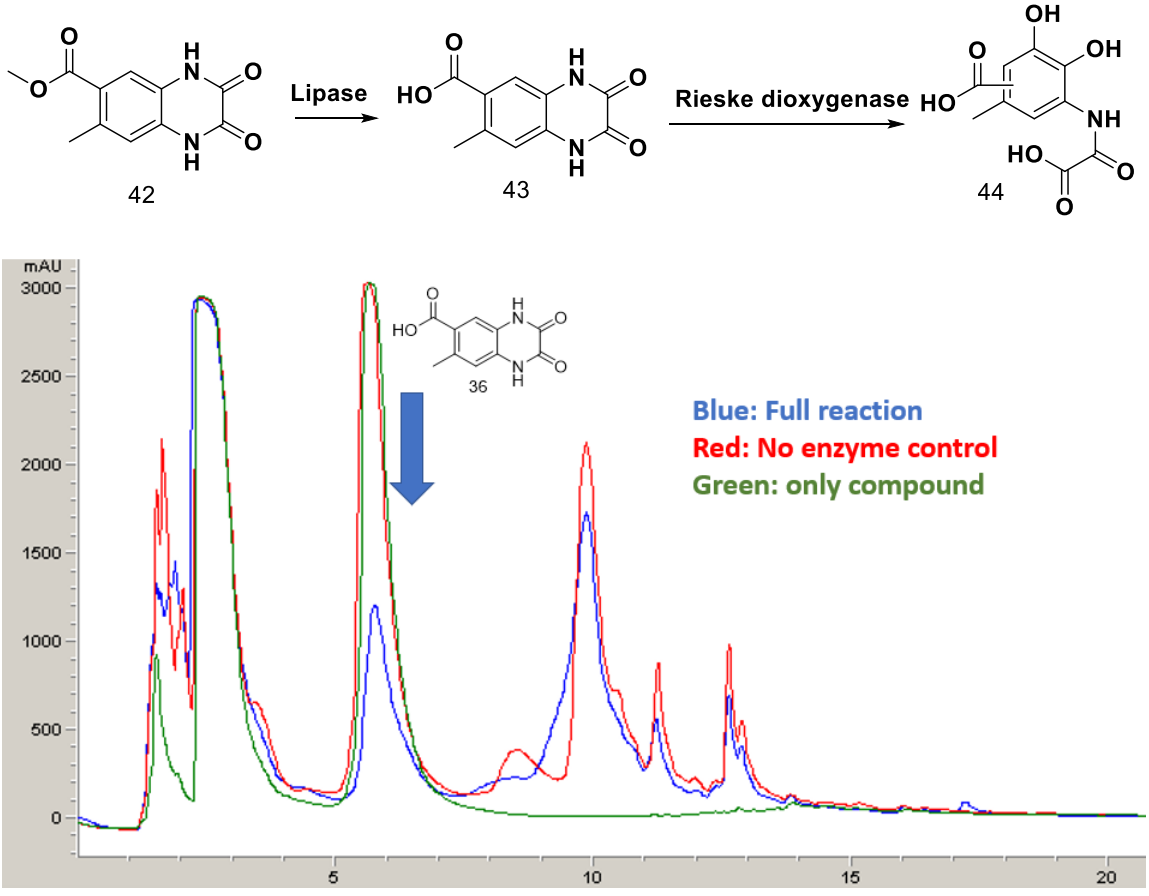

Figure II.13: Activity of quinoxaline dioxygenase with the proposed native substrate. HPLC chromatogram at 254 nm of compound **43** with quinoxaline dioxygenase. Substrate **43** consumption is observed at 6 minutes, but the product elutes at void volume.

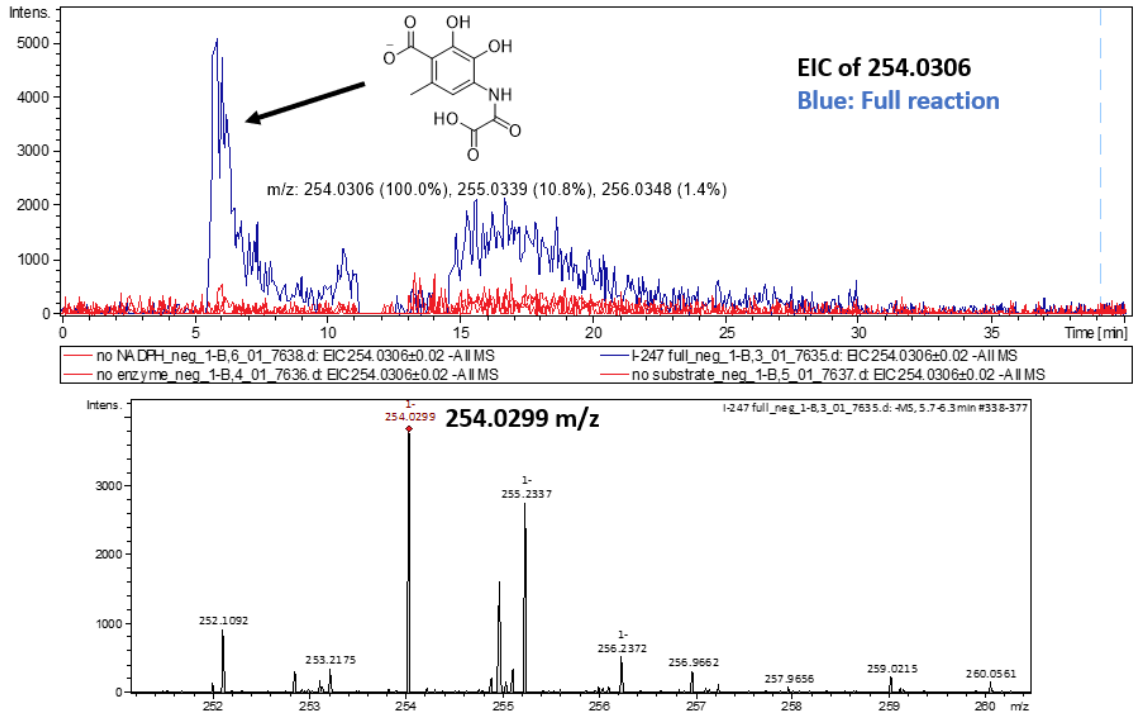

Figure II.14: LC-MS analysis of quinoxaline dioxygenase reaction with proposed native substrate, **43**. The quinoxaline dioxygenase reaction with compound **43** is analyzed on LC-MS. An EIC of [M-H]=254.0306 m/z is only observed in the full reaction.

Mechanistic proposal of quinoxaline dioxygenase

Quinoxaline dioxygenase carries out angular dihydroxylation (**47**) of compound **43** beside the heteroatom, nitrogen. This leads to the opening of the heterocycle and forms a reactive amide **48**. The amide is hydrolyzed to an acid non-enzymatically to form compound **44**. There are two possible sites for dihydroxylation; the synthesis of a product standard is in progress by Sreyashi Sinha. The corresponding mechanism is supported by the mass of product, labeling with heavy water, and model studies with product analog **40**.

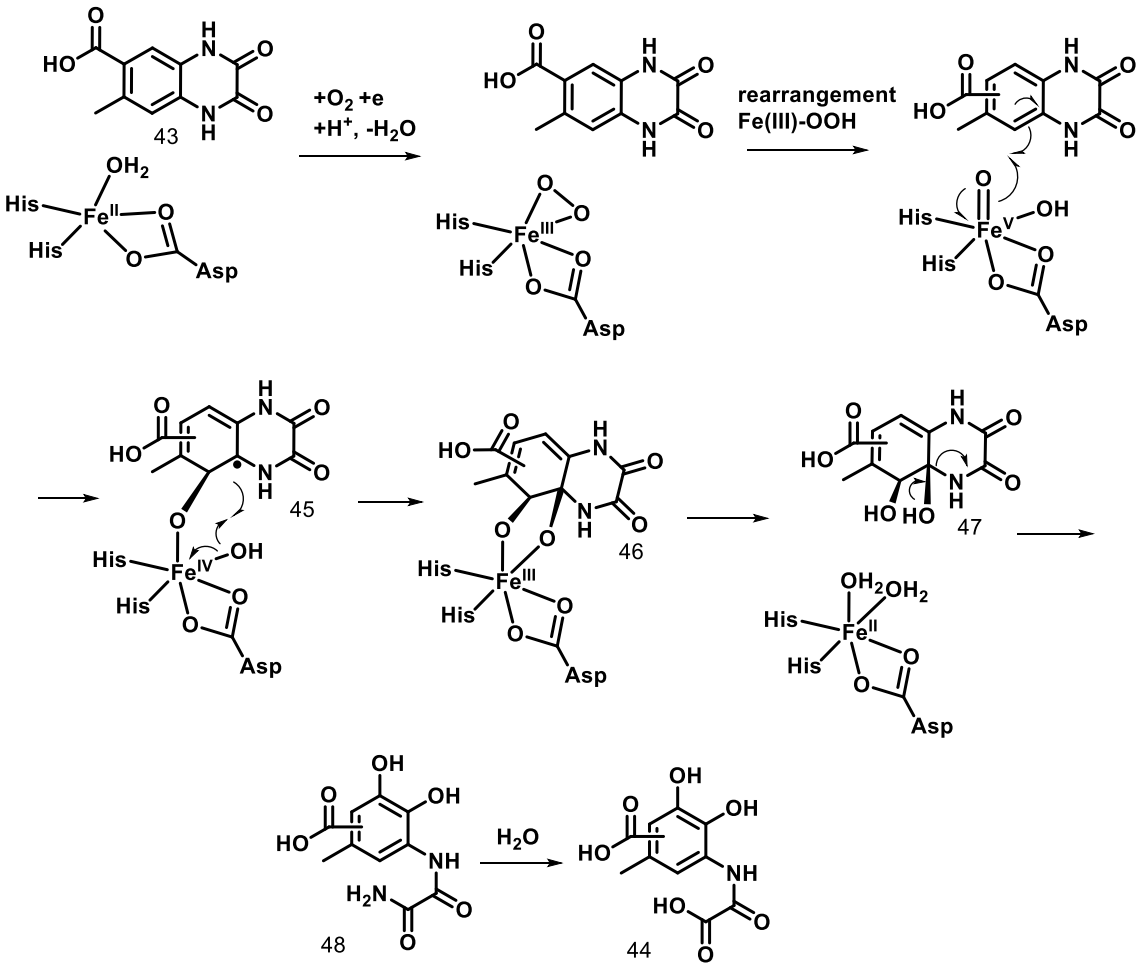

Figure II.15: Mechanistic proposal of quinoxaline dioxygenase activity[10].

Conclusion

Quinoxaline dioxygenase was heterologously expressed in *E.coli* BL21(DE3), and soluble proteins were obtained. The activity of quinoxaline dioxygenase was observed with carboxy-quinoxaline-diamide (**30, 43**), and a catechol product was detected (Figure II.15). According to the hypothesis in Figure II.3, the product of quinoxaline dioxygenase should be the substrate of amidocatechol dioxygenase. Next, we will be testing the activity of the amidocatechol dioxygenase enzyme.

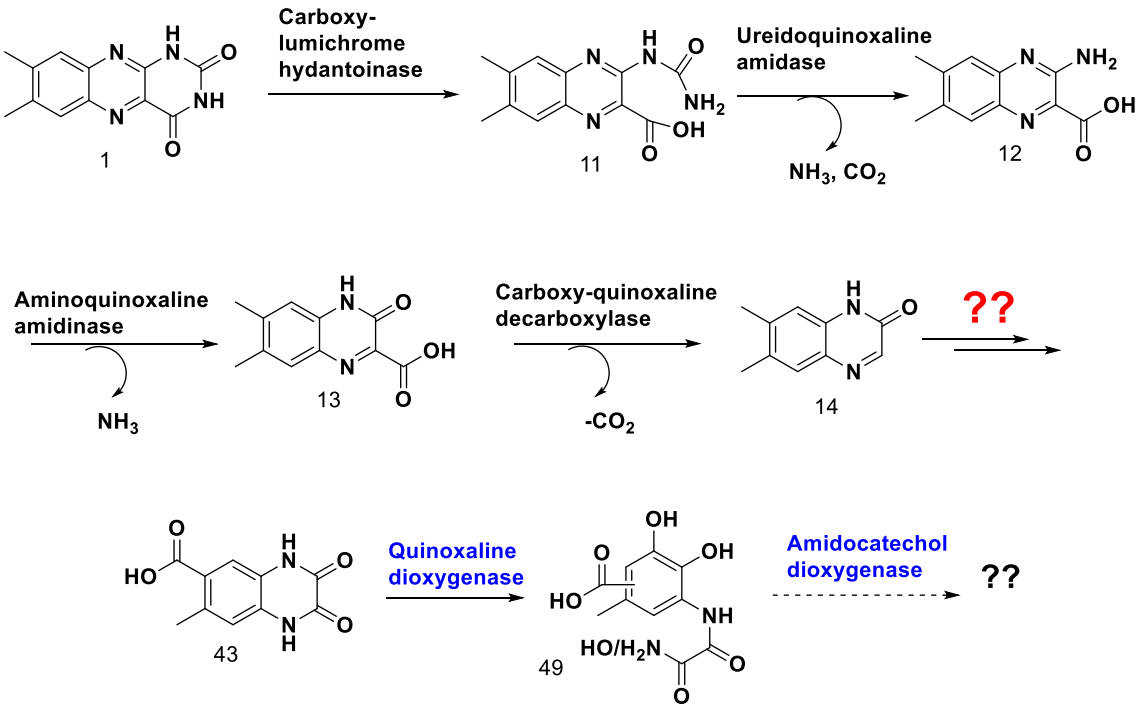

Figure II.16: The current progress in the lumichrome catabolic pathway and questions remained to be answered.

Experimental

Materials

All chemicals were purchased from Sigma-Aldrich unless mentioned otherwise. A dehydrated form of LB medium was purchased from EMD Millipore. IPTG, kanamycin and Ampicillin were purchased from Lab Scientific Inc. HPLC and LC-MS solvents were purchased from VWR. Nickel-NTA affinity column for protein purification was purchased from GE Healthcare. Amicon ultra centrifugal filters (10,000 MWCO) were purchased from Millipore. Econo-pak 10DG desalting columns were purchased from Bio-Rad. Protein overexpression in *E.coli* was carried out in 2.5 L baffled ultra yield flasks

obtained from Thomson Instrument company. $H_2{}^{18}O$ was purchased from Cambridge Isotope Laboratories. Zorbax Eclipse XDB-C18 column (4.6 x 150 mm, 5 μM particles) was obtained from Agilent Technologies.

General method for expression and purification of enzymes

Chemical competent Escherichia coli BL21 (DE3) (Novagen) cells were prepared using standard methods. The cells were freshly transformed with the constructs containing the desired gene with N-terminal hexa-histidine tag. Single colony transformants were grown aerobically for 12-16 hours at 37 °C in 30 mL of LB medium supplemented with recommended quantities of relevant antibiotic. Cells from the starter culture were added to 1.5 L of LB medium supplemented with antibiotic, and the culture was grown aerobically at 37 °C until the A600 was 0.6-0.7. Expression was induced by the addition of IPTG (final concentration=500 μM) and the culture was grown aerobically at 15 °C for an additional ~ 14-16 h at 150 rpm. Cells were harvested by centrifugation at 6,300×g for 25 min at 4 °C (Beckman Coulter Avanti J-E centrifuge with a JA-10 rotor). The medium was discarded and the cell paste (~ 2 g per liter of cell culture) was stored at –80 °C until use. Cells were thawed, resuspended in 20 mL of Lysis Buffer (50 mM potassium phosphate, 5 mM imidazole, pH 7.8, 150 mM NaCl, cooled to 4 °C), Benzonase, Lysozyme, and then lysed by sonication on ice (Misonix Sonicator 3000, pulse 'on' time 1.5 sec, pulse 'off' time 1.5 sec, output level 0.8, for 30 seconds and repeated six times with 10 minutes of cooling between each cycle). Cell debris was removed by centrifugation

at 31,000×g for 45 min at 4 °C (Beckman Coulter Avanti J-E centrifuge with a JA-17 rotor) and the supernatant was clarified by passage through a 0.45 µm syringe filter. The enzyme was purified by nickel affinity chromatography (Ni-NTA) at 4 °C using a 5 mL Hi Trap chelating HP column (GE Healthcare Life Sciences). The resin was charged with 2 column volumes (CV) of 0.1 M NiSO4, washed with 5 CV of filtered water to remove excess nickel, and equilibrated with 2 CV of Lysis Buffer. After loading the filtered protein sample, the resin was washed with 5 CV of Wash Buffer (50 mM potassium phosphate, pH 7.8, 150 mM NaCl, and 30 mM imidazole, cooled to 4 °C). The protein was eluted using elution buffer (50 mM potassium phosphate, pH 7.8, 150 mM NaCl, 250 mM imidazole, cooled to 4 °C). Fractions of 10 mL were collected and analyzed for purity by 12% SDS-PAGE. Nickel affinity column fractions containing the desired protein were pooled and concentrated from ~ 25 mL to ~ 3 mL using a centrifugal filtering device with a 10 kDa MWCO membrane (Millipore) and the buffer was exchanged to Final Buffer (50 mM potassium phosphate, pH 7.5, 150 mM KCl, 30% glycerol, cooled to 4 °C) via Econo-Pac 10DG size exclusion chromatography. Protein purity was determined by SDS-PAGE analysis. Protein concentrations were determined using the absorbance at 280 nm (e280 is estimated using expasy ProtParam tool). Proteins were stored in Final Buffer at –80 °C.

Expression of quinoxaline dioxygenase large subunit, ferredoxin reductase, and Ferredoxin

Quinoxaline dioxygenase large subunit, ferredoxin reductase, and ferredoxin were cloned into pETDuet, pCDFDuet-1, and pTHT vector by genscript. The plasmids were transformed individually into *E.coli* BL21(DE3). The following protocol is the same for the 3 enzymes. An overnight starter culture was grown in LB medium in the presence of antibiotics in the shaking incubator at 37 ℃. A 1.5 liter LB medium was inoculated with the starter culture in the presence of an antibiotic. At OD600 of 0.1-0.2, 100 mg of iron sulfate and L-cysteine were added. The culture was kept at 0 ℃ after the OD600 had reached 0.6-0.8. The protein was induced by the addition of 0.5 mM IPTG and shaken at 15 ℃, 150 rpm for 16 hours. The cells were harvested and stored at -80 ℃ till needed.

Expression of quinoxaline dioxygenase small subunit

The protocol is similar to the one mentioned above except for the addition of iron sulfate and cysteine in the growth medium.

Purification of quinoxaline dioxygenase large subunit, quinoxaline dioxygenase small subunit, ferredoxin reductase, and Ferredoxin

The general purification protocol is followed as described above.

Reconstitution of quinoxaline dioxygenase with carboxy-quinoxaline-diamide

The quinoxaline dioxygenase reaction mixture contains; rieske large α subunit (100 μM), rieske small β subunit (100 μM), ferredoxin (50 μM), ferredoxin reductase (50 μM), compound (1 mM), and NADPH (1 mM) in potassium phosphate buffer (pH 7.5). The reaction was incubated at room temperature for 6 hours, and was filter quenched before being analyzed by HPLC and LC-MS.

Synthetic scheme of methyl 7-methyl-2,3-dioxo-1,2,3,4-tetrahydroquinoxaline-6-carboxylate, 42

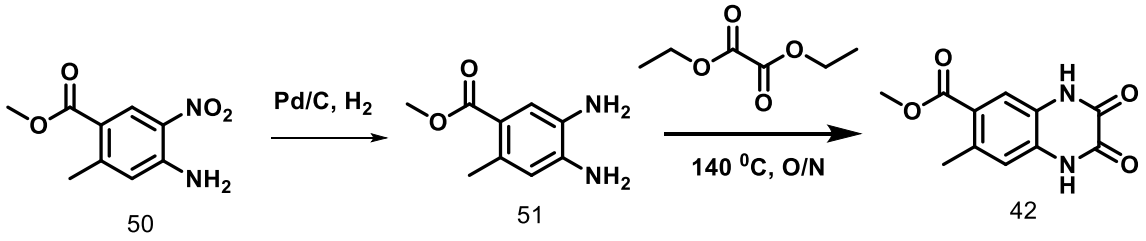

50 51 42

Synthesis of methyl 4,5-diamino-2-methylbenzoate, 51

500 mg of methyl 4-amino-2-methyl-5-nitrobenzoate, 50 mg of palladium/carbon, and 10 mL anhydrous methanol are added to an argon filled round bottom flask. The flask is flushed with a balloon of hydrogen gas. A hydrogen filled balloon is connected and left overnight. The next day, the reaction mixture is filtered using 0.45 μm filter and rotovapped to give a pure reduced product.

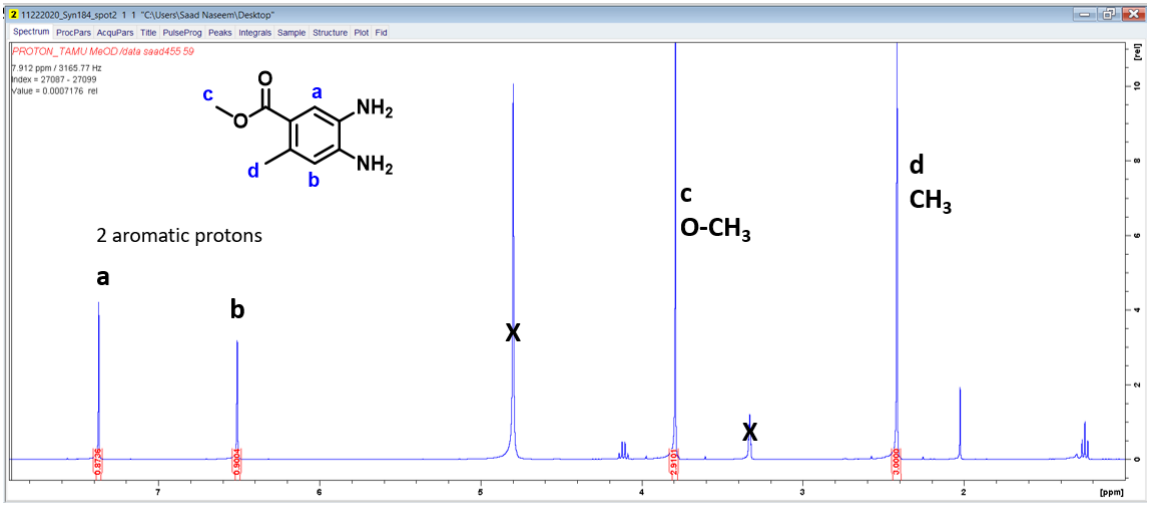

Synthesis of methyl 7-methyl-2,3-dioxo-1,2,3,4-tetrahydroquinoxaline-6-carboxylate, 42

Methyl 4,5-diamino-2-methylbenzoate is condensed with diethyl oxalate at 140 °C for around 16 hours. The product is collected as precipitate.

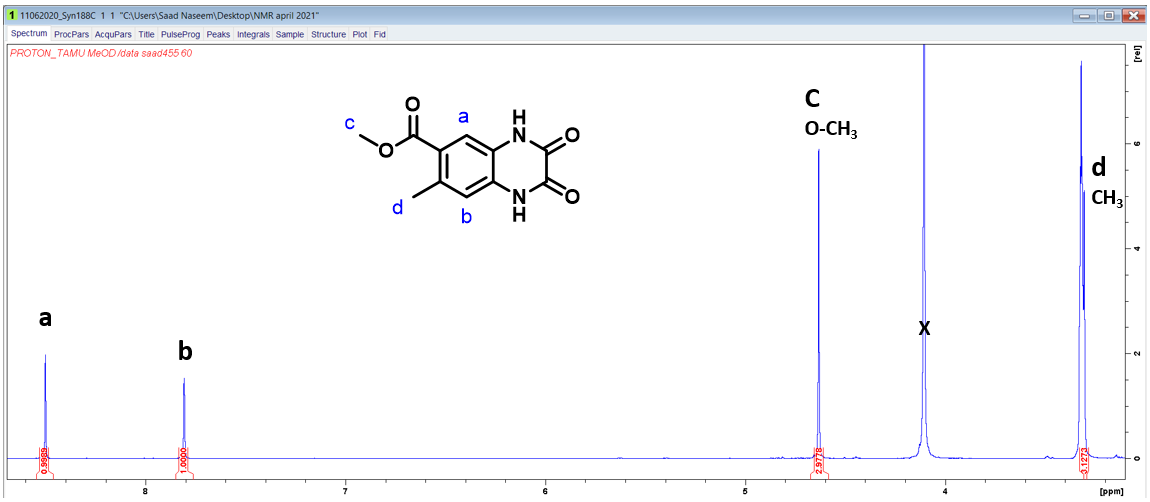

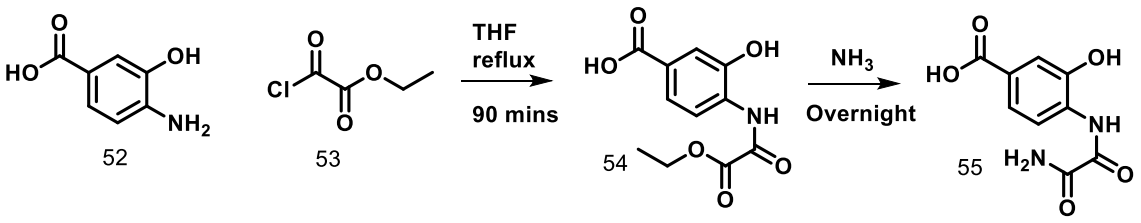

Synthesis of 4-(2-ethoxy-2-oxoacetamido)-3-hydroxybenzoic acid, 54

A stirred solution of 4-amino-3-hydroxybenzoic acid (200mg, 1.3 mmol), dry THF, and ethyl-2-chloro-oxoacetate (1 equivalent) was refluxed for 90 minutes. The reaction was filtered to give a white solid residue.

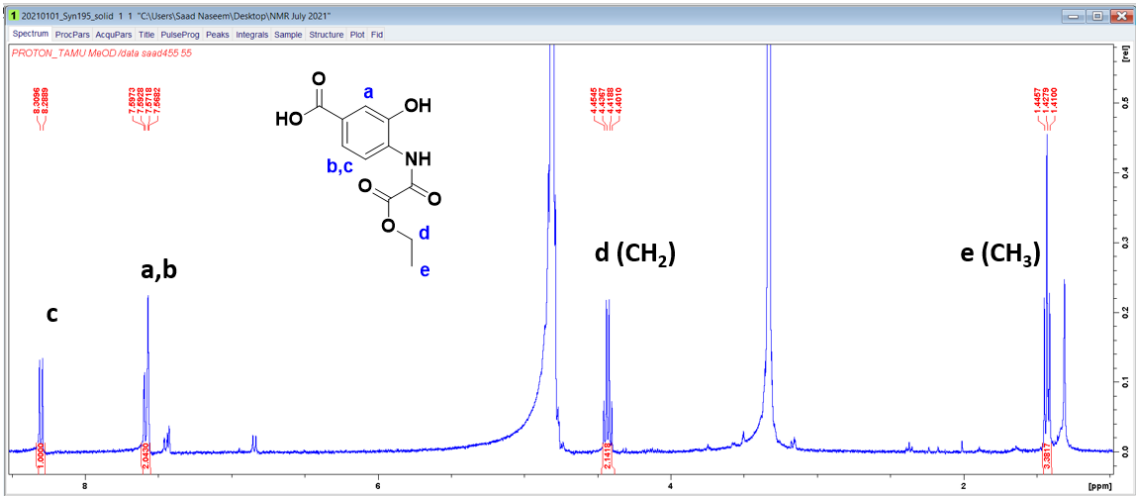

Synthesis of 4-(2-amino-2-oxoacetamido)-3-hydroxybenzoic acid, 55

50 mg of 4-(2-ethoxy-2-oxoacetamido)-3-hydroxybenzoic acid is dissolved in dry methanol and stirred with 1 equivalent of methanolic ammonia for 5 hours at room temperature. The reaction mixture was rotovapped to give a pure product.

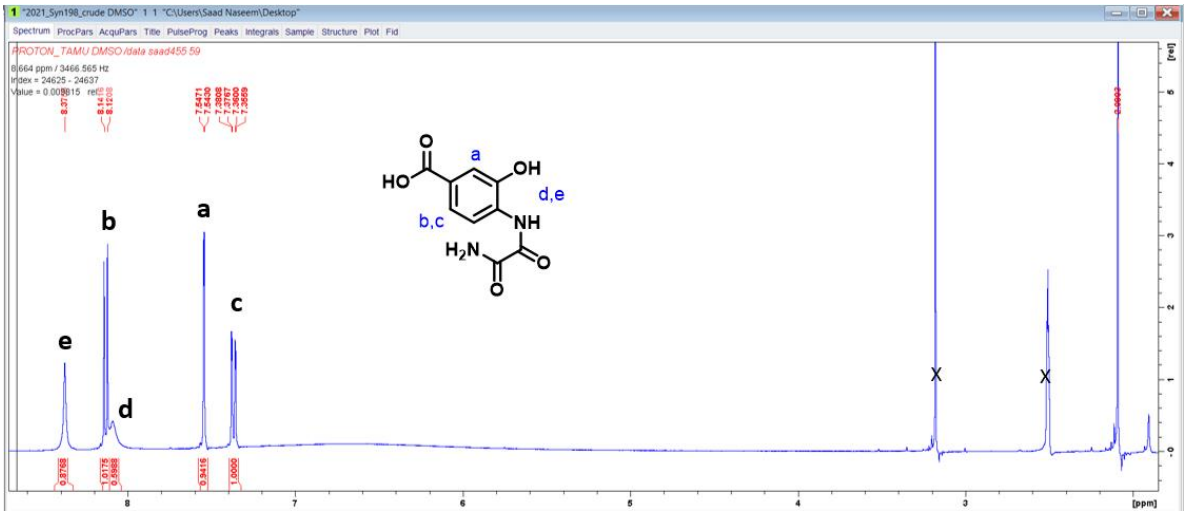

HPLC Parameters

An Agilent 1260 HPLC equipped with a quaternary pump was used. The system included a diode array UV-visible detector, and eluted compounds were detected using absorbance at 220, 254, 280, 300, 320, 340 and 420 nm. Analysis was performed on a Zorbax Eclipse XDB-C18 column (4.6 x 150 mm, 5 µm particles, Agilent Technologies)

HPLC analysis using a linear gradient, at a flow rate of 1 mL/min was used with absorbance detection at 254 nm. Solvent A is water, solvent B is 100 mM K2HPO4, pH 6.6, and solvent C is methanol: 0 min, 100% B; 5 min, 100 % B; 12 min, 48 % A, 40 % B, 12 % C; 14 min, 48 % A, 30 % B, 22 % C; 18 min, 32 % A, 10% B, 58% C; 20 min, 100 % B; 25 min 100 % B.

LC-MS Parameters

Samples were analyzed by reverse-phase HPLC on an Agilent 1200 HPLC system equipped with a diode array UV-Vis detector, a thermostatic autosampler

(10 °C) and a Supelcosil LC-18-T column (15 cm × 3 mm, 3 µm particles), maintained at 22 °C. The LC eluent consisted of a gradient of methanol/water (3:1) with 5 mM ammonium acetate buffer, pH 6.6 (0.4 mL/min flow rate). The percentages of ammonium acetate buffer (B) and methanol/water (M) at time t varied according to the following scheme: (t,M,B): (0,0,100), (2,0,100), (10,35,65), (15,57.5,42.5), (18,100,0), (23,100,0); (26,0,100); (33,0,100). Compounds were detected using absorbance at 254 S5nm. UV-Vis spectra (190 – 640 nm) were also collected and evaluated. Mass data were collected using an in-line Bruker Daltonics micrOTOF-Q II ESI-Qq-TOF mass spectrometer (HyStar) in negative ion mode.

CHAPTER III

FUNCTIONAL CHARACTERIZATION OF AMIDOCATECHOL DIOXYGENASE

Introduction

Catechol dioxygenase is primarily found in the degradation pathways of aromatic compounds[6]. They linearize 1,2-dihydroxybenzenes, catechol, and subsequent processing leads the product to central metabolism. Catechol dioxygenase allows nature to break down stable aromatic compounds and use them as a carbon source and energy for growth.

Catechol dioxygenase incorporates both molecules of molecular oxygen, O_2, into the substrate. Depending on the position of ring cleavage, the catechol dioxygenases can be termed intradiol or extradiol dioxygenase. Both types of dioxygenase make use of iron at the catalytic center to initiate the chemistry. Other differences include the iron-binding site; extradiol dioxygenase has 2-His-1-carboxylate binding the ferrous Fe(II) ion. Meanwhile, intradiol dioxygenase has a mononuclear ferric Fe(III) coordinated by 2-His-2-tyrosine residues (Figure III.1).

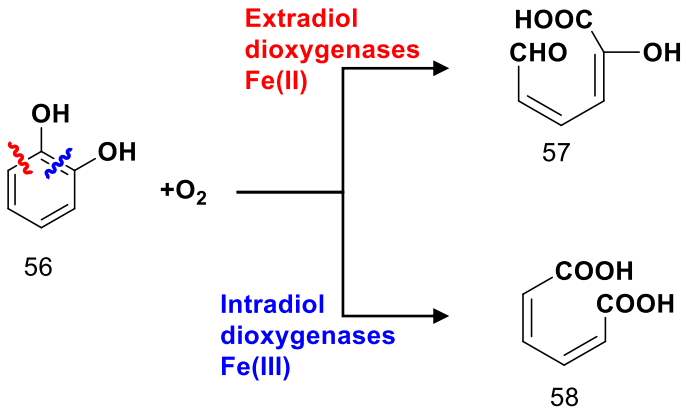

Figure III.1: Extradiol and intradiol dioxygenases differ by the oxidation state of mono-nuclear iron and the position of aromatic cleavage. Extradiol dioxygenase cleaves adjacent to the two phenolic hydroxy groups to give an aldehyde and an acid (**57**). Meanwhile, intradiol dioxygenase cleaves between the two hydroxy phenolic groups to give a dicarboxylic acid product (**58**).

The product of the quinoxaline dioxygenase reaction (**49**) is proposed to be the substrate of amidocatechol dioxygenase or deacetylase (Figure III.2). The proposal was tested by a coupled reaction of quinoxaline dioxygenase with amidocatechol or deacetylase. A demethyl-quinoxaline-diamide-substrate analog (**30**) was tested in the coupled reaction due to the ease of analysis on HPLC.

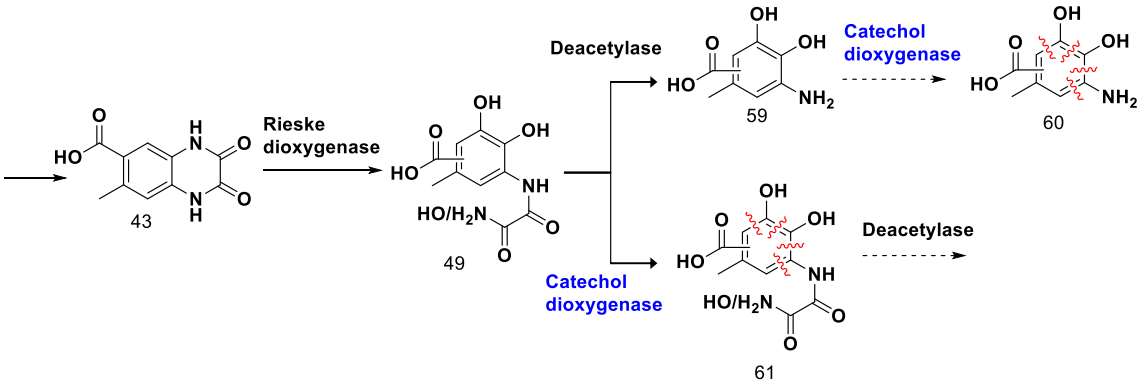

Figure III.2: The product of quinoxaline dioxygenase is a catechol with an amide linkage. The product can be the substrate of deacetylase followed by amidocatechol dioxygenase or vice versa. The position of cleavage is more likely to be an extradiol.

Results and Discussion

Expression and purification of Amidocatechol dioxygenase

The gene of amidocatechol dioxygenase was cloned into pTHT (a derivative of pet28b) with an N-terminal His_6-tag by genscript. A general expression protocol was followed except that 100-150 mg of ferrous ammonium sulfate and 0.5 mM IPTG were added at OD_{600} = 0.6-0.8 and shaken at 15 °C for 16-18 hours. A general protein purification protocol was followed, and soluble protein was successfully eluted using nickel-affinity chromatography.

Activation of Amidocatechol dioxygenase

The amidocatechol dioxygenase has a high sequence similarity with extradiol dioxygenases, in which the catalytic cycle initiates with ferrous ion [Fe^{2+}]. The enzyme is reconstituted with ferrous ion and used immediately with the substrate. The enzyme (300 uM) is reconstituted by diluting it into 10 mM potassium phosphate buffer pH 7.5, 10 mM

Cleland's reagent, 250 mM imidazole, and 2 mM ferrous ammonium sulfate. After incubation on ice for 30 minutes, the enzyme is desalted into 100 mM potassium phosphate buffer pH 7.5, and 500 uM substrate is added. The reaction usually reaches completion within 30 minutes, and it is analyzed by HPLC, LC-MS, and UV-vis spectroscopy.

Coupled assay of amidocatechol dioxygenase and deacetylase with quinoxaline dioxygenase

The quinoxaline dioxygenase reaction with compound **30** is filter quenched after 3 hours, followed by the addition of reconstituted amidocatechol dioxygenase (100 μM) or deacetylase (100 μM). After 30-60 minutes, the reaction is filter quenched and analyzed by HPLC.

The coupled reaction of quinoxaline dioxygenase and deacetylase showed no consumption of the quinoxaline dioxygenase reaction product (**34**). In contrast, the coupled reaction of quinoxaline dioxygenase and amidocatechol dioxygenase turns yellow. HPLC shows the quinoxaline dioxygenase product (**34**) consumption at 3.2 minutes and a new peak at 1.6 minutes (Figure III.3). The UV-vis spectra of the product at 1.6 minutes have a lambda max at 400 nm, which is characteristic of extradiol dioxygenase products. The product of quinoxaline dioxygenase is identified as the substrate of amidocatechol dioxygenase.

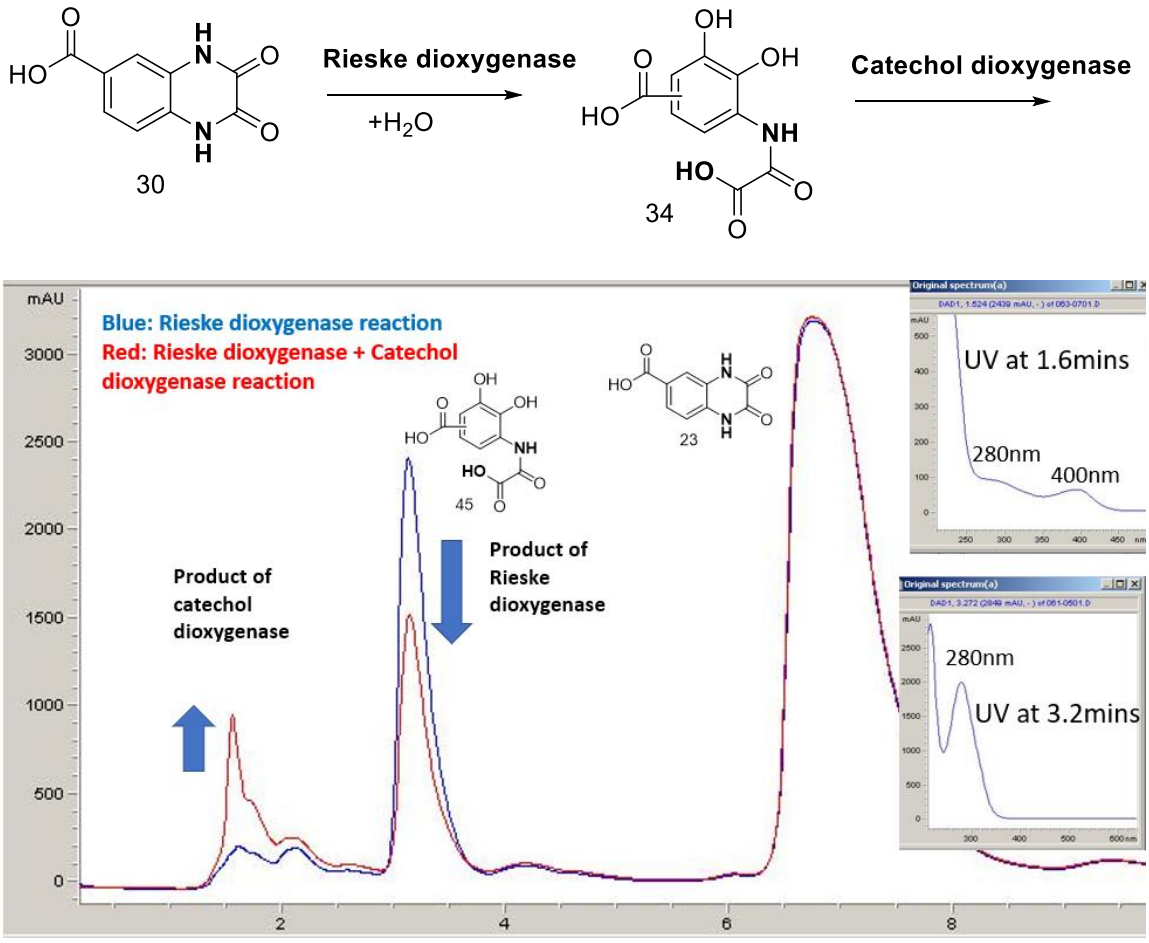

Figure III.3: The HPLC chromatogram of quinoxaline dioxygenase and amidocatechol dioxygenase coupled reaction (red) and quinoxaline dioxygenase reaction only (blue) with demethyl-substrate analog **30**. Amidocatechol dioxygenase consumes the product of quinoxaline dioxygenase at 3.2 minutes, and a new peak at 1.6 minutes is detected. The UV-vis spectra of the amidocatechol dioxygenase product is typical of extradiol cleavage of aromatic compounds with lambda max at 400 nm.

Conclusion

The functional characterization of quinoxaline dioxygenase led us to the substrate of amidocatechol dioxygenase. Another graduate student, Sreyashi Sinha, is characterizing the product of amidocatechol dioxygenase. Meanwhile, I investigated the

enzymes responsible for hydroxylation of the heterocycle of compound **14** and oxidation of methyl to form compound **43**.

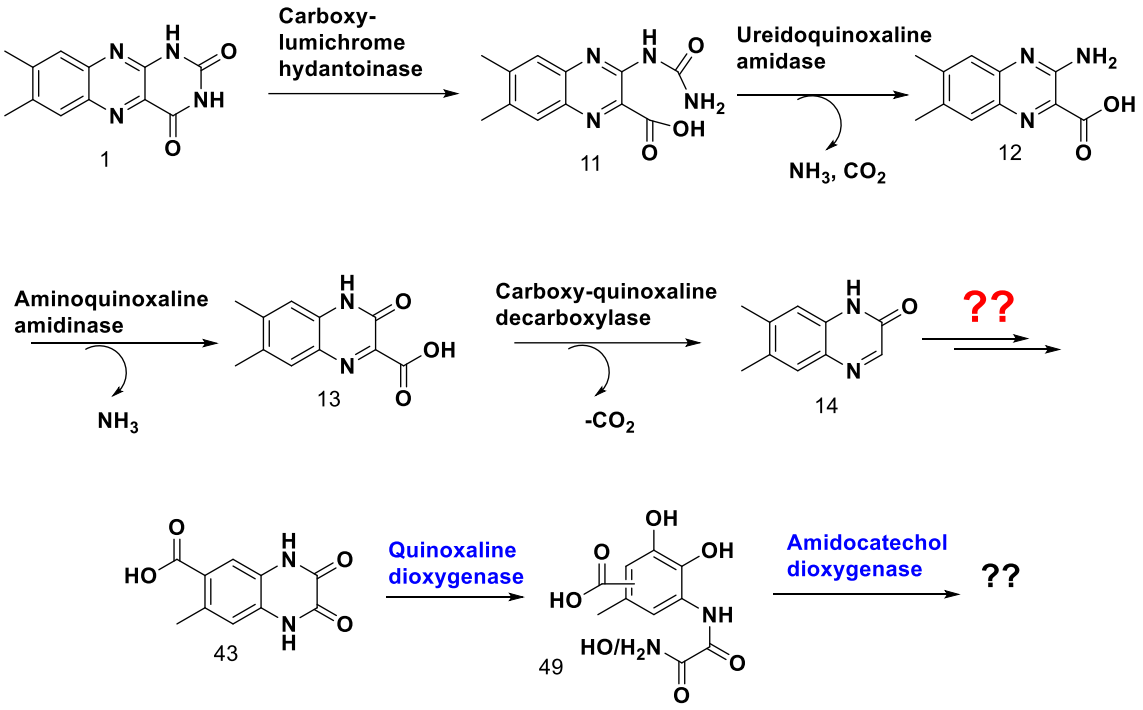

Figure III.4: Quinoxaline dioxygenase and amidocatechol dioxygenase is reconstituted. The next challenge is to discover the enzymes responsible for the oxidation of the methyl to carboxylic acid.

CHAPTER IV

EXPRESSION, PURIFICATION, AND RECONSTITUTION OF QUINOXALINE OXIDASE

Introduction

Mononuclear molybdenum enzymes are spread throughout living organisms. In prokaryotes, they are responsible for essential roles in metabolism and catabolism[11]. Only around 50 molybdenum-containing enzymes have been purified and biochemically characterized till 2016[12]. The study on these enzymes has been hindered due to challenges in heterologous expression, low yield, reactive nature of the complex molybdopterin cofactor, and low occupancy of the cofactor in the purified enzymes.

The prokaryotic molybdenum enzymes fall into four families (Figure IV.1) based on the bound cofactor[11]; (i) aldehyde oxidoreductase family utilizing bis-pyranopterin cofactor that usually contains a tungsten atom (ii) xanthine oxidase family utilizing molybdenum cofactor (Moco, **63**) or molybdopterin-cytosine-dinucleotide cofactor (MCD, **65**) (iii) dimethylsulfoxide (DMSO) reductase family using bis-molybdopterin-guanine-dinucleotide cofactor (bis-MGD, **64**) and (iv) sulfite oxidase family using a molybdenum cofactor (Moco, **63**).

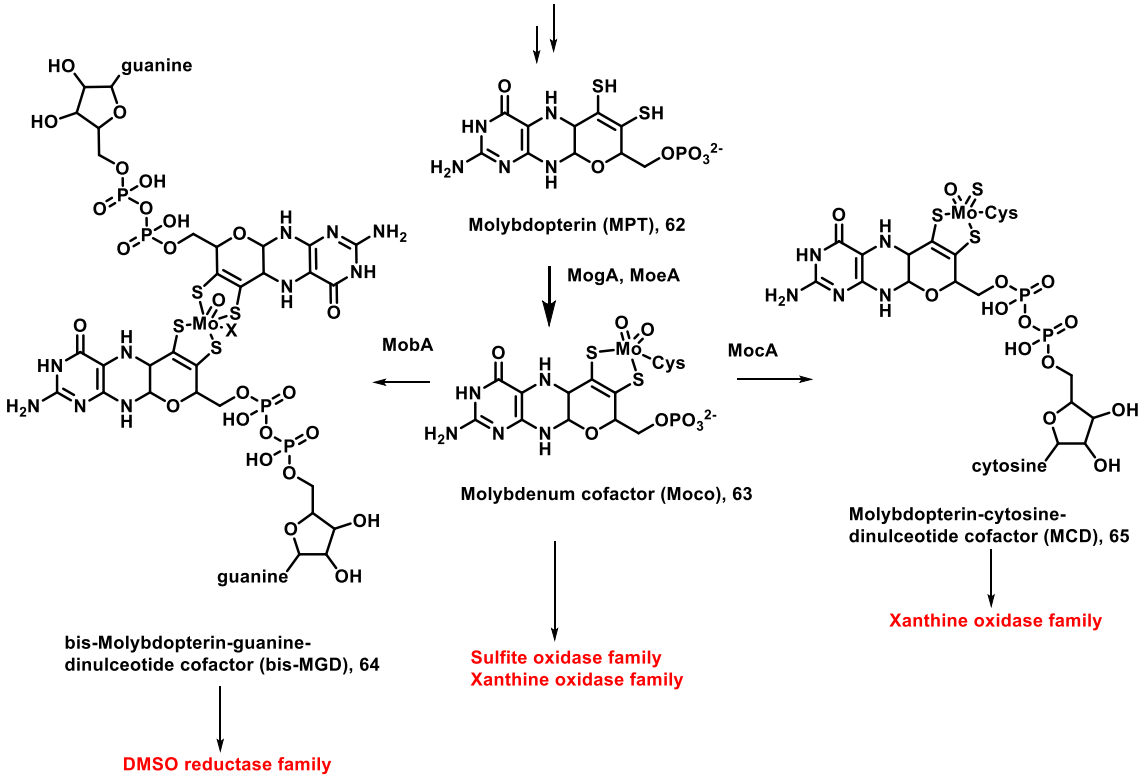

Figure IV.1: Cofactor structures of the four families of mononuclear molybdenum enzymes.

The xanthine oxidase family seems to be the most relevant in our pathway among the four families of molybdenum enzymes. Xanthine oxidase carries out oxidative hydroxylation of a carbon center in aromatic heterocycles or an aldehyde. Unlike quinoxaline dioxygenase and amidocatechol dioxygenase that inserts molecular oxygen into the substrate, xanthine oxidase utilizes the oxygen from water (Figure IV.2).

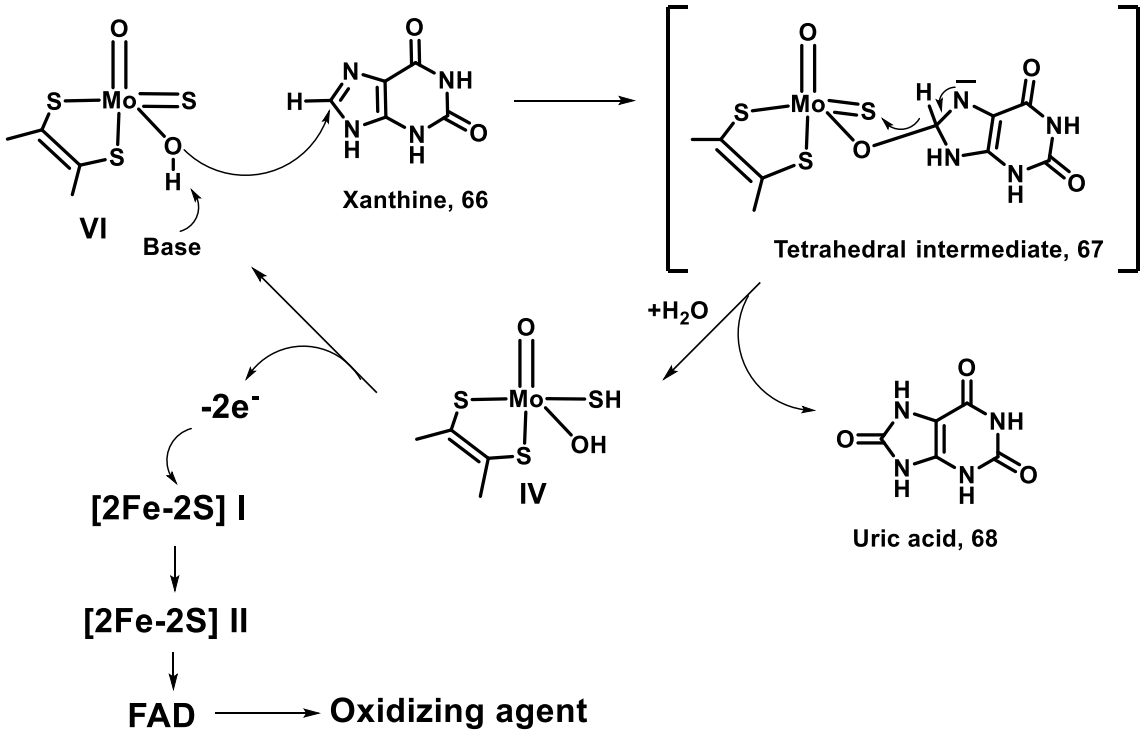

Figure IV.2: The oxidative hydroxylation of xanthine to uric acid by xanthine oxidase.

Xanthine oxidase is usually 150 kDa in size and contains three domains; an N-terminal [2Fe-2S] domain contains two [2Fe-2S] clusters, flavin adenine dinucleotide (FAD) domain, and a C-terminal molybdopterin cofactor (Moco) domain. The catalytic cycle initiates with Mo(VI) and hydroxy ligand as a nucleophile onto the electropositive carbon center of an aromatic heterocycle, xanthine (**66**). This leads to a tetrahedral intermediate (**67**), supported by DFT calculations, and hydride transfer from the substrate to Mo(IV)=S. The cofactor hydrolyzes and releases the hydroxylated product, uric acid (**68**). Then two electrons are transferred from Mo(IV) cofactor to the [2Fe-2S] I-cluster then [2Fe-2S] II-cluster of ferredoxin. This is followed by electron transfers to FAD in the ferredoxin reductase domain and then finally to an oxidizing agent (Figure IV.2).

Proposed role of Quinoxaline oxidase

Based on xanthine oxidase's role in converting xanthine (**66**) to uric acid (**68**), we propose that quinoxaline oxidase may catalyze oxidative hydroxylation of the electropositive carbon besides the nitrogen in the heterocycle.

The substrate of quinoxaline dioxygenase, carboxy-quinoxaline-diamide (**43**), has a carboxylic acid instead of methyl; this leads to three proposed substrates for quinoxaline oxidase, as shown in Figure IV.3. Proposal B and C differ in the position of the carboxylic acid for the substrate of quinoxaline oxidase (compounds **69** and **70**).

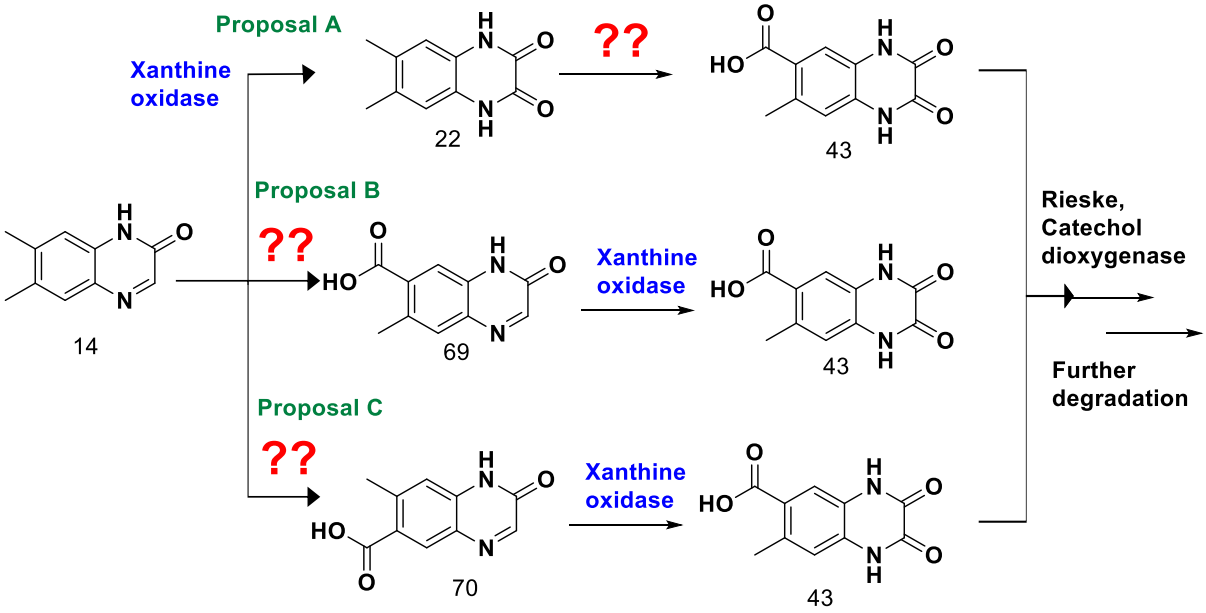

Figure IV.3: The proposed role of quinoxaline oxidase in the lumichrome catabolic pathway.

Results and Discussion

Expression and purification of quinoxaline oxidase:

The expression and purification of quinoxaline oxidase have been a hurdle in this project. Despite various attempts by other graduate students and me, this protein could not be expressed for many months. Finally, I discovered that the quinoxaline oxidase gene's Open Reading Frame (ORF) in the Uniprot and NCBI databases was incorrect. After testing more than 20 expression conditions, 3 plasmid constructs; the below-described condition expressed active quinoxaline oxidase.

The [2Fe-2S] domain, FAD domain, and molybdenum core domain were cloned into pMAL-c2E-TEV vector using Gibson assembly. The vector was transformed into *E.coli TP1000* cells (Courtesy Dr. Russ Hille, UC Riverside), a knockout of mobAB genes belonging to molybdopterin cofactor biosynthesis. *E.coli TP1000* cells have previously been used to express xanthine oxidases because it increases the occupancy of the Moco and MCD cofactor in the expressed molybdenum enzymes (Figure IV.1). After expression, the protein was purified using nickel-affinity chromatography. The presence of the C-terminal-His8-tagged-quinoxaline oxidase was confirmed with western blot using an anti-His tag antibody.

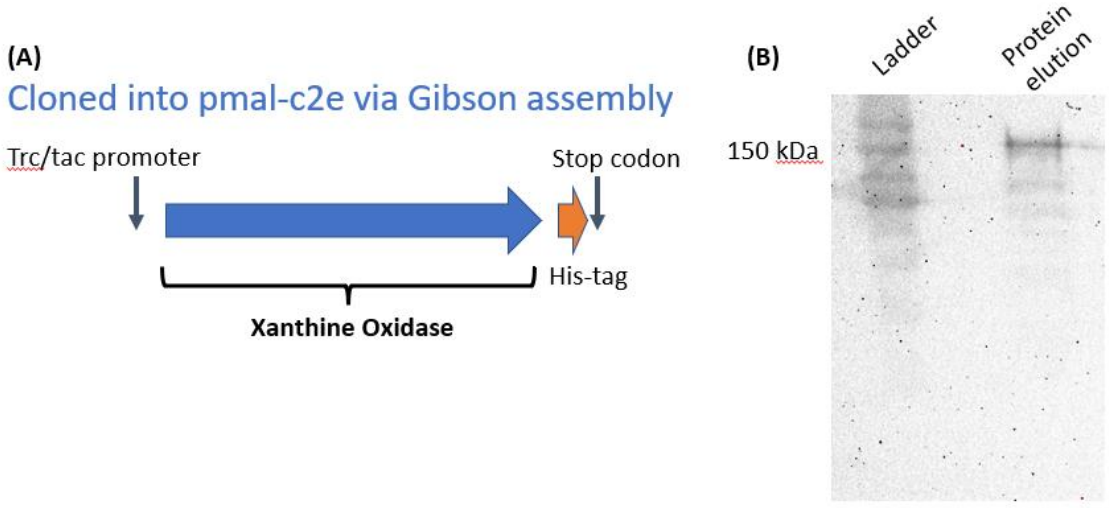

Figure IV.4: A) The construct map of quinoxaline oxidase in pMAL-c2E-TEV vector. B) The western blot image of quinoxaline oxidase elution using an anti-His tag antibody.

Activity assay of quinoxaline oxidase to test Proposal A

The activity of quinoxaline oxidase is tested with compound **14** (1 mM) in the presence of an oxidizing agent, potassium ferricyanide (0.5 mM). The reaction was filter quenched after 6 hours and analyzed by HPLC. HPLC analysis detected a new peak at 29.2 minutes in the full reaction. The product was confirmed as dimethyl-quinoxaline-diamide **22** based on LC-MS, UV-vis spectroscopy, and retention time on HPLC (Figure IV.5).

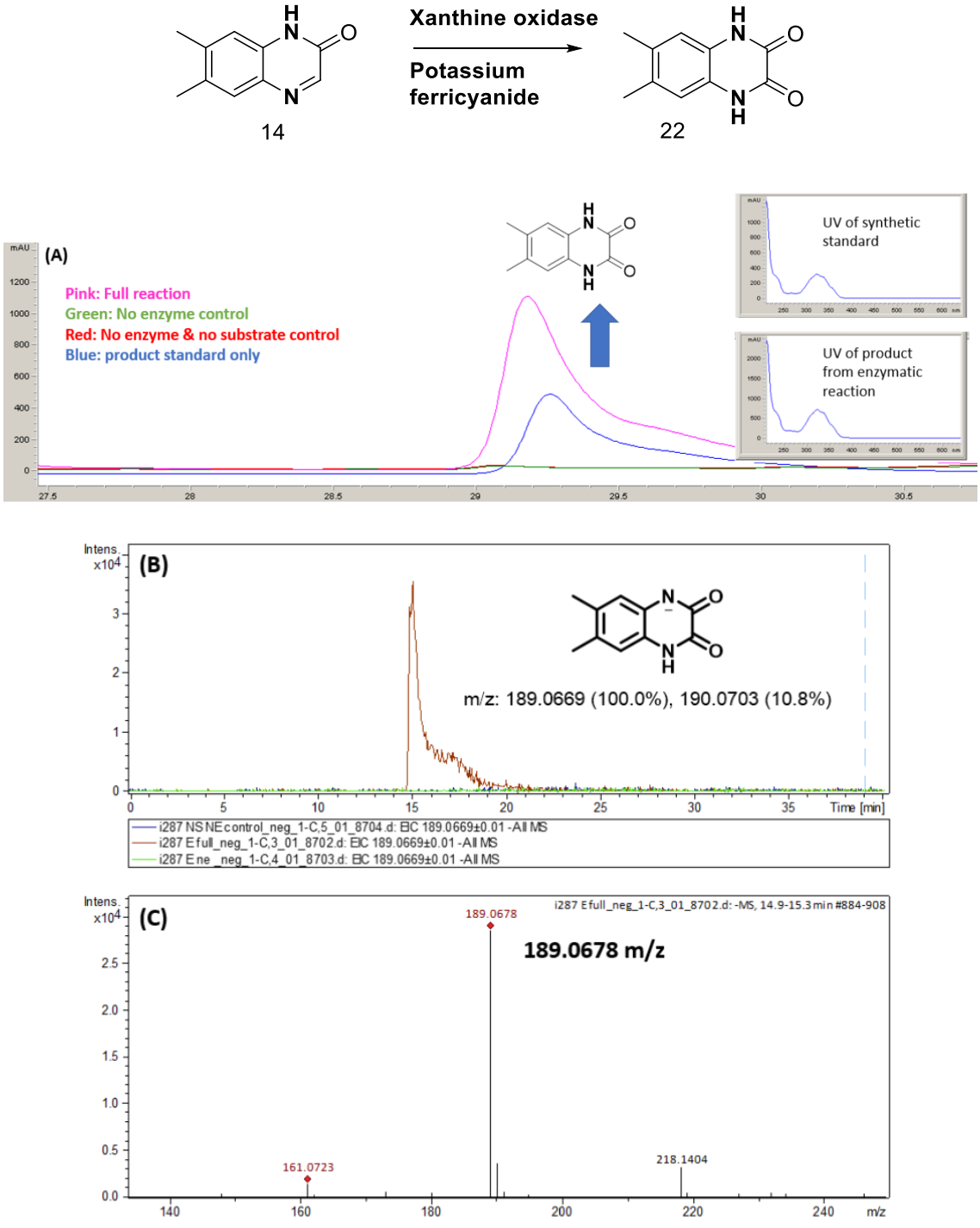

Figure IV.5: Activity assay of compound **14** with quinoxaline oxidase to test proposal A (A) HPLC chromatogram at 254 nm shows product formation at 29.2 minutes. The retention time and UV-vis spectrum of the enzymatic product match the product standard (**22**). (B) The Extracted Ion

Chromatogram (EIC) at 189.0669 m/z shows product formation only in the full reaction. (C) The mass matches the proposed product structure (**22**).

Activity assay of quinoxaline oxidase to test Proposal B and C

The substrate of quinoxaline dioxygenase suggests that the methyl is oxidized to carboxylic acid by other enzymes in catabolic strain. The oxidation of methyl may occur before or after the oxidative hydroxylation of heterocycle by quinoxaline oxidase. We would like to see if the carboxy-quinoxaline-amide **(69** or **70)** is the substrate of quinoxaline oxidase (Figure IV.3 Proposal B and C). If compound **69** or **70** is not the substrate, that will provide evidence that oxidation of methyl takes place on the product of quinoxaline oxidase in the catabolic sequence.

The two demethyl-carboxy-analogs (**27** and **28**) were prepared and tested with quinoxaline oxidase in the presence of the oxidizing agent. Consumption of both the substrate analogs (**27**, **28**) was observed, and HPLC and LC-MS detected the formation of carboxy-quinoxaline-diamide (**30**).

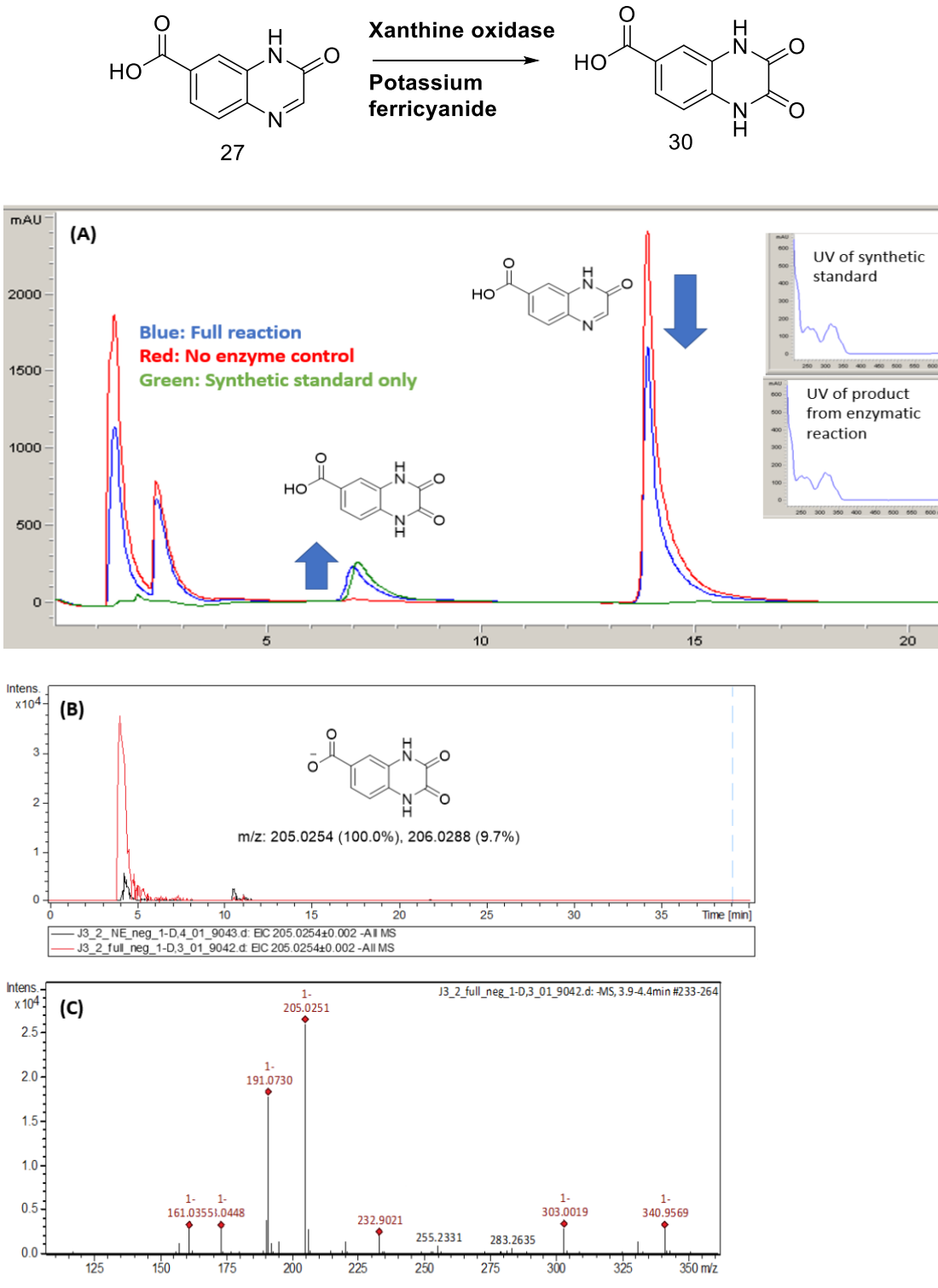

Figure IV.6: Activity assay of compound **27** with quinoxaline oxidase (A) HPLC chromatogram at 254 nm shows product formation at 7.2 minutes. The retention time and UV-vis of the enzymatic

product match the product standard **23**. (B) The Extracted Ion Chromatogram (EIC) at 205.0254 m/z shows product formation only in the full reaction. (C) The mass matches the proposed product structure **23**.

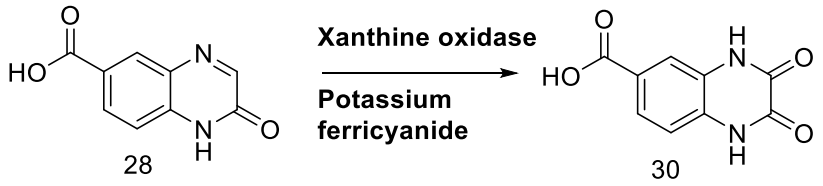

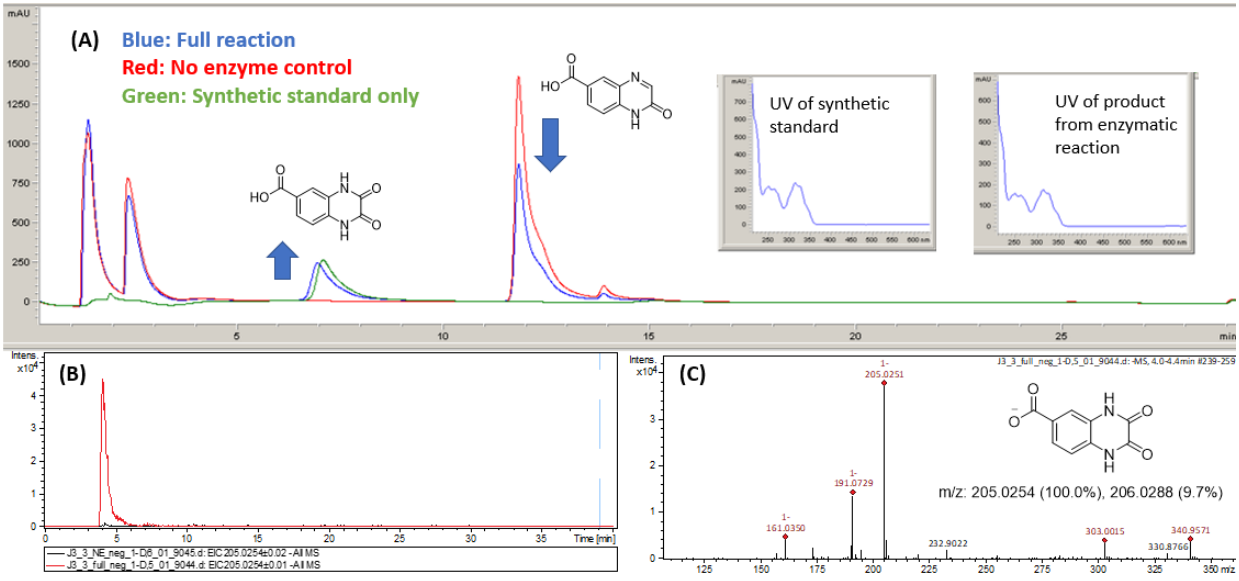

Figure IV.7: Activity assay of compound **28** with quinoxaline oxidase (A) HPLC chromatogram at 254 nm shows product formation at 7.2 minutes. The retention time and UV-vis of the enzymatic product match the product standard **30**. (B) The Extracted Ion Chromatogram (EIC) at 205.0254 m/z shows product formation only in the full reaction. (C) The mass matches the proposed product structure **30**.

Conclusion

Quinoxaline oxidase was successfully overexpressed and purified in *E.coli* TP1000 cells (Figure IV.4). The activity assays with compounds **14, 27, 28** showed nucleophilic hydroxylation at the electropositive carbon center beside the nitrogen. The results suggest that the oxidation of the methyl group may occur before or after the activity

of quinoxaline oxidase. The remaining enzymes in the lumichrome catabolic cluster (deacetylase and aldehyde dehydrogenase) can not oxidize methyl to carboxylic acid. The next challenge was to find the enzymes responsible for the oxidation of the methyl group in the *P. simplex*.

Experimental

General methods and materials

Molecular biology manipulations were carried out using standard techniques. PCR amplifications were performed using a C1000 automatic thermocycler (Bio-Rad) and Integrated DNA Technologies synthesized oligonucleotide primers. Phusion DNA polymerase was obtained from New England BioLabs. The cloning vector was purchased from Novagen. pMAL-c2E-TEV vector was provided by Dr. James Sacchettini (Texas A&M University). Plasmid mini-prep and PCR purification kits were acquired from Qiagen. DNA fragments were purified from agarose gels with the GIAquickgel extraction kit from Qiagen. All restriction enzymes and T4 DNA ligase were purchased from New England Biolabs. Gibson assembly kit was purchased from NEB. DNA sequencing was performed in Eton biosciences. *Escherichia coli* strains DH5α were used as recipients for transformations during plasmid construction as well as for plasmid propagation and storage.

Expression of quinoxaline oxidase

The quinoxaline oxidase gene was cloned into pMAL-c2E-TEV vector using the general procedure of Gibson assembly kit by NEB. The sequence was confirmed by Eton biosciences. The plasmid was transformed into chemical competent *E.coli* TP1000 cells (courtesy of Dr. Russ Hille, UC Riverside). The transformed colony was inoculated into a starter culture for 12 hours. Then a larger (1.5 L) culture was inoculated with 15 mL of starter culture. The larger culture has ampicillin, sodium molybdate salt (1 mM), L-cysteine (200 mg), ferrous ammonium sulfate (200 mg), IPTG (20 μM) and shaken at 100 rpm, 22 °C for 24 hours. The cells from the 9 liter LB culture were collected with centrifugation and stored in liquid nitrogen until further use.

Purification of quinoxaline oxidase

A general protein purification protocol was used with minor modifications. The protein purification took place inside the glove box because the molybdopterin cofactor is oxygen sensitive. In addition, the cell lysate was not passed through a 0.45 μm filter before loading onto the nickel-NTA column. After protein purification, the protein was stored in liquid nitrogen.

Assay conditions of the reconstitution of quinoxaline oxidase with quinoxaline-amide (Compounds 14, 27, 28)

A mixture of quinoxaline oxidase, compound (1mM), potassium ferricyanide (1 mM) in tris buffer (pH 7.5) was incubated for 6 hours at room temperature. The reaction was filter quenched and analyzed by HPLC and LC-MS.

Synthesis of 2-oxo-1,2-dihydroquinoxaline-6-carboxylic acid, 28

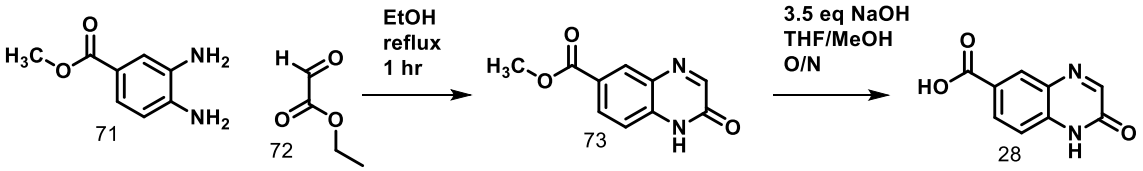

Synthesis of dihydroquinoxaline-6-carboxylate, 73

A modified procedure of patent application WO2020065613A1 was followed. Methyl 3,4-diaminobenoate (2 grams), ethyl glyoxylate (4 mL) was refluxed in methanol for 2 hours. The precipitate was collected to give the desired product.

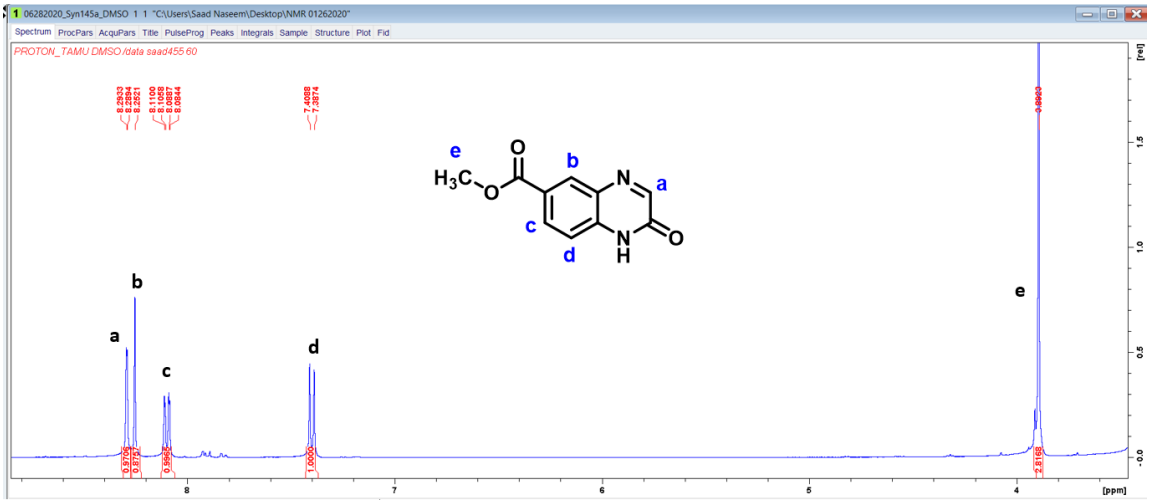

Synthesis of 2-oxo-1,2-dihydroquinoxaline-6-carboxylic acid, 28

A modified procedure of patent application WO2015161142A1 was followed. To a solution of methyl 2-oxo-1,2-dihydroquinoxaline-6-carboxylate in methanol (5 mL) and THF (5 mL) was added 3.5 equivalent of sodium hydroxide (0.24 mL of 4M NaOH) and stirred overnight at room temperature. The mixture was quenched with 1N HCl aqueous to bring the pH of the solution to 2-3. The precipitate was collected by vacuum filtration and washed with methanol, and dried to give the desired product.

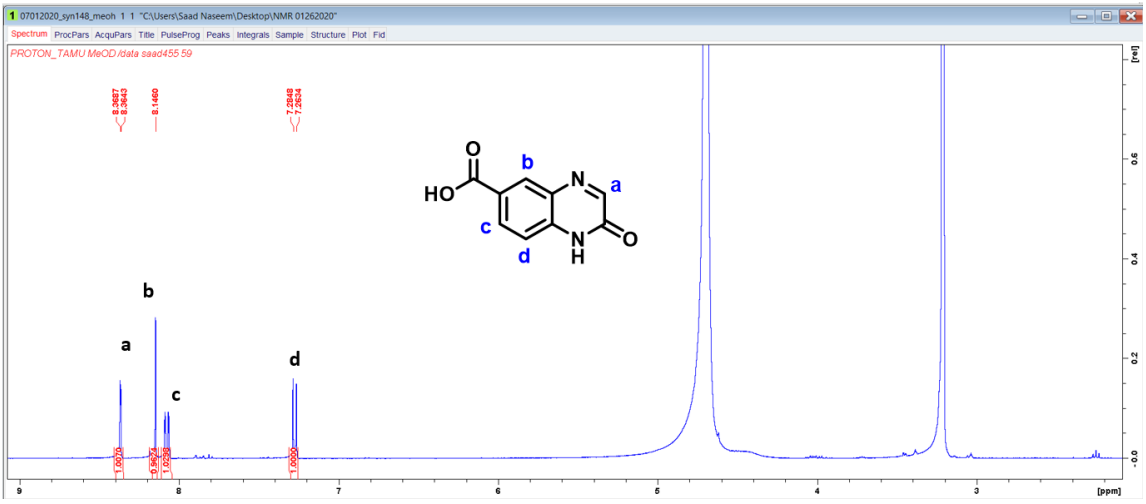

CHAPTER V

DISCOVERY AND RECONSTITUTION OF LUMICHROME MONOOXYGENASE INVOLVED IN HYDROXYLATION OF LUMICHROME

Introduction

Functional characterization of quinoxaline dioxygenase revealed that only the carboxy-quinoxaline-diamide **43** is its substrate. It raises two questions (I) which enzymes are responsible for the oxidation of methyl to carboxylic acid? (II) where in the catabolic sequence is the carboxy group introduced? (Figure V.1) Our previous work shows that thiamin pyrophosphate-dependent carboxyquinoxaline decarboxylase and quinoxaline oxidase can catalyze reaction on carboxy-substrate analogs (Figure IV.6, Figure IV.7).

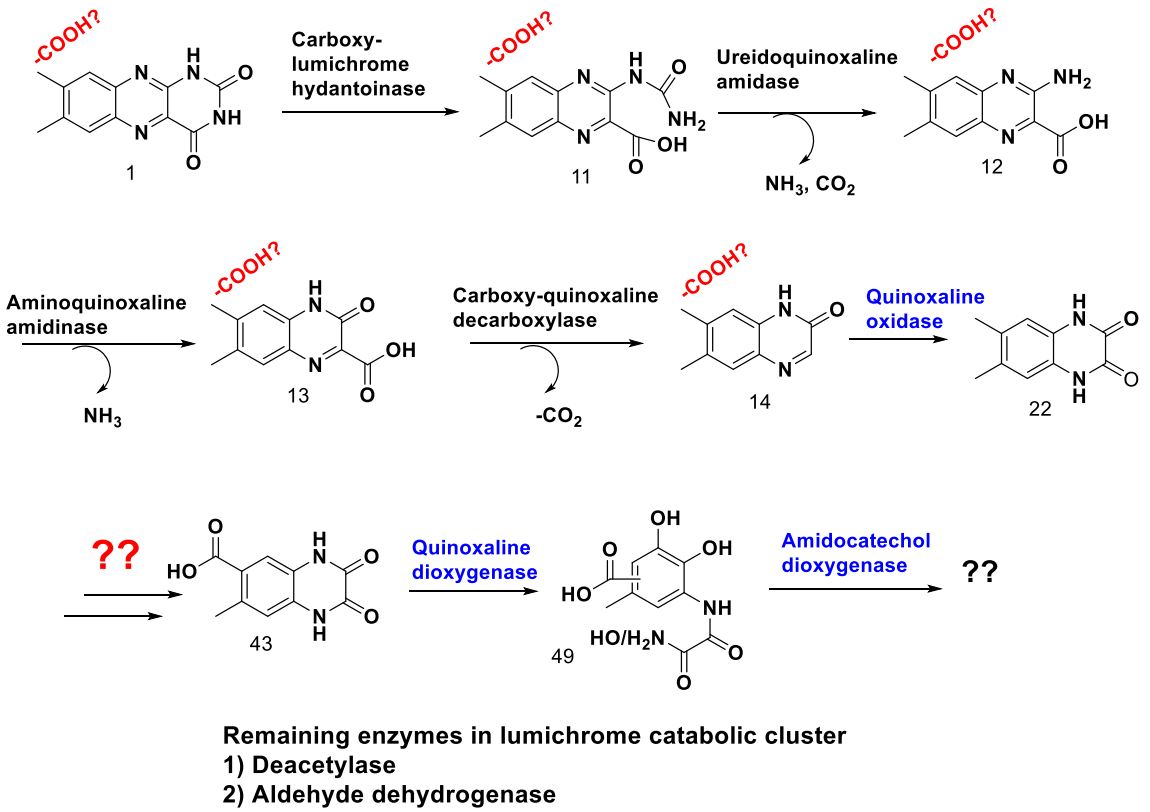

Figure V.1: Summary of progress and questions in the lumichrome catabolic cluster. We have successfully shown the activity of carboxy-lumichrome hydantoinase, Ureidoquinoxaline amidase, aminoquinoxaline amidinase, TPP-carboxyquinoxaline decarboxylase, quinoxaline oxidase, quinoxaline dioxygenase, and amidocatechol dioxygenase. The critical question is to discover the enzyme(s) responsible for the oxidation of methyl and identify their substrate.

Results and Discussion

Discovery of lumichrome monooxygenase and NDMA-dependent hydroxymethyl-lumichrome oxidase

Nature will have to use a flavin or metal-dependent monooxygenase to oxidize the methyl group. EFI-EST/GNT tools were used to discover a cytochrome P450 (lumichrome monooxygenase) and an N,N-dimethyl-4-nitrosoaniline-dependent alcohol dehydrogenase (NDMA-hydroxymethyl-lumichrome oxidase) located further away from

the lumichrome catabolic cluster in *Pimelobacter simplex* (Figure V.2). The two enzymes were also present in other organisms (*Nocardioides nitrophenolious*, *Nocardiodes Soli*) with a putative lumichrome catabolic cluster.

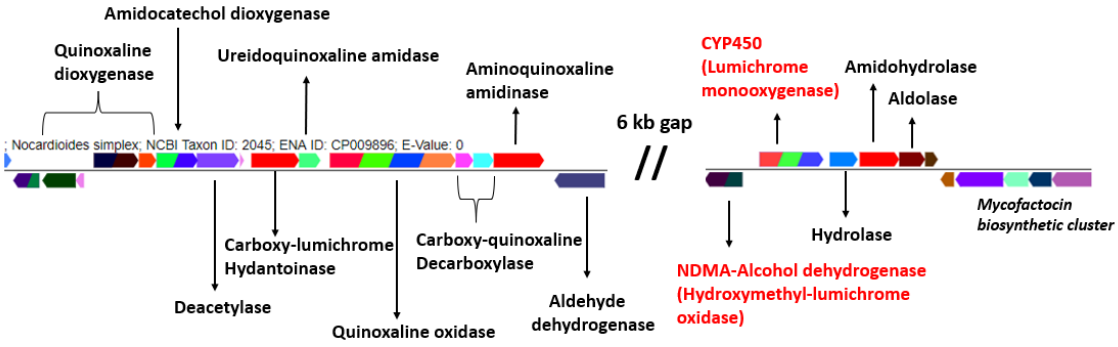

Figure V.2: Discovery of lumichrome monooxygenase and hydroxymethyl-lumichrome oxidase. The complete catabolic cluster of lumichrome in *Pimelobacter Simplex*.

Mechanistic hypothesis for the oxidation of methyl to carboxylic acid

We propose that lumichrome monooxygenase will hydroxylate the substrate **74**, followed by oxidation to aldehyde **76** by hydroxymethyl-lumichrome oxidase, and subsequently, the aldehyde dehydrogenase will form a carboxylic acid **77** (Figure V.3).

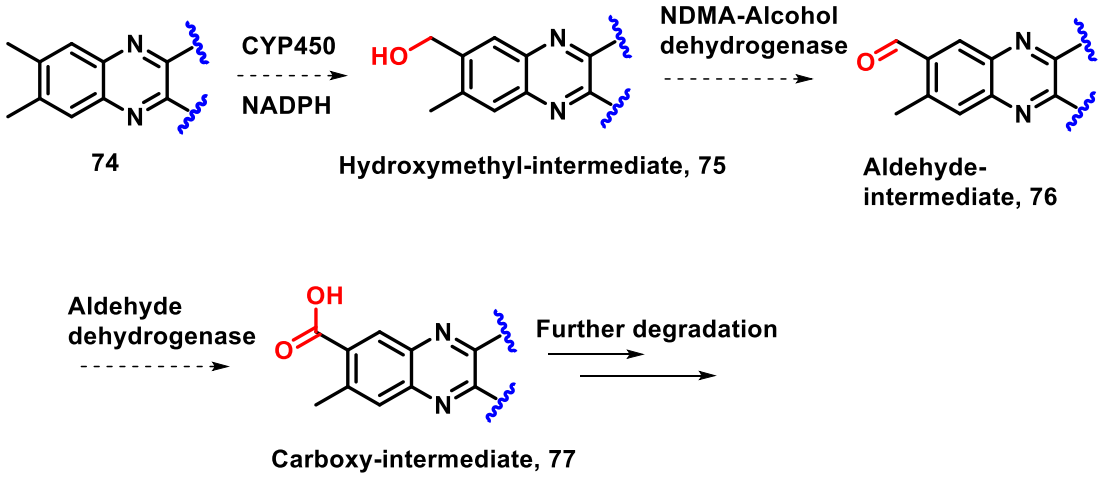

Figure V.3: Proposal for formation of carboxy-intermediate within the lumichrome catabolic cluster.

'Self-sufficient' Lumichrome monooxygenase enzyme

Cytochrome P450 enzymes usually require reducing partners to provide electrons for forming the iron(IV)-oxo cofactor. Iron(IV)-oxo is the reactive species that carry out hydrogen atom abstraction, followed by a rebound to hydroxylate the substrate. Using the NCBI domain search of lumichrome monooxygenase, I found the gene has an N-terminal heme binding site, FMN reductase domain, and ferredoxin domain with [2Fe-2S] cluster binding site (Figure V.4). The discovered lumichrome monooxygenase would not require any external reducing partner proteins; therefore, it is named a 'self-sufficient' lumichrome monooxygenase enzyme[13-14].

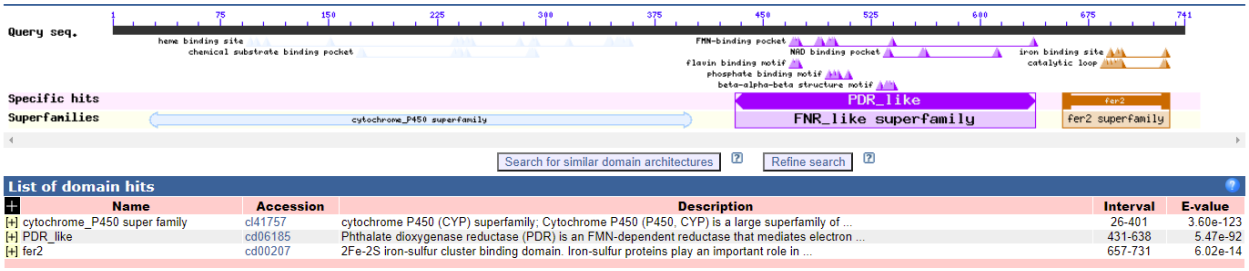

Figure V.4: Domain search of lumichrome monooxygenase in *Pimelobacter simplex*. The domain search shows an N-terminal cytochrome P450 heme binding site, followed by FMN-dependent reductase and a C-terminal ferredoxin.

Expression and purification of Lumichrome monooxygenase

The lumichrome monooxygenase gene was cloned into pTHT by Genscript and heterologously expressed in *E. coli* BL21(DE3). The expression culture (1.5 liters) was provided with 100 mg iron(II) ammonium sulfate, 100 mg L-cysteine, and 1 mM d-aminolevulinic acid to increase the biosynthesis of [2Fe-2S] cluster and heme in *E. coli*. The N-terminally His-tagged protein was purified by Ni-NTA affinity chromatography (Figure V.5).

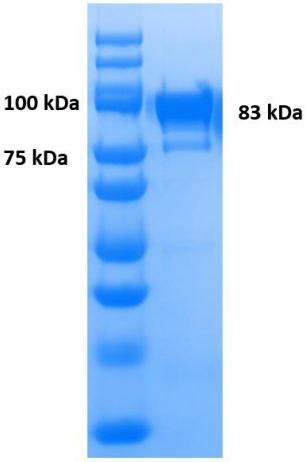

Figure V.5: SDS-PAGE of a lumichrome monooxygenase. The molecular weight of lumichrome monooxygenase is 83 kDa.

Activity assay of lumichrome monooxygenase with lumichrome

The assay contains lumichrome monooxygenase enzyme (50 uM), lumichrome (~1 mM), and NAD(P)H (1 mM). The reaction is filter quenched after 6 hours and analyzed on HPLC and LC-MS. All the intermediates of the lumichrome catabolic pathway were tested as substrates for the lumichrome monooxygenase enzyme (Figure V.6). Lumichrome, as a substrate to lumichrome monooxygenase, formed a new peak at 26 minutes on HPLC. A time-dependent increase of the product and consumption of NADPH is demonstrated (Figure V.7). The new peak has a mass of [M-H]= 257.0680 m/z. The mass corresponds to hydroxymethyl-lumichrome **78**; the position of hydroxy could not be confirmed by LC-MS alone.

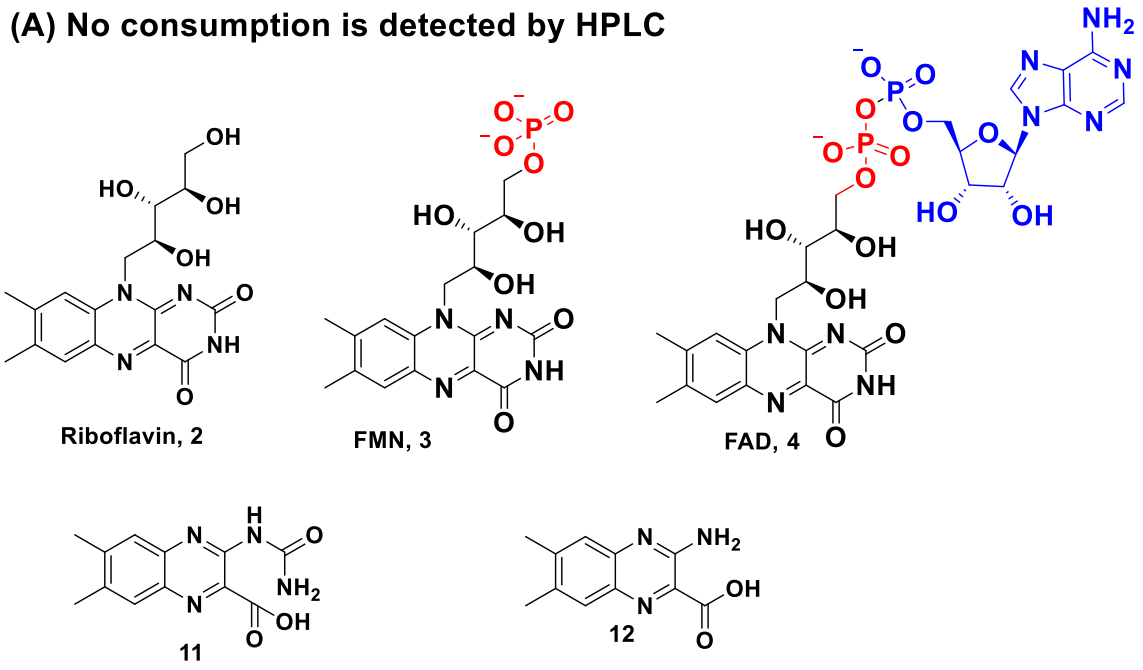

Figure V.6: The following compounds were tested for activity with lumichrome monooxygenase.

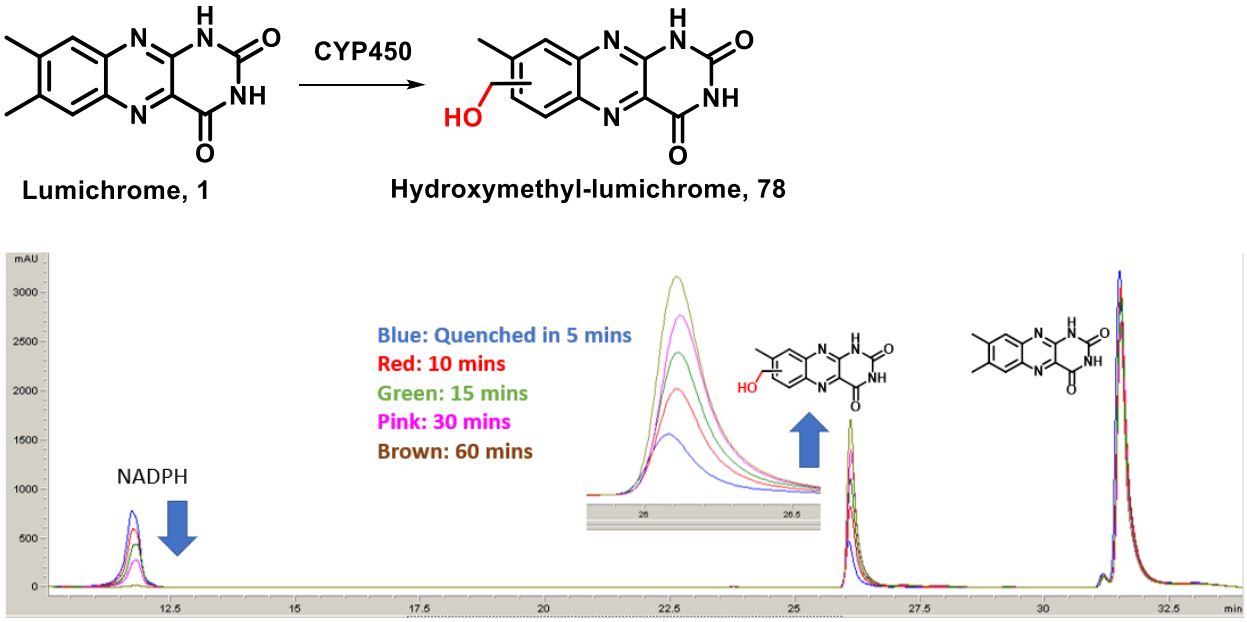

Figure V.7: Reconstitution of lumichrome monooxygenase. HPLC chromatogram shows a time-dependent increase of a new peak at 26 minutes.

Comparison of NADH and NADPH as a reducing agent

Lumichrome monooxygenase is active with both NADH and NADPH as reducing agents. The native reducing agent is determined by comparing product formation with NADH and NADPH as reducing agents. The reactions were heat quenched in 10 minutes and analyzed by HPLC. NADH as a reducing agent leads to higher product formation; therefore, NADH is more likely to be a physiological reducing agent for lumichrome monooxygenase.

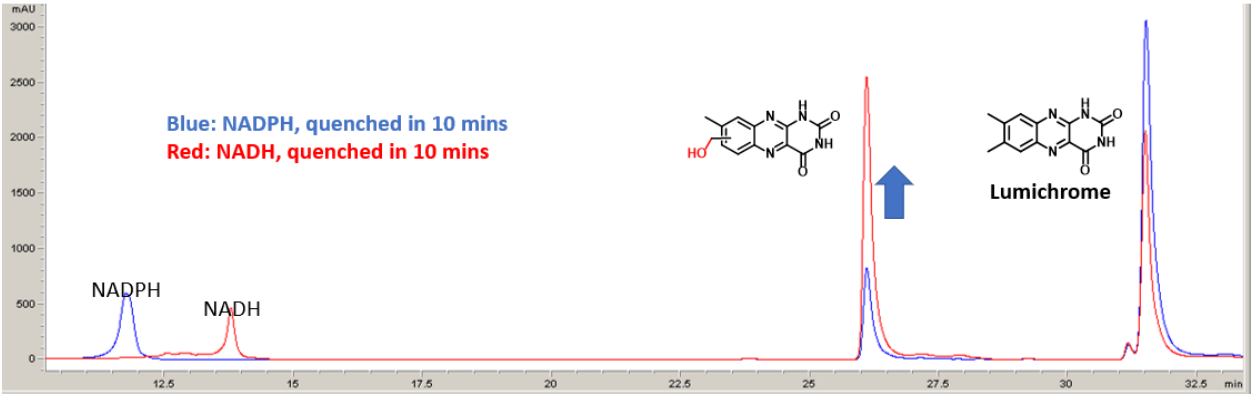

Figure V.8: Yield of product formation by NADH and NADPH. Higher product formation is observed with NADH as a reducing agent (red) than NADPH (blue).

Overnight incubation with excess reducing agent:

Interestingly, an overnight incubation of lumichrome, lumichrome monooxygenase, NAD(P)H, NAD(P)H regeneration system (glucose-6-phosphate, glucose-6-phosphate dehydrogenase) formed 3 new peaks (14.8 mins, 26.0 mins, and 28.0 mins) on the HPLC chromatogram (Figure V.9). The 3 peaks have a UV spectra similar to lumichrome, and the LC-MS suggests that peak 1 has a mass of [M-H]=271.0472 m/z, peak 2 has [M-H]=257.0680 m/z, and peak 3 has [M-H]=255.0523 m/z. The mass of three peaks corresponds to carboxy-lumichrome **80**, hydroxymethyl-lumichrome **78**, and aldehyde-lumichrome **79**, respectively. The regiochemistry of the oxidation on the C7 or C8 methyl is not yet known.

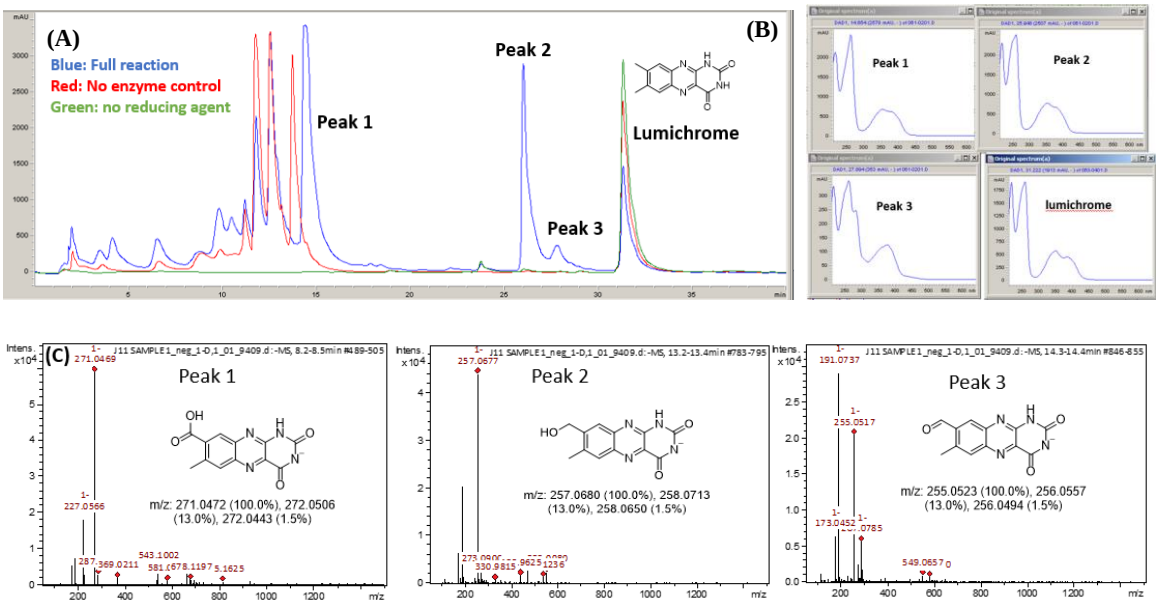

Figure V.9: Overnight reaction of lumichrome monooxygenase with lumichrome forms three new peaks in the full reaction. The UV-vis and LC-MS suggest that peak 1 is carboxy-lumichrome **80**, peak 2 is hydroxymethyl-lumichrome **78**, and peak 3 is aldehyde-lumichrome **79**.

Mechanistic proposal for the over-oxidation of lumichrome

The over-oxidation of lumichrome by lumichrome monooxygenase enzyme supports multiple catalytic turnovers when incubated for long hours in the presence of an excess reducing agent.

Conclusion

I have discovered a 'self-sufficient' lumichrome monooxygenase and NDMA-dependant hydroxymethyl-lumichrome oxidase in *Pimelobacter simplex*. Lumichrome monooxygenase enzyme is reconstituted with lumichrome as a substrate, and a product with mass corresponding to hydroxymethyl-lumichrome **78** is detected. Next, we would

like to investigate the enzymes responsible for converting 7-(or 8)-hydroxy-lumichrome (**78**) to 7-(or 8)-carboxy-lumichrome (**80**).

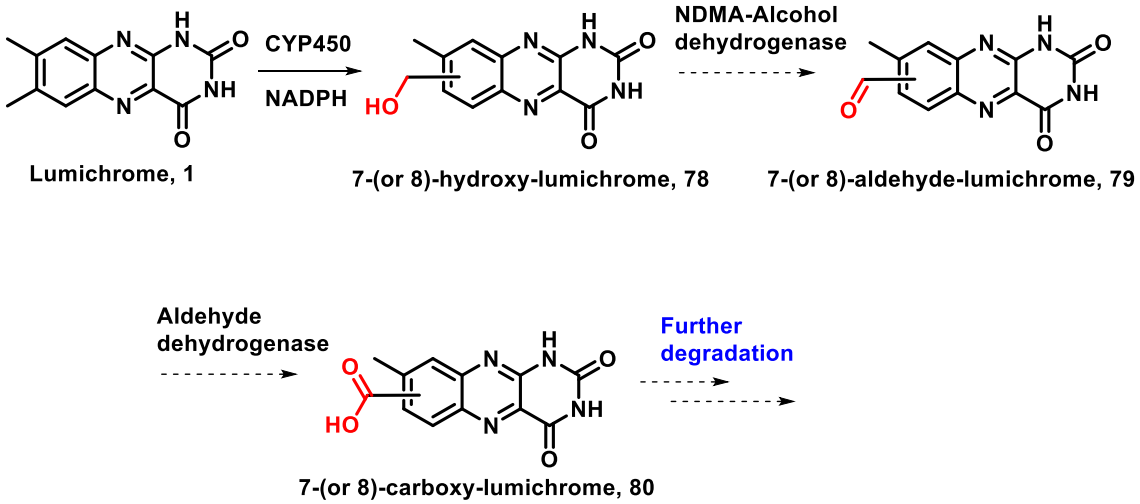

Figure V.10: Proposal for the introduction of carboxylic acid on lumichrome in *Pimelobacter simplex*.

Experimental procedure:

Assay condition of lumichrome monooxygenase to over oxidize hydroxy-lumichrome

The assay conditions were; lumichrome monooxygenase (100 μM), lumichrome (1-2 mM), NADPH (1 mM), and NADPH regeneration system (10 mM glucose-6-phosphate, 1 unit glucose-6-phosphate dehydrogenase) in potassium phosphate buffer (pH 7.5).

CHAPTER VI

FUNCTIONAL CHARACTERIZATION OF N,N-DIMETHYL-4-NITROSOANILINE (NDMA)-DEPENDENT HYDROXYMETHYL-LUMICHROME OXIDASE

Introduction

Lumichrome monooxygenase can hydroxylate the C7 or C8 methyl of lumichrome. We propose that an hydroxymethyl-lumichrome oxidase transforms the alcohol (**78**) to an aldehyde (**79**), followed by aldehyde dehydrogenase to further oxidize to carboxy-lumichrome (**80**).

Adjacent to lumichrome monooxygenase, I discovered a gene annotated as N,N-dimethyl-4-nitrosoaniline (NDMA)-dependent alcohol dehydrogenase that usually oxidizes alcohol to an aldehyde (Figure V.2). These are zinc(II) containing enzymes with a tightly bound NAD(H) that does not dissociate during the catalytic cycle. Instead, a second substrate (NDMA, **81**) acts as an external redox partner and regenerates the cofactor (NAD) for multiple turnovers[15].

NDMA-hydroxymethyl-lumichrome oxidase is proposed to oxidize the hydroxymethyl-lumichrome **78** to an aldehyde-lumichrome **79** (Figure VI.1). During catalysis, a hydride transfer from substrate to NAD will form NADH and an aldehyde-lumichrome (**79**). The non-exchangeable cofactor, NADH, will be oxidized to NAD^+ by the external redox partner N,N-dimethyl-4-nitrosoaniline (NDMA, **81**).

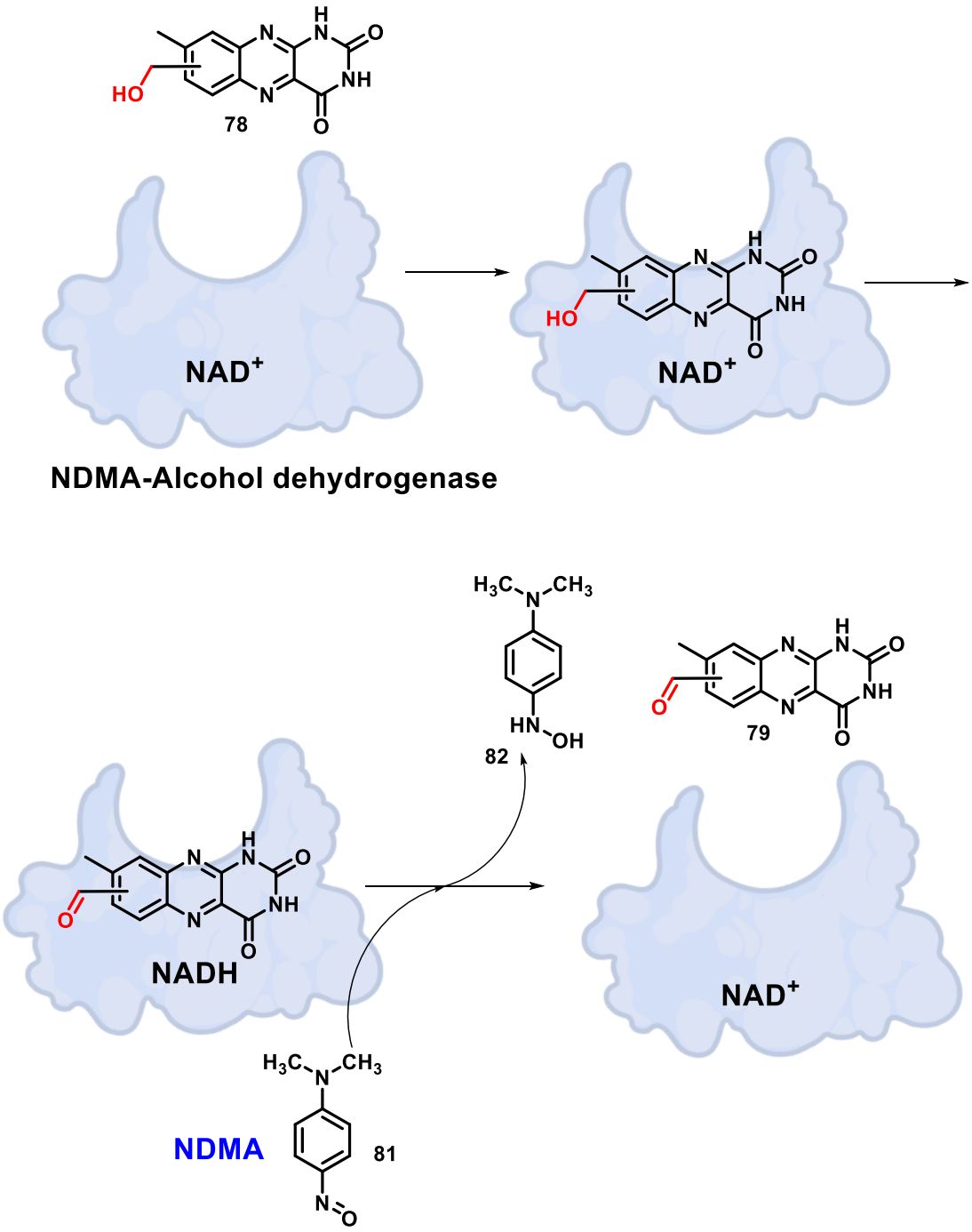

Figure VI.1: The proposed catalytic cycle of NDMA-dependent hydroxymethyl-lumichrome oxidase. The NAD(H) cofactor is non-exchangeable and will remain inside the active site. Meanwhile, NDMA will act as an external oxidizing agent.

Results and Discussion

Overexpression and purification of NDMA-Hydroxymethyl-lumichrome oxidase

The gene was synthesized and cloned into a pETDuet vector by Genscript. The plasmid was overexpressed in BL21(DE3) and loaded onto nickel affinity chromatography but eluted an impure protein. To improve the solubility and purity of eluted protein, it was co-expressed with chaperone proteins (GroEL-GroES), but there was no improvement in the purity of the eluted protein. Then the gene was subcloned using Gibson assembly into pMAL-c2E-TEV vector (derivative of pMAL-c2E vector, courtesy James Sacchettini lab) with a maltose-binding protein fusion tag on the N-terminal of the enzyme. Expression and purification resulted in pure NDMA-hydroxymethyl-lumichrome oxidase (Figure VI.2).

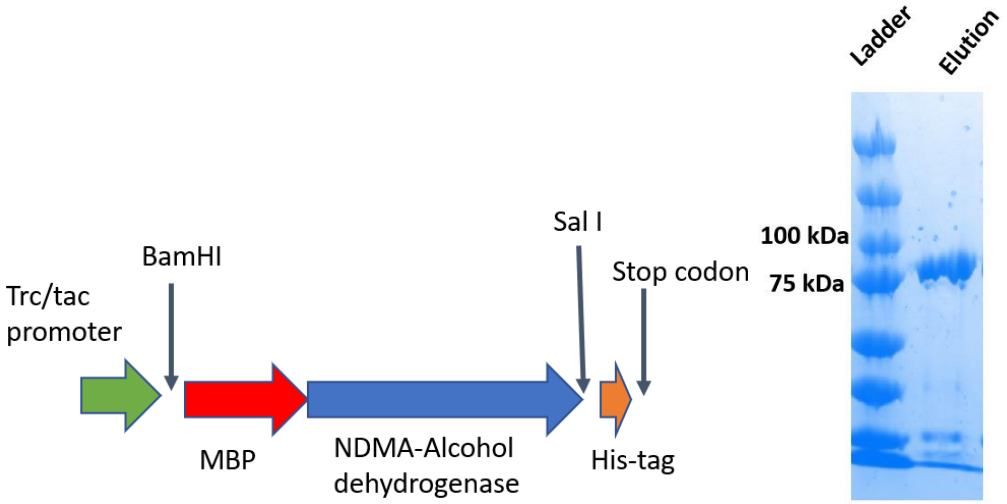

Figure VI.2: Cloning and purification of hydroxymethyl-lumichrome oxidase. The design of the construct with NDMA- hydroxymethyl-lumichrome oxidase has an N-terminal maltose-binding protein fusion tag, and the C-terminal has a His-tag. The SDS-PAGE of 84 kDa maltose-binding protein-tagged NDMA- hydroxymethyl-lumichrome oxidase.

NAD(H) bound NDMA-Hydroxymethyl-lumichrome oxidase

Usually, enzymes come bound with cofactors. The physiological cofactor of NDMA-hydroxymethyl-lumichrome oxidase was determined by analyzing heat-quenched enzyme on HPLC. The NDMA-hydroxymethyl-lumichrome oxidase comes bound with NAD and NADH.

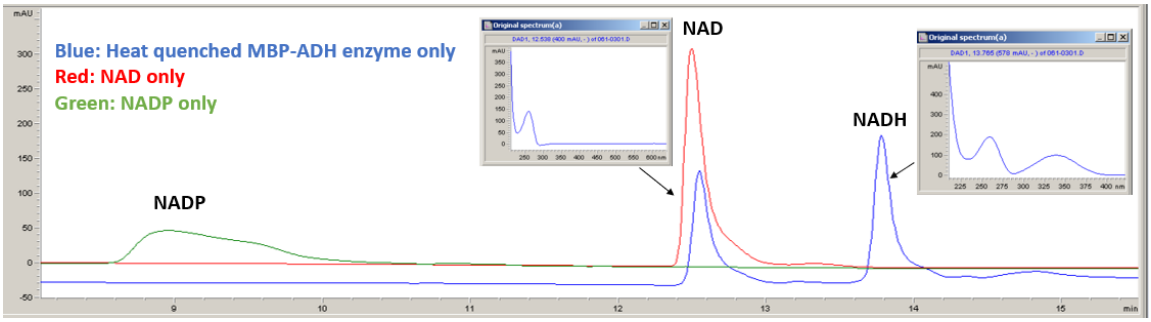

Figure VI.3: HPLC chromatogram at 254 nm of heat quenched NDMA-hydroxymethyl-lumichrome oxidase. The enzyme comes bound with NAD (12.5 mins) and NADH (13.8 mins).

Reconstitution of NDMA-dependent hydroxymethyl-lumichrome oxidase

The NDMA-hydroxymethyl-lumichrome oxidase catalyzed reaction was reconstituted by a coupled reaction with lumichrome and lumichrome monooxygenase. Lumichrome (~1mM), NADH (2mM), and lumichrome monooxygenase (50uM) were incubated in potassium phosphate buffer pH 7.5 at 25 °C for 3 hours. After the filter quench, NDMA-hydroxymethyl-lumichrome oxidase (50 uM), NDMA (1 mM) were added, and the reaction mixture was analyzed by HPLC and LCMS after 3 hours.

NDMA-hydroxymethyl-lumichrome oxidase consumes hydroxymethyl-lumichrome **78** (26.5 mins), and a new peak at 14.8 mins was detected on HPLC. The new

peak has a mass of [M-H]=271.0472 corresponding to carboxy-lumichrome **80**. HPLC and LC-MS did not detect aldehyde-lumichrome **79**. The NDMA-hydroxymethyl-lumichrome oxidase is carrying out two catalytic turnovers by oxidizing hydroxy-lumichrome to aldehyde-lumichrome and then carboxy-lumichrome (**80**) (Figure VI.4).

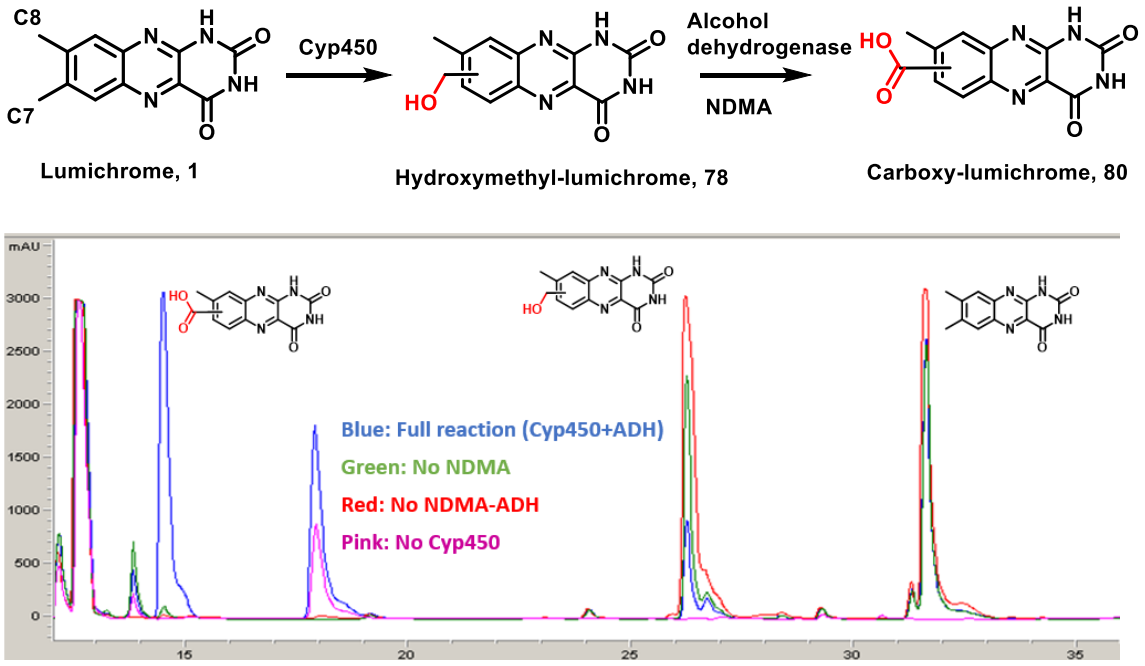

Figure VI.4: Coupled assay of lumichrome with lumichrome monooxygenase and NDMA-hydroxymethyl-lumichrome oxidase. lumichrome monooxygenase catalyzed hydroxylation of lumichrome to form hydroxymethyl-lumichrome (**78**) at 26.5 mins. A coupled assay with NDMA-hydroxymethyl-lumichrome oxidase consumes the hydroxy-lumichrome at 26.5 mins and a new peak at 14.8 mins is detected. The mass suggest that the peak at 14.8 mins is carboxy-lumichrome (**80**).

NDMA as an oxidizing agent

Many oxidizing agents and electron carriers (phenazine methosulfate, cytochrome C, methyl viologen, potassium ferricyanide, and dichlorophenolindophenol (DCIP)) were screened for the activity of NDMA-hydroxymethyl-lumichrome oxidase. Only NDMA

and DCIP showed product formation. Amongst DCIP and NDMA, NDMA as an electron acceptor resulted in higher product formation (Figure VI.5).

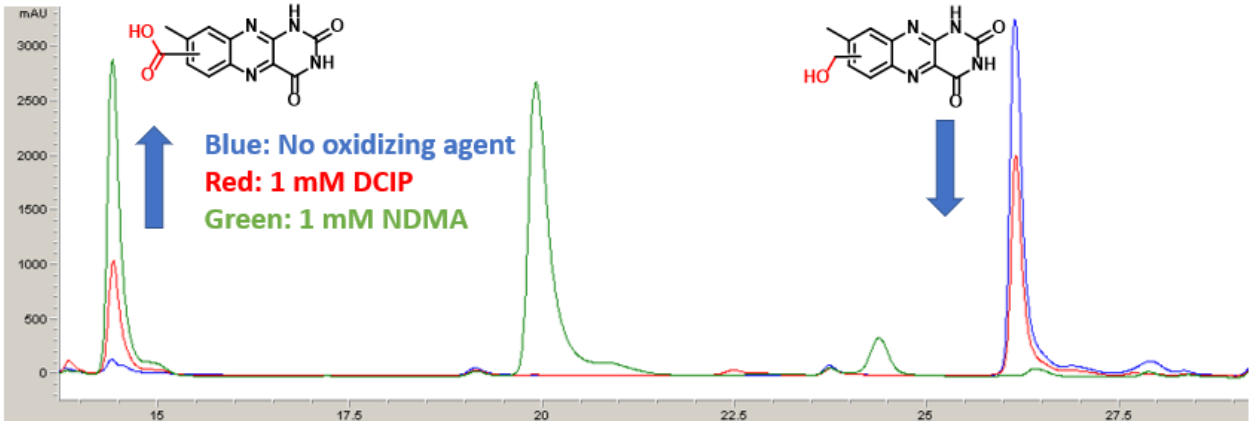

Figure VI.5: HPLC chromatogram of NDMA-hydroxymethyl-lumichrome oxidase reaction using DCIP (red) and NDMA (green) as an oxidizing agent. NDMA results in higher product formation than DCIP.

Mechanistic proposal of NDMA-hydroxymethyl-lumichrome oxidase:

The NDMA-hydroxymethyl-lumichrome oxidase carries out two catalytic turnovers to oxidize hydroxymethyl-lumichrome **78** to carboxy-lumichrome **80** at the expense of two molecules of NDMA. The aldehyde-lumichrome **79** intermediate remains tightly bound inside the enzyme and does not leak out (

Figure VI.6).

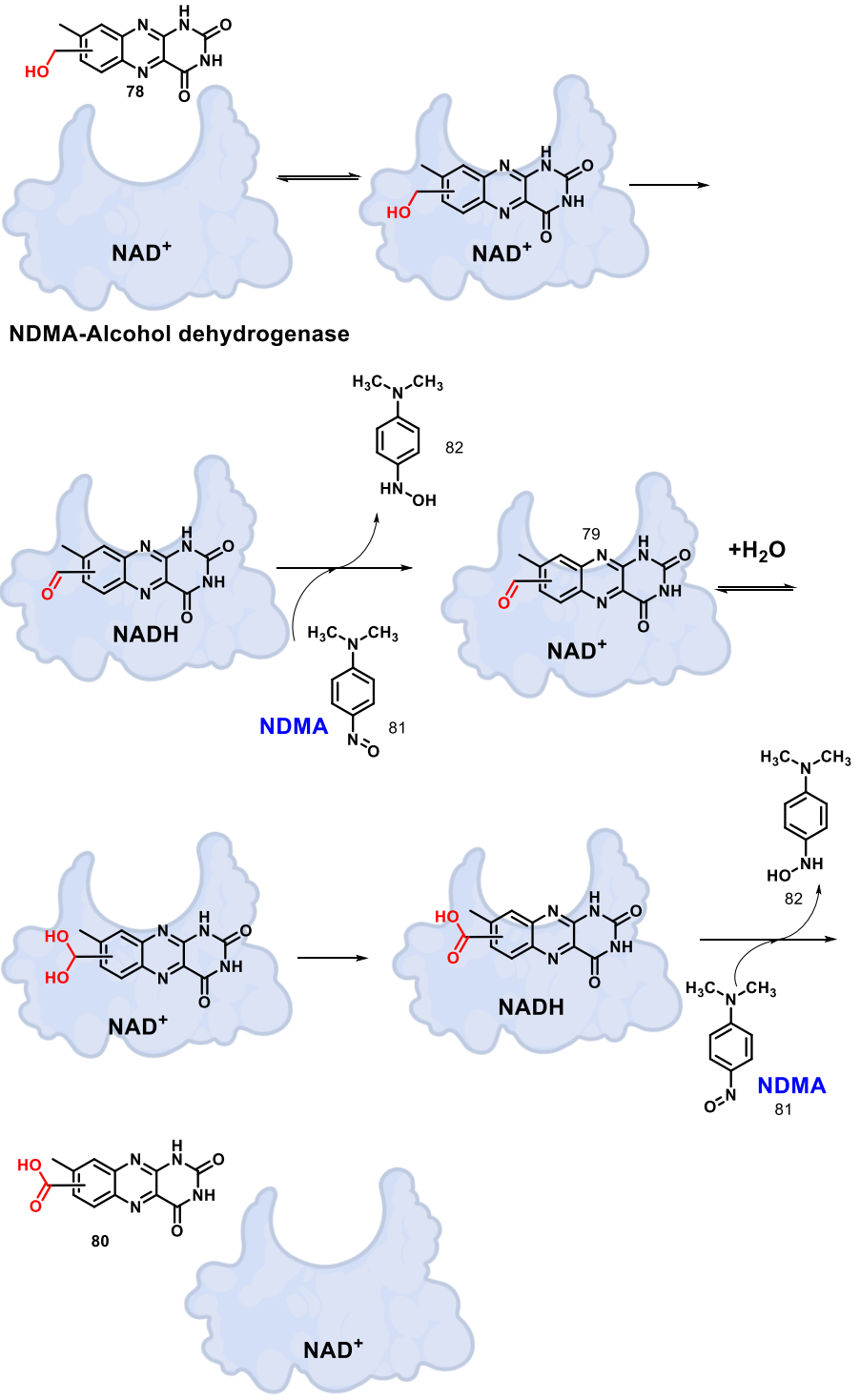

Figure VI.6: Mechanistic proposal for the NDMA-dependent hydroxymethyl-lumichrome oxidase catalyzed reaction.

Aldehyde-lumichrome (**79**) is proposed as an intermediate of the reaction. The proposal was tested by feeding aldehyde-lumichrome **79** to NDMA-hydroxymethyl-lumichrome oxidase. Total consumption of aldehyde-lumichrome was observed, and a peak corresponding to carboxy-lumichrome (**80**) was detected (Figure VI.7). This shows that the enzyme can bind the intermediate aldehyde and further oxidize it to an acid.

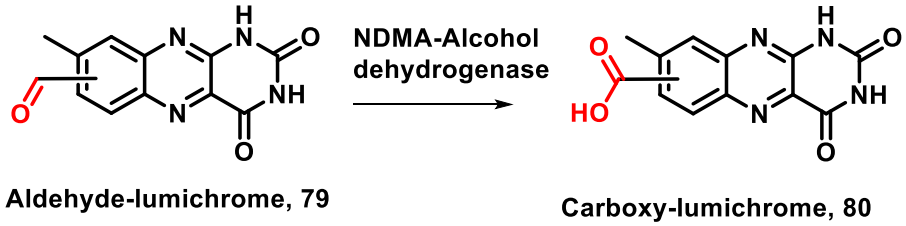

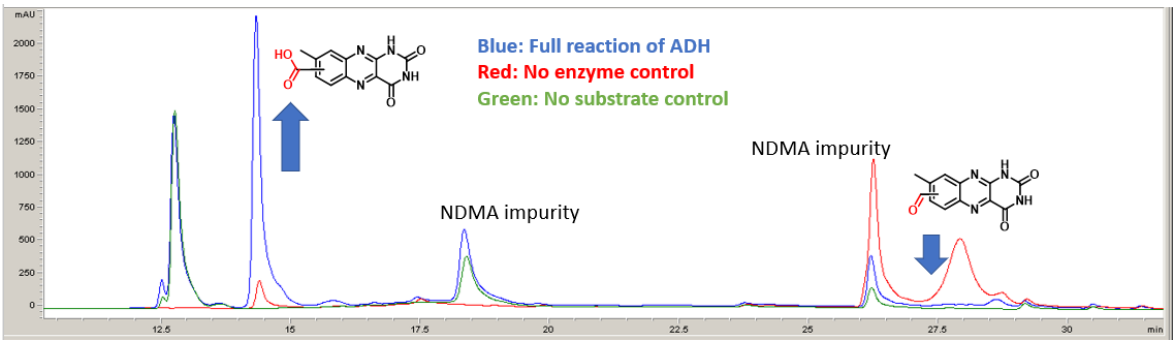

Figure VI.7: Feeding of aldehyde-intermediate to NDMA-hydroxymethyl-lumichrome oxidase. Aldehyde-lumichrome is tested as a substrate for NDMA-hydroxymethyl-lumichrome oxidase. Total consumption of aldehyde-lumichrome and a peak corresponding to carboxy-lumichrome (**80**) (14.8 mins) is detected.

Physiological electron acceptor for NDMA-hydroxymethyl-lumichrome oxidase

I have reconstituted the activity of NDMA-hydroxymethyl-lumichrome oxidase using an artificial electron acceptor, NDMA. To determine the physiological electron acceptor of the enzyme, I searched for the biosynthetic genes of electron carrier molecules in the neighborhood of lumichrome catabolic genes. Besides the lumichrome catabolic

cluster, I discovered the mycofactocin biosynthetic gene cluster. The neighboring genes are annotated as MftA, MftB, MftE, MftD, and MftF involved in mycofactocin biosynthetic pathway (Figure VI.8). There is literature precedence that mycofactocin is an electron carrier for mycobacterial dehydrogenases with non-exchangeable NAD cofactors[16-17].

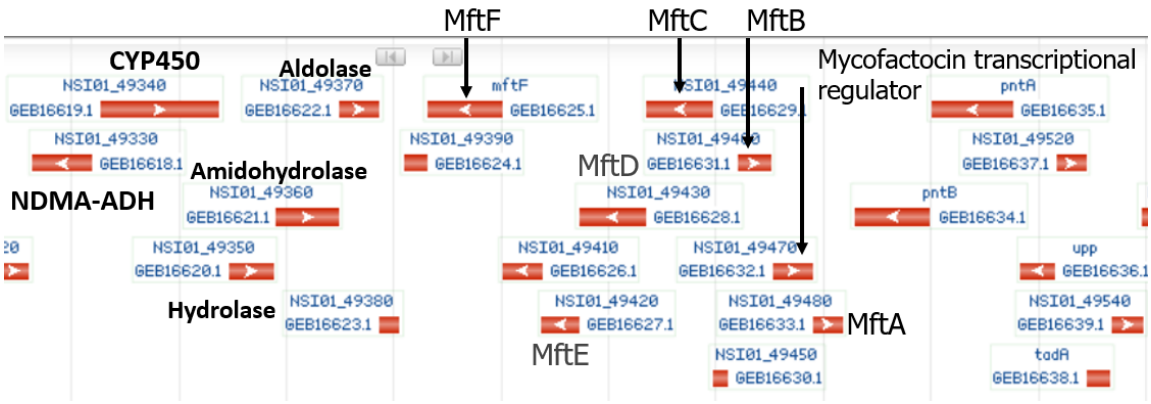

Figure VI.8: Neighboring mycofactocin biosynthetic gene cluster. The neighboring genes of NDMA-hydroxymethyl-lumichrome oxidase and lumichrome monooxygenase are annotated as MftABDEF involved in the mycofactocin biosynthetic pathway.

Characterization of the product of Hydroxymethyl-lumichrome oxidase

LC-MS data suggests the lumichrome monooxygenase catalyzes hydroxylation on the methyl (C8 or C7) of lumichrome, and NDMA-hydroxymethyl-lumichrome oxidase further oxidizes to carboxy-lumichrome (**80**)(Figure VI.9). The exact position of oxidation (C8 or C7) could not be determined by LC-MS alone. I synthesized the carboxy-lumichrome standard and analyzed it on HPLC to confirm the assignment of oxidation on lumichrome in the catabolic pathway.

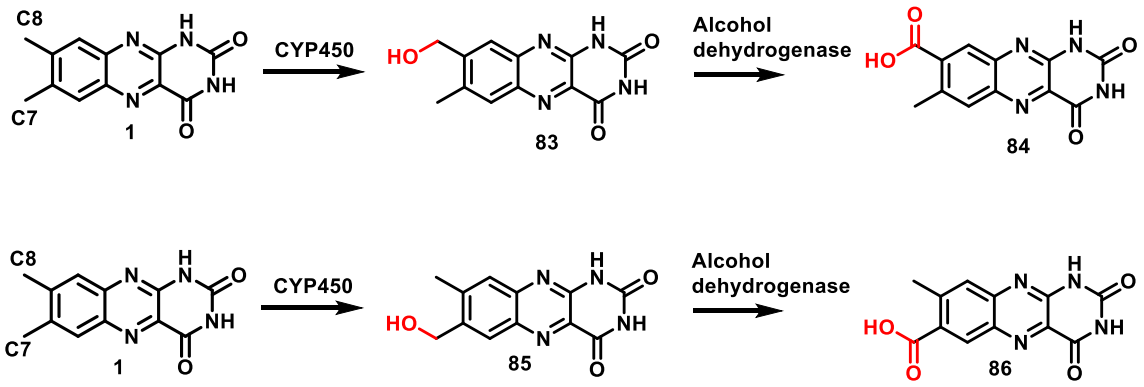

Figure VI.9: Two possibilities of regioisomers. The oxidation may occur on C8 or C7 position of lumichrome.

First, a mixture of 7-carboxy-lumichrome **86** and 8-carboxy-lumichrome **84** was synthesized and found to separate sufficiently on a C18 reverse-phase HPLC column (Figure VI.11). Then the synthetic standard of 7-carboxy-lumichrome **86** was synthesized and overlayed with the native enzymatic reaction of lumichrome monooxygenase and NDMA-hydroxymethyl-lumichrome oxidase. The retention time on HPLC and UV spectra were identical for the 7-carboxy-lumichrome **86** synthetic standard, and the product of coupled NDMA-hydroxymethyl-lumichrome oxidase and lumichrome monooxygenase catalyzed reaction with lumichrome (Figure VI.10).

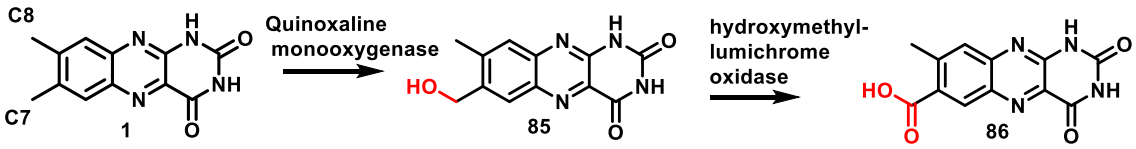

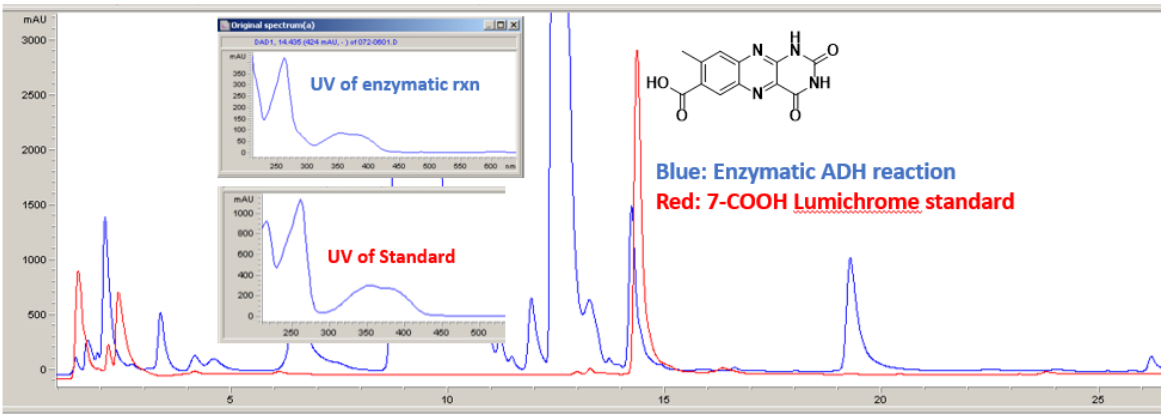

Figure VI.10: Overlay of 7-carboxy-lumichrome **86** standard and NDMA-hydroxymethyl-lumichrome oxidase enzymatic reaction. The enzymatic reaction has a product peak at 14.8 mins with the same retention time to 7-carboxy-lumichrome synthetic standard **86**.

Conclusion

Using EFI-EST/GNT tools, I discovered a lumichrome monooxygenase and NDMA-hydroxymethyl-lumichrome oxidase involved in the lumichrome catabolic pathway. NDMA-hydroxymethyl-lumichrome oxidase carries out two catalytic turnovers to oxidize hydroxy-lumichrome to 7-carboxy-lumichrome (**86**). The position of oxidation on lumichrome is confirmed by comparing retention time on HPLC with the 7-carboxy-lumichrome synthetic standard and native enzymatic reaction.

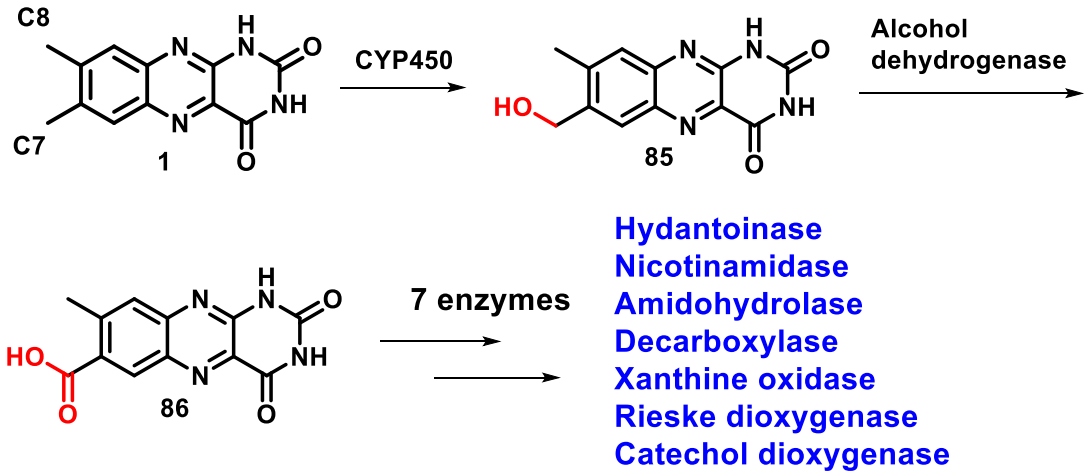

Experimental procedure

Cloning of NDMA-dependent hydroxymethyl-lumichrome oxidase into pMAL-c2E-TEV vector

General Gibson assembly protocol was followed.

Synthesis of the mixture of C7-carboxy-lumichrome and C8-carboxy-lumichrome, 84 & 86

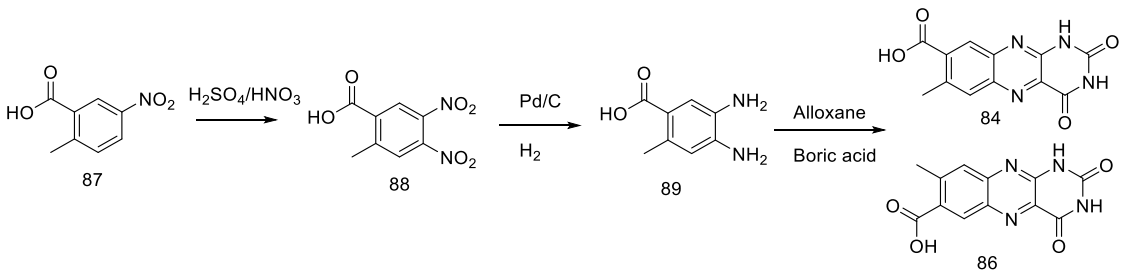

Preparation of 2-methyl-4,5-dinitrobenzoic acid, 88

The nitration was carried out by a modified procedure of S. Puvvala et al. (Synthesis 2017, 49, 2768–2774). A mixture of sulfuric acid (50 mL) and nitric acid (50 mL) was cooled in ice for 30 minutes. Next, 2-methyl-4-nitrobenzoic acid (9 grams) was added slowly while maintained under argon atmosphere. The reaction mixture was allowed to cool to room temperature and stirred overnight, and then quenched by pouring into ice-cold water. The resulting precipitate was filtered and dried to form a product. The product was used for the next reaction without further purification.

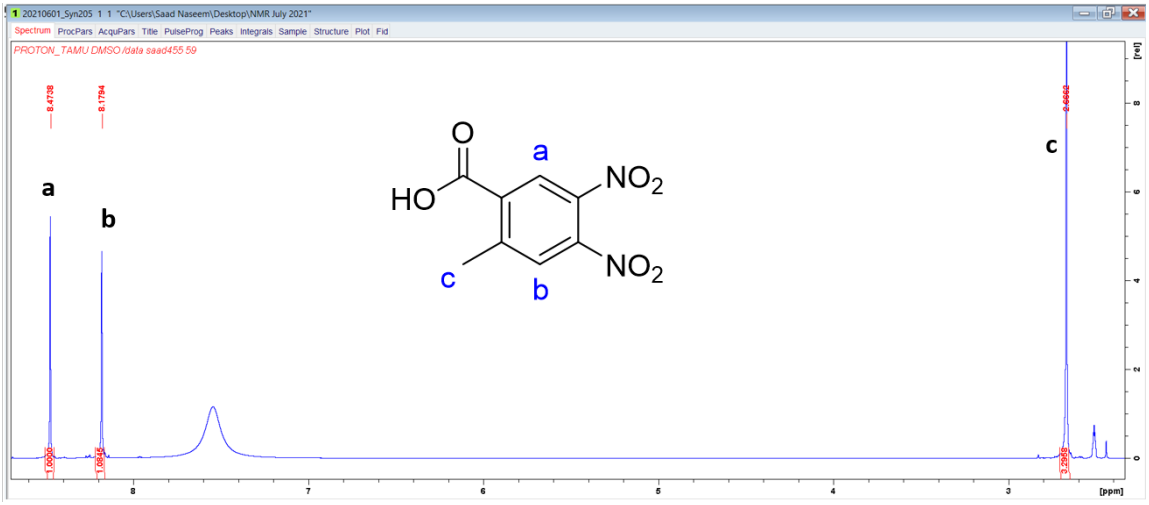

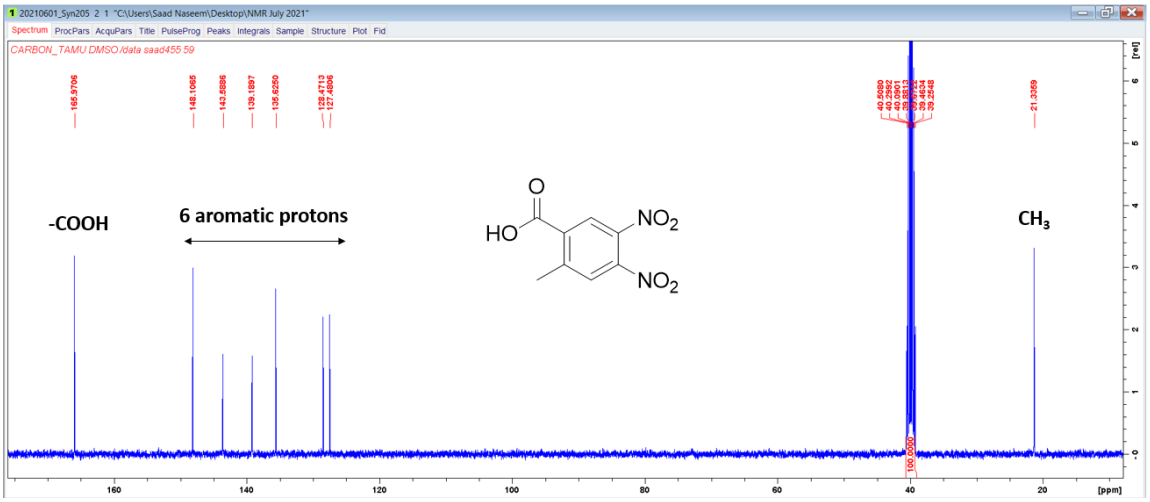

Preparation of 4,5-diamino-2-methylbenzoic acid, 89

The reduction was carried out using a modified procedure of patent WO 2012/149157. 2-methyl-4,5-dinitrobenzoic acid (2 gram) was reduced with 30% palladium/carbon, 20 mL anhydrous methanol, and hydrogen gas in a balloon. The reaction mixture was run overnight and filtered using a 0.45 uM filter. The product was of sufficient purity to carry out the subsequent reaction.

Preparation of the mixture of C7-carboxy-lumichrome and C8-carboxy-lumichrome, (84, 86)

2-methyl-4,5-diaminobenzoic acid (420 mg) was dissolved in acetic acid (20 mL), followed by alloxane (405 mg) and boric acid (157 mg). The reaction was run overnight; the mixture was filtered and washed with acetic acid and ethyl ether the next day. The product was analyzed by NMR to show 2:1 regioisomers of C8 and C7-carboxy-lumichrome.

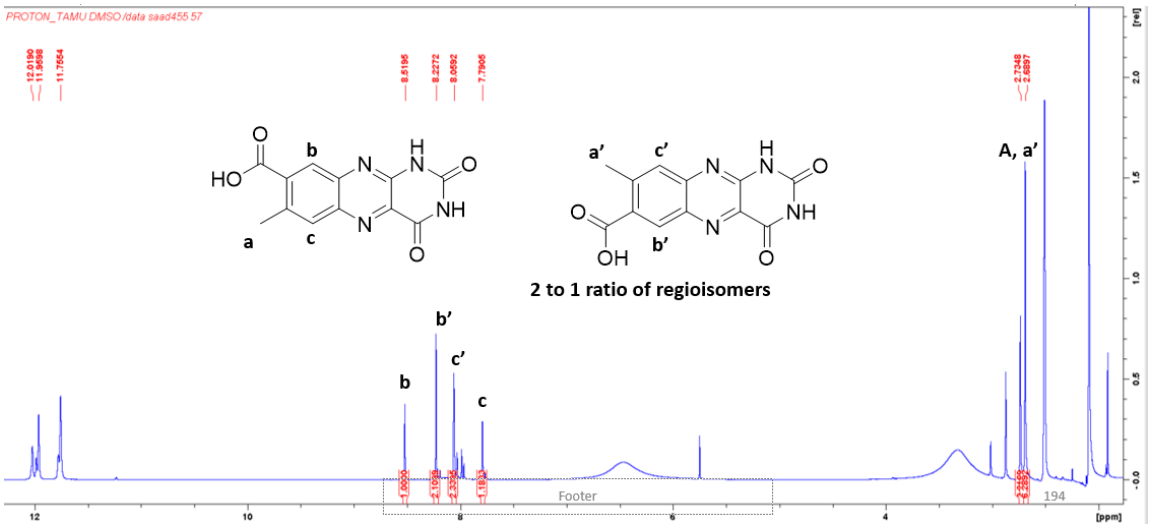

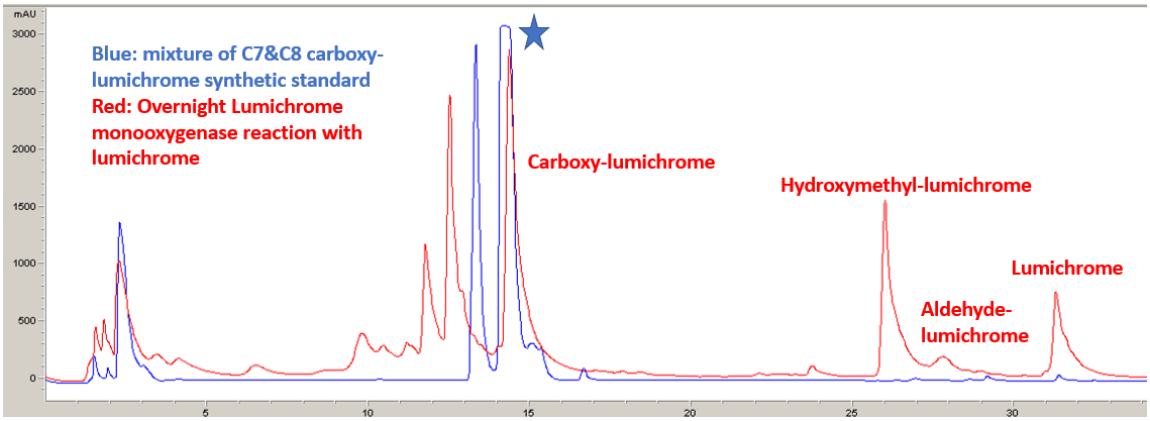

Figure VI.11: Overlay of overnight lumichrome monooxygenase reaction and the C7&C8-carboxylumichrome synthetic standards. One regioisomer in the mixture has the same retention time as the enzymatic carboxy-lumichrome product.

Synthesis of 7-carboxy-lumichrome, 86

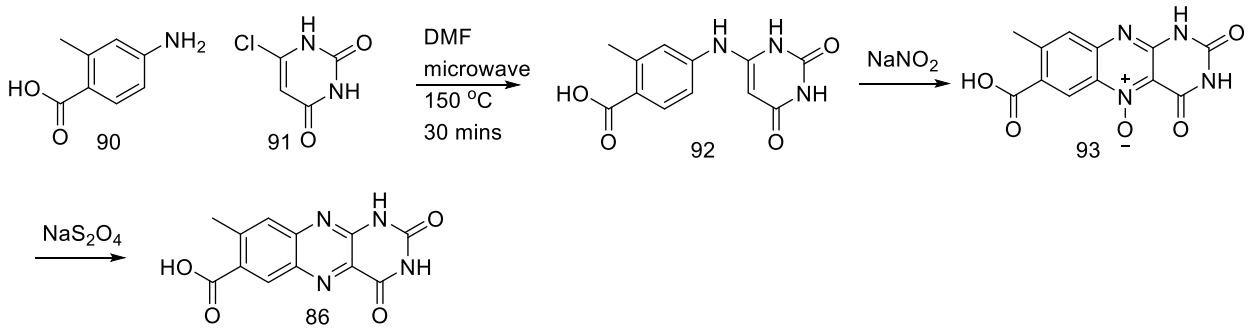

Synthesis of 4-((2,6-dioxo-1,2,3,6-tetrahydropyrimidin-4-yl)amino)-2-methylbenzoic acid, 92

A modified procedure of patent application EP2422817A1 and Chemical Communication, 2015, 51, 12036-12039 was followed. 2-methyl-4-aminobenzoic acid (500 mg), 6-chloro-uracil (242 mg) was dissolved in 2 mL of DMF. The reaction was microwaved at 150 °C for 30 mins. After cooling, the reaction was treated with ether and the crude product was isolated by centrifuge.

Synthesis of 7-carboxy-8-methyl-2,4-dioxo-1,2,3,4-tetrahydrobenzo[g]pteridine 5-oxide, 93

A modified procedure of patent application EP2422817A1 was followed. To the stirred solution of X (250 mg) in acetic acid (5 mL) at 0 °C was added sodium nitrite (332 mg) portion wise. The reaction was carried out for 2-3 hours and then filtered and washed with water.

Synthesis of 7-carboxy-lumichrome, 86

The nitroso compound (7-carboxy-8-methyl-2,4-dioxo-1,2,3,4-tetrahydrobenzo[g]pteridine 5-oxide) was reduced with dithionite (5 equivalents) in DMF for 2-3 hours. The solvent was evaporated and the leftover product was analyzed by HPLC.

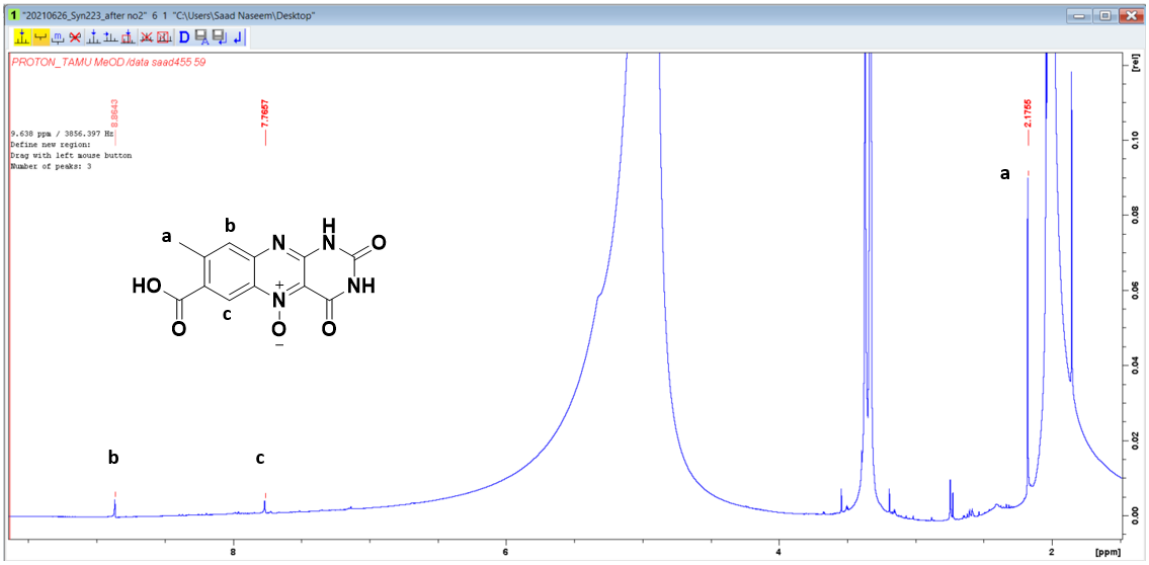

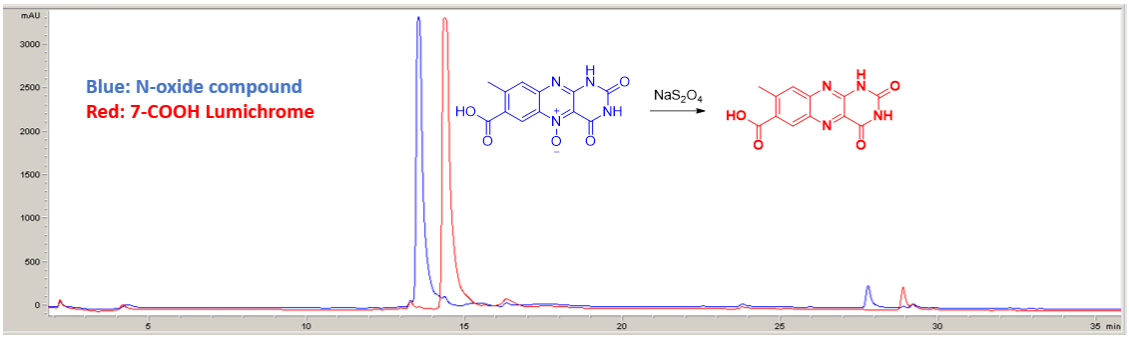

Figure VI.12: HPLC chromatogram of the dithionite reduction of 7-carboxy-nitroso-lumichrome (blue) to 7-carboxy-lumichrome (red).

CHAPTER VII

COUPLED REACTIONS OF DOWNSTREAM ENZYMES

Introduction

We successfully demonstrated that lumichrome is the substrate of lumichrome monooxygenase to form 7-hydroxymethyl-lumichrome (**85**). The 7-hydroxy-lumichrome is the substrate of NDMA-hydroxymethyl-lumichrome oxidase and forms the corresponding 7-carboxy-lumichrome (**86**). To support the relevance of these reactions in the lumichrome catabolic pathway, I carried out coupled reactions of synthesized 7-carboxy-lumichrome (**86**) with carboxy-lumichrome hydantoinase, Ureidoquinoxaline amidase, and aminoquinoxaline amidinase. The three enzymes, carboxy-lumichrome hydantoinase, Ureidoquinoxaline amidase, and aminoquinoxaline amidinase, have previously been studied without carboxylated intermediates (Figure I.5).

Results and discussion

Coupled reaction

The synthesized 7-carboxy-lumichrome **86** is tested with carboxy-lumichrome hydantoinase, Ureidoquinoxaline amidase, and aminoquinoxaline amidinase enzymes. The substrate consumption and product formation of individual enzymes will support the relevance of the carboxylic acid in the lumichrome catabolic pathway.

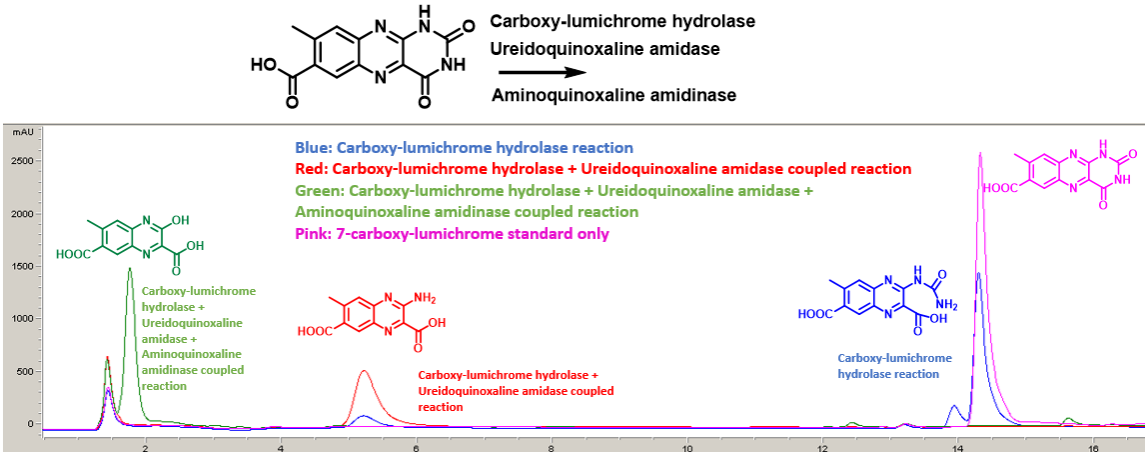

Figure VII.1: Coupled reactions of 7-carboxy-lumichrome (**86**) with carboxy-lumichrome hydantoinase, Ureidoquinoxaline amidase and aminoquinoxaline amidinase. 7-carboxy-lumichrome is consumed by carboxy-lumichrome hydantoinase to form a new peak at 14 mins (blue). This product is consumed by Ureidoquinoxaline amidase to form a new compound at 5.2 mins (red). The product of carboxy-lumichrome hydantoinase and Ureidoquinoxaline amidase reaction is consumed by aminoquinoxaline amidinase to form a new peak at 1.8 mins (green).

7-carboxy-lumichrome **86** (14.5 mins) is consumed in the presence of carboxy-lumichrome hydantoinase to form a product at 14.0 mins (Figure VII.1). The peak at 14.0 mins (product of carboxy-lumichrome hydantoinase) is consumed by Ureidoquinoxaline amidase and forms a compound at 5.2 mins. The product of the Ureidoquinoxaline amidase reaction is the substrate of aminoquinoxaline amidinase, and a compound at 1.8 mins is formed in the coupled reaction.

Based on our previous studies of carboxy-lumichrome hydantoinase, Ureidoquinoxaline amidase, and aminoquinoxaline amidinase enzymes, we have proposed the following structures as shown in the figure.

Proposed lumichrome catabolic pathway in Pimelobacter simplex

I have reconstituted (i) lumichrome monooxygenase enzyme, (ii) NDMA-dependent hydroxymethyl-lumichrome oxidase, (iii) quinoxaline oxidase, (iv) quinoxaline dioxygenase, and (v) amidocatechol dioxygeanse in the lumichrome catabolic pathway. The discovery and activity of lumichrome monooxygenase and NDMA-dependent hydroxymethyl-lumichrome oxidase led us to propose 7-carboxy-lumichrome (**86**) as the substrate of carboxy-lumichrome hydantoinase (Figure VII.2). The corresponding carboxylated substrates are proposed for the subsequent downstream enzymes (Ureidoquinoxaline amidase, aminoquinoxaline amidinase, carboxyquinoxaline decarboxylase, quinoxaline oxidase, quinoxaline dioxygenase, and amidocatechol dioxygenase).

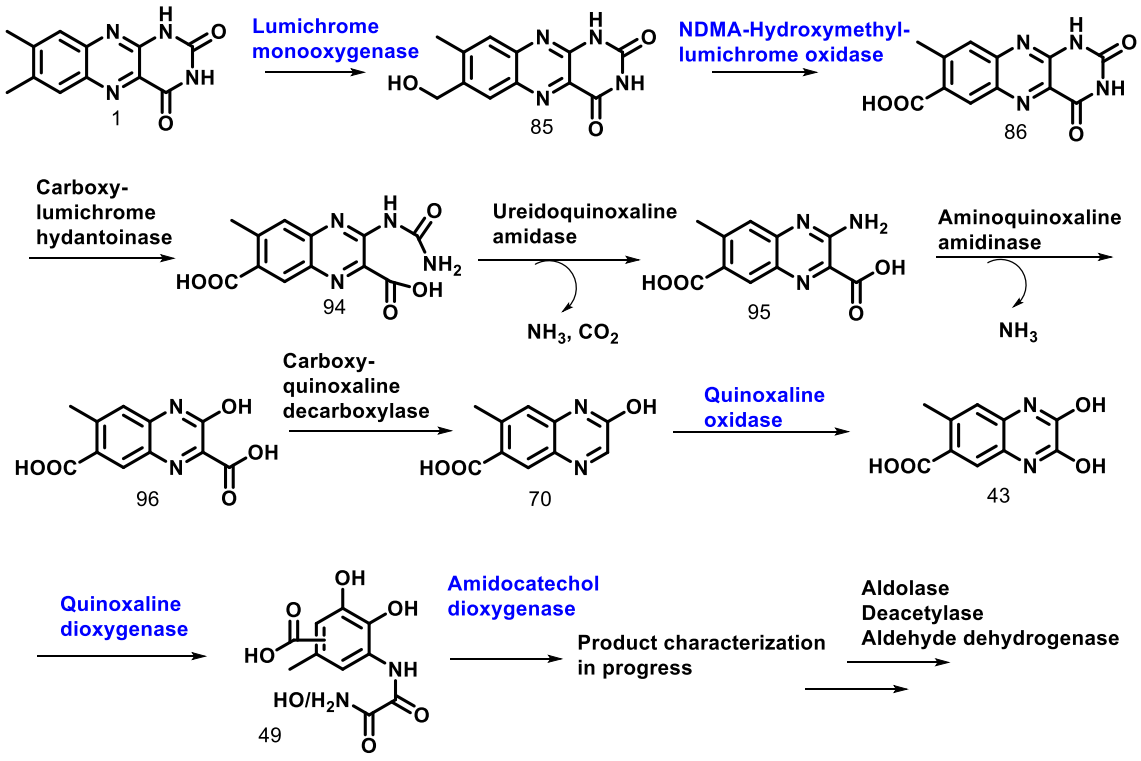

Figure VII.2: Current picture of lumichrome catabolic pathway in *Pimelobacter simplex*.

Conclusion

The solubility of lumichrome in buffer or water is less than 80 µM. Nature has developed a strategy to increase the solubility of lumichrome by oxidizing the methyl of lumichrome to a carboxylic acid. The introduction of carboxylic acid makes it easier for its breakdown and use as carbon and nitrogen sources and increases the organism's chances of survival.

CHAPTER VIII

MECHANISTIC STUDIES OF CARBON-SULFUR BOND FORMING CYTOCHROME P450 ENZYME, CXND, IN CHUANGXINMYCIN BIOSYNTHESIS

Introduction

Carbon-sulfur bond formation in natural product biosynthesis has intrigued researchers for many years[18]. The method of the incorporation of sulfur into secondary metabolites remains poorly understood. The mechanistic investigation of carbon-sulfur bond-forming cytochrome P450 monooxygenase will provide insight into the strategy nature adopts to form C-S bonds.

Chuangxinmycin (**104**), an indole alkaloid, was found to be effective against gram-positive and gram-negative bacteria as a tryptophanyl tRNA synthetase inhibitor[19]. Its analogs have also shown improved antibacterial activity; hence, the scaffold holds the potential to develop potent antibiotics. Genes responsible for chuangxinmycin biosynthesis were identified recently by *Hong et al.* and *Zhange et. al.* [20-21]. The biosynthesis of chuangxinmycin requires the formation of two carbon-sulfur bonds using different strategies. The first bond is made using a sulfur carrier protein (SCP), CxnE[22],

similar to ThiS in thiamin biosynthesis; the second by CxnD, a cytochrome P450 enzyme[23].

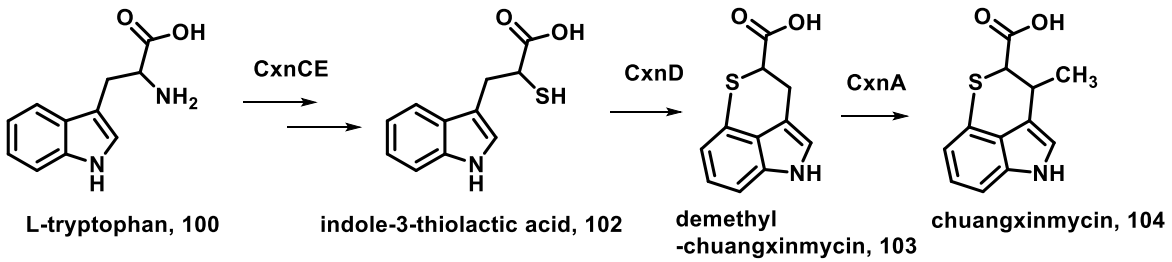

Figure VIII.1: Proposed biosynthetic pathway of chuangxinmycin (104).

The biosynthetic gene cluster of chuangxinmycin, isolated from *Actinoplanes tsinanensis*, contains a cytochrome P450 monooxygenase named CxnD. Recently, Shi *et al.* reported the biochemical studies and structure of CxnD[23]. They propose a diradical mechanism for the formation of demethyl-chuangxinmycin **3**. In this section, I report systematic mechanistic studies of CxnD and discuss two plausible mechanistic proposals for C-S bond formation via aryl radical anion intermediate or a (2-3)-epoxyindole intermediate. Intriguingly, indole-3-propanoic acid, as a substrate analog of CxnD releases five shunt products. Characterization of the products provides evidence for (2-3)-epoxyindole intermediate in the formation of C-S bond by CxnD.

Results and discussion

Expression and purification of CxnD

The CxnD sequence was codon-optimized for expression in *E. coli* and cloned into a pTHT expression vector (a derivative of pET28b vector with a TEV protease cleavage site after the N-terminal His-tag) and co-expressed with pGro7 in *E.coli* C41 cells. 1 mM of ∂-aminolevulinic acid was added after culture reached OD_{600} of 0.1, and protein expression was induced with 0.1 mM of IPTG at OD_{600} of 0.6-0.8. The overexpressed protein was purified using Ni-NTA-affinity chromatography (Figure VIII.2). The eluted protein has an absorbance at 418 nm, characteristic of heme-bound protein. Quantification via pyridine hemochrome assay indicates that only 10 % of the purified enzyme was heme bound[24].

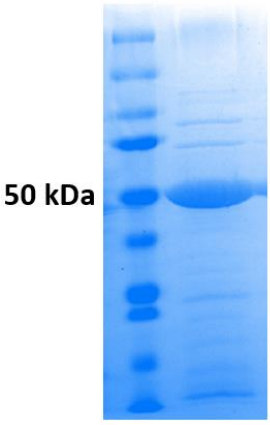

Figure VIII.2: SDS-PAGE of purified CxnD (47 kDa)

Functional characterization of CxnD

To reconstitute the activity of CxnD, the proposed substrate of CxnD-catalyzed reaction, indole-3-thiolactic acid (**102**), was synthesized according to the modified literature procedure[25]. After screening many chemical reducing agents and *E.coli* ferredoxin and ferredoxin reductase system, finally, CxnD (25 μM) formed a product in the presence of compound **102** (~1 mM), spinach ferredoxin (10 μM), spinach ferredoxin-NADP+ reductase (0.05 unit), and NADPH (2 mM) (Figure VIII.3). A product is detected by HPLC and LC-MS only in the full reaction. The product is identified as demethyl-chuangxinmycin **103** by MS analysis and UV-VIS spectrum. The UV-VIS spectrum of the product was red-shifted, as expected, because of electron donation by sulfur to the indole[20].

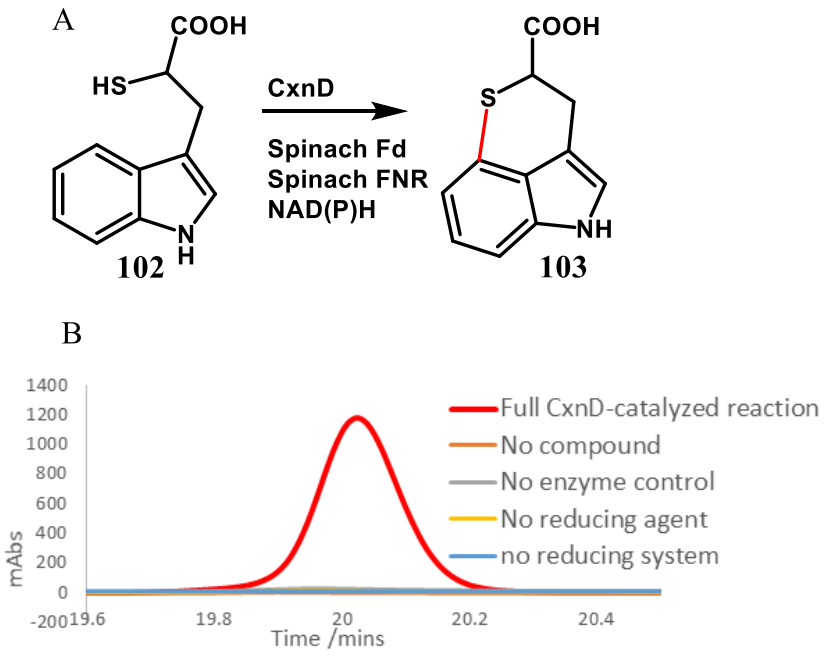

Figure VIII.3**:** (A) CxnD-catalyzed reaction (B) HPLC chromatogram of CxnD-catalyzed reaction at 300 nm shows compound **103** eluting at 20 mins in the full reaction only (red).

The reconstitution of CxnD set a solid foundation to carry out mechanistic studies of the enzyme. We have proposed two mechanisms of CxnD-catalyzed C-S bond formation from **102** to **103** (Figure VIII.4).

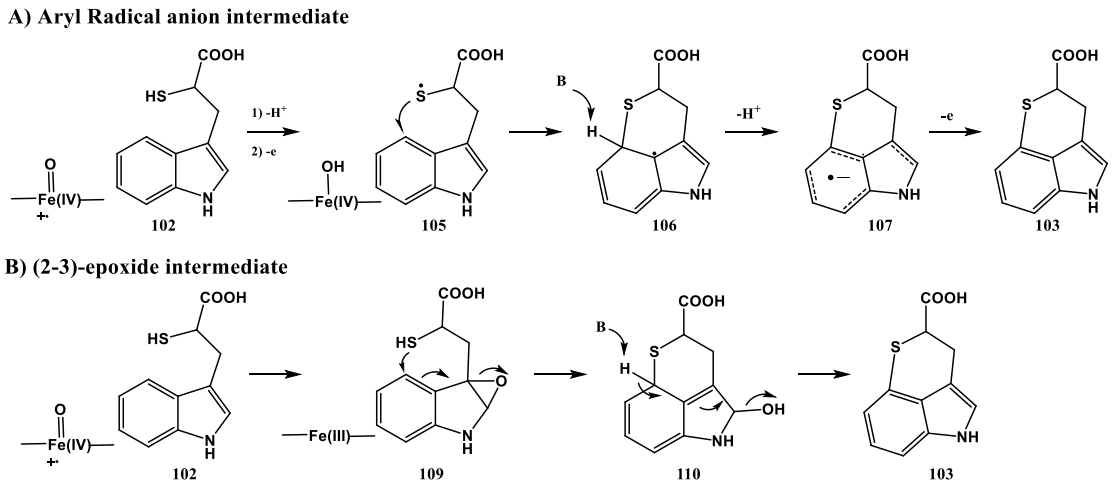

Figure VIII.4: Mechanistic proposals for CxnD-catalyzed reaction via (a) Aryl radical anion intermediate (b) (2,3)-epoxide intermediate

Table 2: The compounds tested on CxnD and their products. *Compounds synthesized

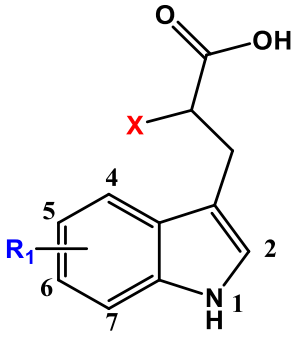

Compound	R_1	X	Product
138*	4, Br	SH	-
143*	5, Br	SH	-
112*	6, Br	SH	113
153*	7, Br	SH	-
108	H	OH	-
111	H	CH_3	-
114	H	H	115*, 116, 117, 118
170	N_1=S	H	171*
172*	N-CH_3	H	177*
137*	4, I	SH	-

Carbon-sulfur bond formation via Aryl-radical anion intermediate

The first proposal (Figure VIII.4A) performs C-S bond formation via radical anion intermediate **107**. The iron(IV)-oxo generates a thiyl radical **105** that adds to the C4-position of indole. The deprotonation of the C4 proton will form an aryl radical anion **107** followed by the loss of an electron, leading to demethyl-chuangxinmycin **103**. Trapping

of aryl radical anion intermediate is possible using halogenated substrate via $S_{RN}1$ substitution reaction. A halogenated aryl radical anion undergoes substitution/hydrogen atom abstraction reactions resulting in the loss of bromide and an aryl radical that a hydrogen atom donor quenches (Figure VIII.5). This strategy has been successful in probing MqnE and MqnC-catalyzed reactions in our lab[26].

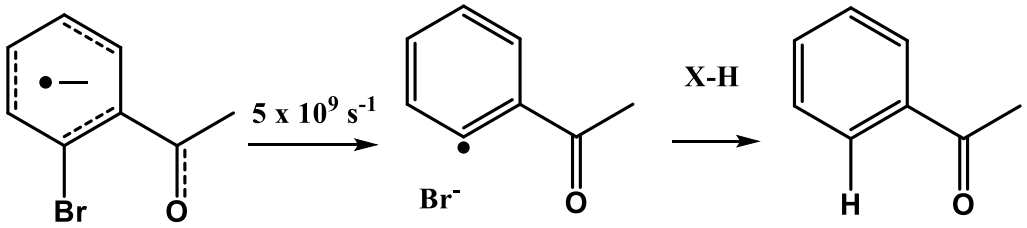

Figure VIII.5: A halogenated aryl radical anion undergoes substitution/hydrogen atom abstraction reactions resulting in the loss of bromide and an aryl radical that a hydrogen atom donor quenches.

Bromo analogs of the substrate (Table 2), compounds **112**, **138**, **143**, **153** were synthesized and tested with CxnD. A loss of bromide from the substrate and the formation of demethyl-chuangxinmycin **103** will provide evidence for aryl radical anion intermediate. CxnD consumed only 6-bromo as a substrate analog **112**, and a new compound with a different retention time from demethyl-chuangxinmycin **103** was observed (Figure VIII.6). LC-MS analysis revealed a new peak corresponding to the mass of 6-bromo-demethyl-chuangxinmycin **113**, only in the full reaction. In the CxnD-catalyzed reaction of 6-bromo analog, bromine retention argued against the aryl radical anion intermediate, **107**.

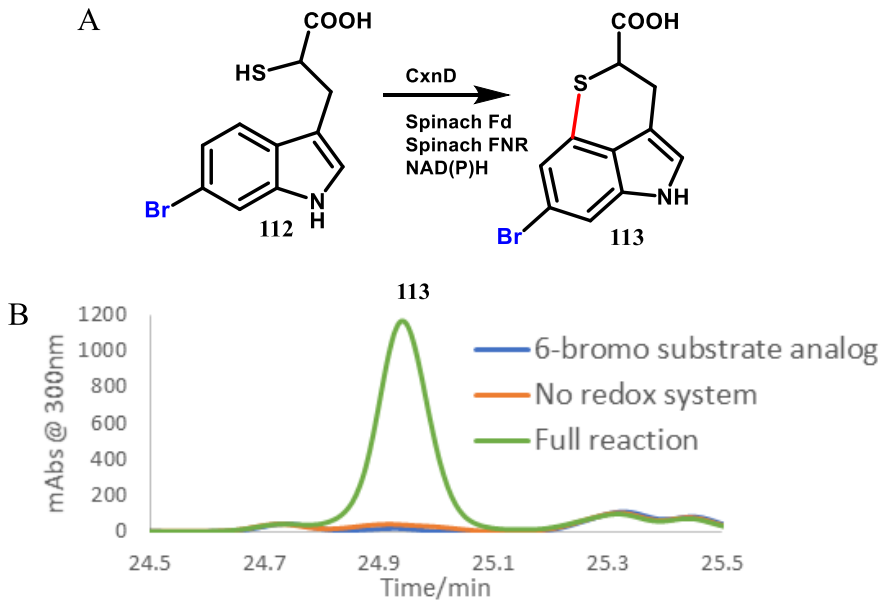

Figure VIII.6: (A) Reaction catalyzed by CxnD on 6-Bromo analog (**112)** to form 6-Bromo-demethylchuangxinmycin (**113)** (B) HPLC chromatogram of the reaction shows a new peak in the full reaction at 25 mins.

Carbon-sulfur bond formation via (2-3)-epoxide intermediate

Alternatively, the iron(IV)-oxo may form an epoxide at the C2-C3 position of indole (Figure VIII.4B). The thiol adds to the C4-position (**109**), and subsequent deprotonation and loss of water will lead to the product (**103**). To investigate if the CxnD-catalyzed reaction went via epoxidation (Figure VIII.4B), we substituted the thiol group of **1** with -OH (**108**), -CH_3 (**111**), & -H (**114)** and tested for activity with CxnD. The proposed mechanism does not require thiol at a 2' position to initiate chemistry, and we would likely detect intermediates and shunt products of the reaction. Only indole-3-propanoic acid **114** is consumed, and five new products were detected via HPLC and LC-MS (Figure VIII.7). Coelution, LC-MS, and UV-VIS spectroscopic studies identified some products as 4-hydroxyindole-3-propanoic acid **115**, 2-oxoindole-3-propanoic acid

116, indole-3-acrylic acid **117**, and 4-(2-formamidophenyl)-4-oxobutanoic acid **118**. The coelution data for all the compounds is shown in the experimental section.

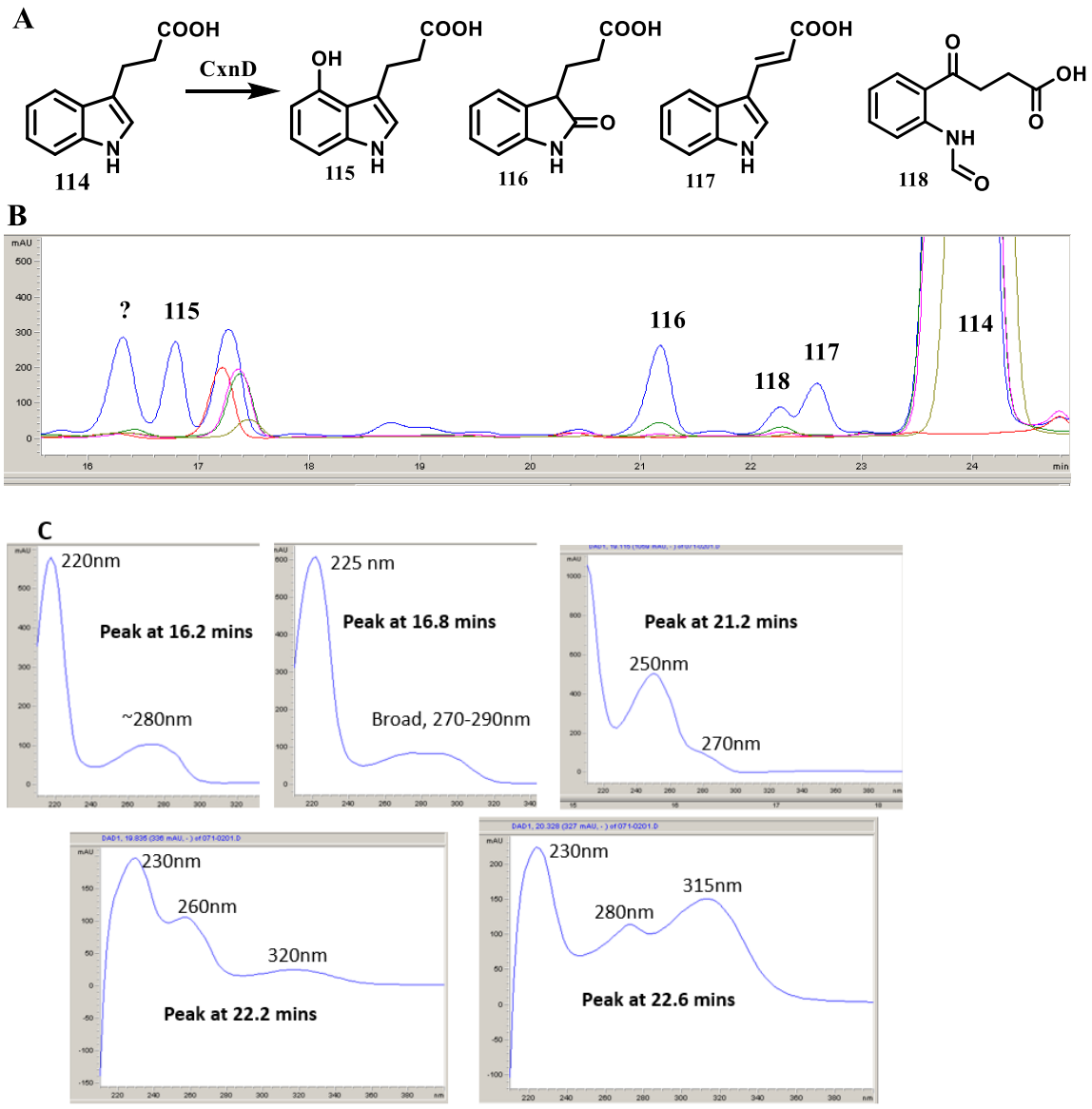

Figure VIII.7: (A) Shunt products released in the CxnD catalyzed reaction with indole-3-propanoic acid **114** (B) HPLC chromatogram (220 nm) of the CxnD-catalyzed reaction with indole-3-propanoic acid **114** forms five new compounds.(C) The UV-vis spectra of all the shunt products was helpful in identifying the compounds.

(2-3)-epoxyindole intermediate can explain the formation of all the shunt products of indole-3-propanoic acid **114**. We propose that after forming epoxyindole, the intermediate leaks out of the active site and non-enzymatically forms the shunt products (Figure VIII.8). Similar to MarE enzyme in maremycin biosynthesis[27], 2-oxoindole-3-proponoic acid **116** is proposed to form by (2-3)-hydride shift on epoxyindole and ketone formation at the C2 position. Indole-3-acrylic acid **117** is proposed to form by deprotonation at C1' beside the carbocation of C3. Followed by another deprotonation at C2', and loss of water will lead to indole-3-acrylic acid **117**. 4-hydoxyindole-3-propanoic acid **115** is proposed to form by water addition at C4 position of (2-3)-epoxyindole. Subsequent deprotonation and loss of water will lead to 4-hydroxyindole-3-propanoic acid. Lastly, 4-(2-formamidophenyl)-4-oxobutanoic acid **118** is proposed to form via epoxyindole intermediate **119**. Another round of oxidation by iron(IV)-oxo, where the electrophilic addition of iron(IV)-oxo on C2 or C3 position occurs. Subsequent ketone formation and cleavage of the C2-C3 bond will form the final compound **118**. A similar mechanism has been proposed for tryptophan dioxygenase (TDO)[28].

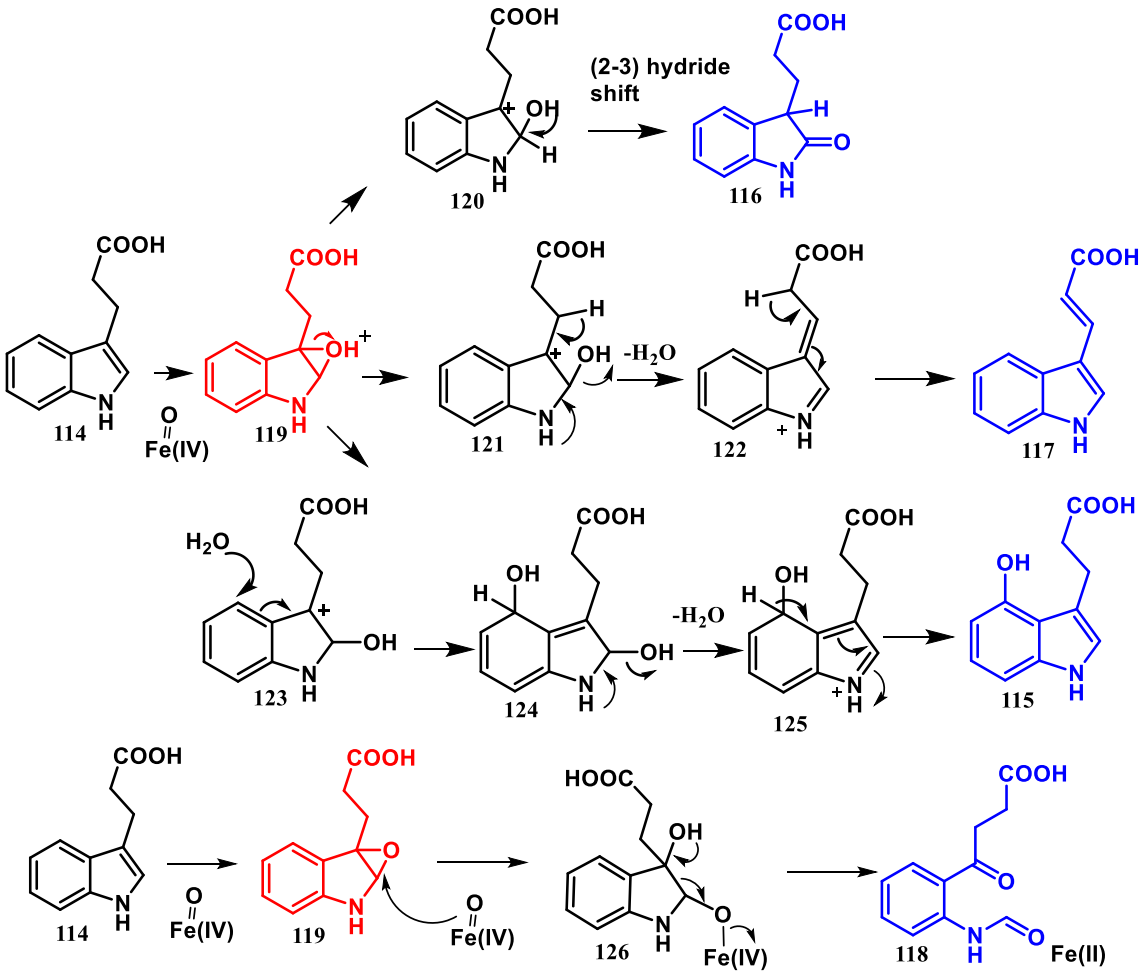

Figure VIII.8: Proposed mechanism for the leaked products.

To test our proposal, we attempted to synthesize (2,3)-epoxyindole-3-propanoic acid (**119**) and feed the intermediate to the CxnD. Indole-3-propanoic acid (**114**) was oxidized with OXONE according to literature procedures for the synthesis of epoxyindoles[29-30]. Unfortunately, due to the high reactivity of epoxyindole we were unable to isolate it. On the other hand, we detected compounds **116** and **118** as products of indole-3-propanoic acid oxidation. Demonstrating the two shunt products are formed via a (2-3)-epoxide intermediate.

The formation of shunt products formed by indole-3-propanoic acid as a substrate can be explained via epoxide mechanism (Figure VIII.9). Consumption of **114** provides evidence that indole is within the iron(IV)-oxo proximity, and the chemistry initiates at the C2-C3 of indole rather than the thiol substituent.

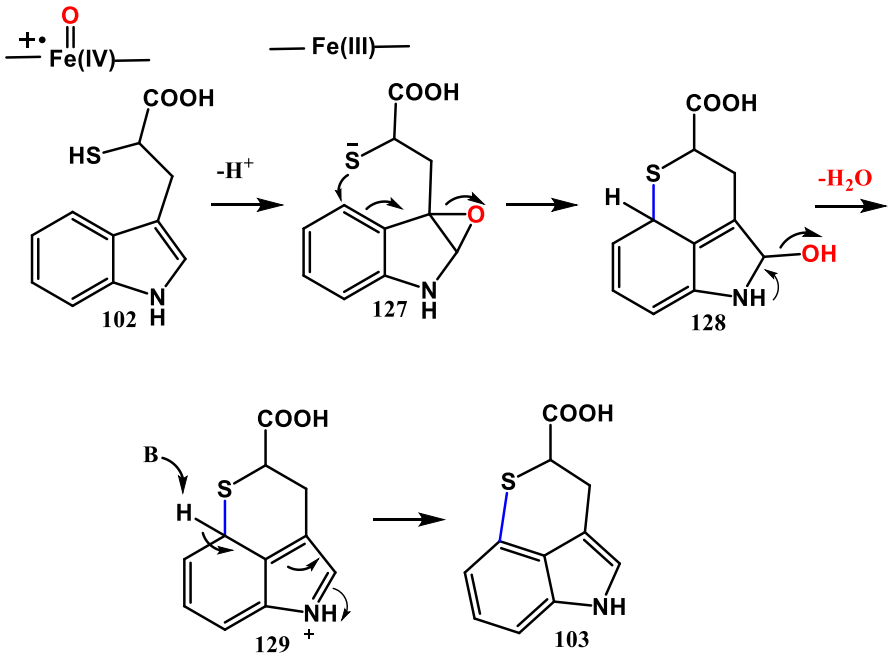

Figure VIII.9: Mechanistic proposal for CxnD catalyzed carbon-sulfur bond formation via (2,3)-epoxyindole intermediate.

Conclusion

We were successfully able to reconstitute carbon-sulfur bond formation of indole-3-thiolactic acid (**102**) to form demethyl-chuangxinmycin (**103**) by CxnD. To investigate the two plausible mechanisms via i) aryl radical anion intermediate ii) (2-3)-epoxyindole intermediate, several substrate analogs were tested with CxnD. Bromo-substituted substrate analogs ruled out the carbon-sulfur bond formation via aryl radical anion

intermediate. Indole-3-propanoic acid as a substrate analog of CxnD released multiple products that provide evidence for epoxyindole intermediate formation.

Experiemental procedures

Co-elution of 4-hydroxyindole-3-propionic acid, 115

Indole-3-propanoic acid as a substrate analog releases 5 shunt products. LC-MS analysis suggested multiple compounds with one more oxygen incorporation. The position of oxygen was determined by synthesizing multiple hydroxylated indole-3-propanoic acid standards and coeluted with the enzymatic reaction mixture. 4-hydroxyindole-3-propanoic acid coelutes with the enzymatic reaction peak at 16.3 minutes. Further support from LC-MS and UV-vis spectra confirm the product characterization.

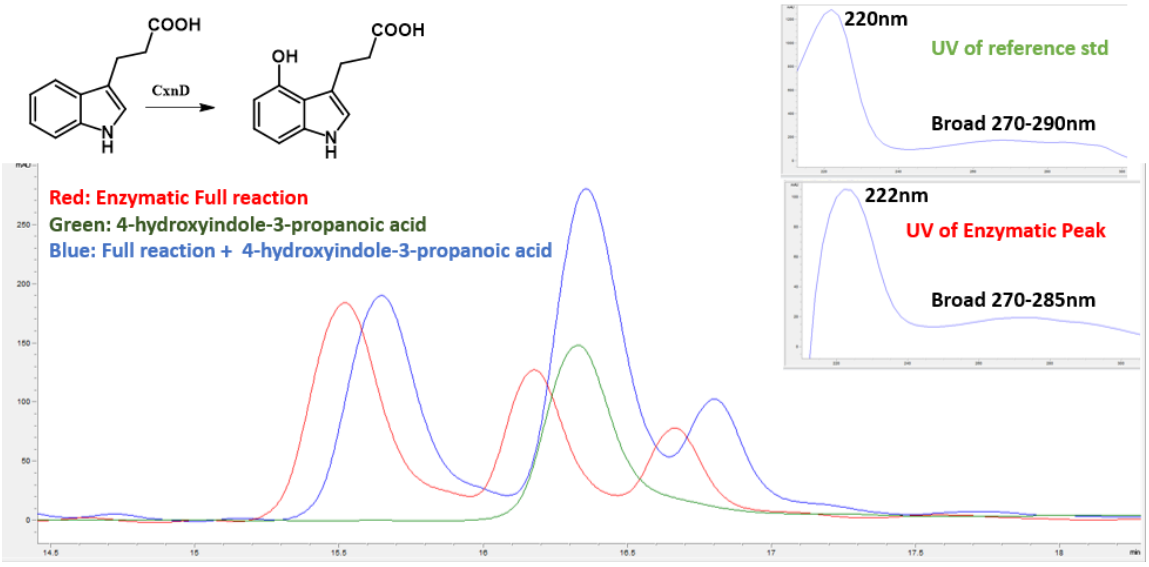

Figure VIII.10: 4-hydroxyindole-3-propanoic acid coelutes with the enzymatic reaction peak at 16.3 minutes.

Co-elution of 2-oxoindole-3-propanoic acid, 116

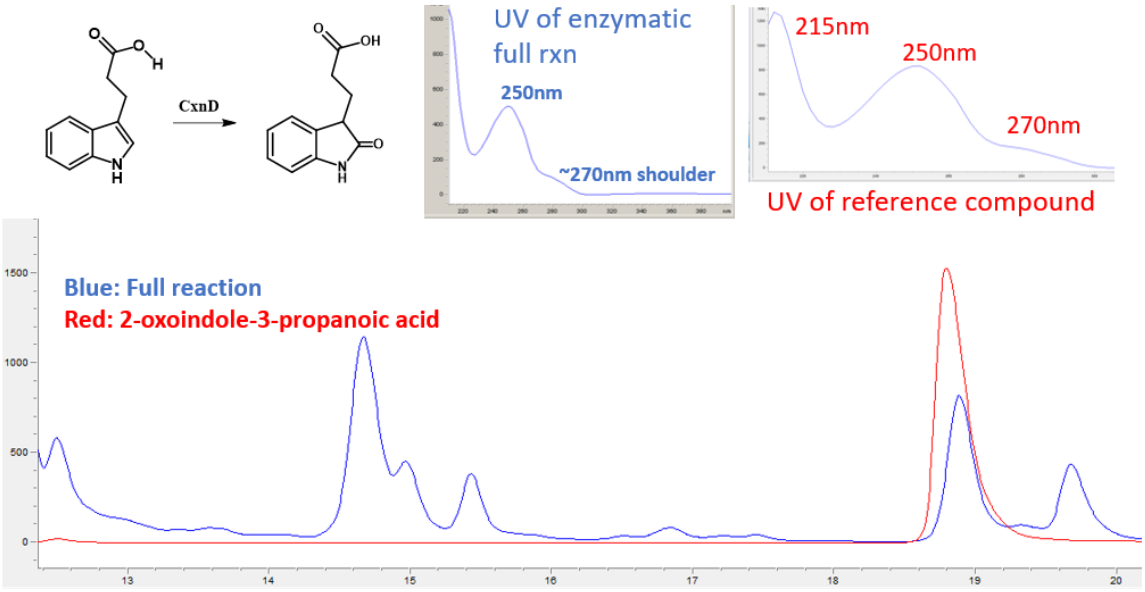

Figure VIII.11: 2-oxoindole-3-propanoic acid standard coelutes with the enzymatic reaction peak at around 19 minutes. The distinct UV-vis spectra further confirm the assignment.

s

Co-elution data with indole-3-acrylic acid, 117

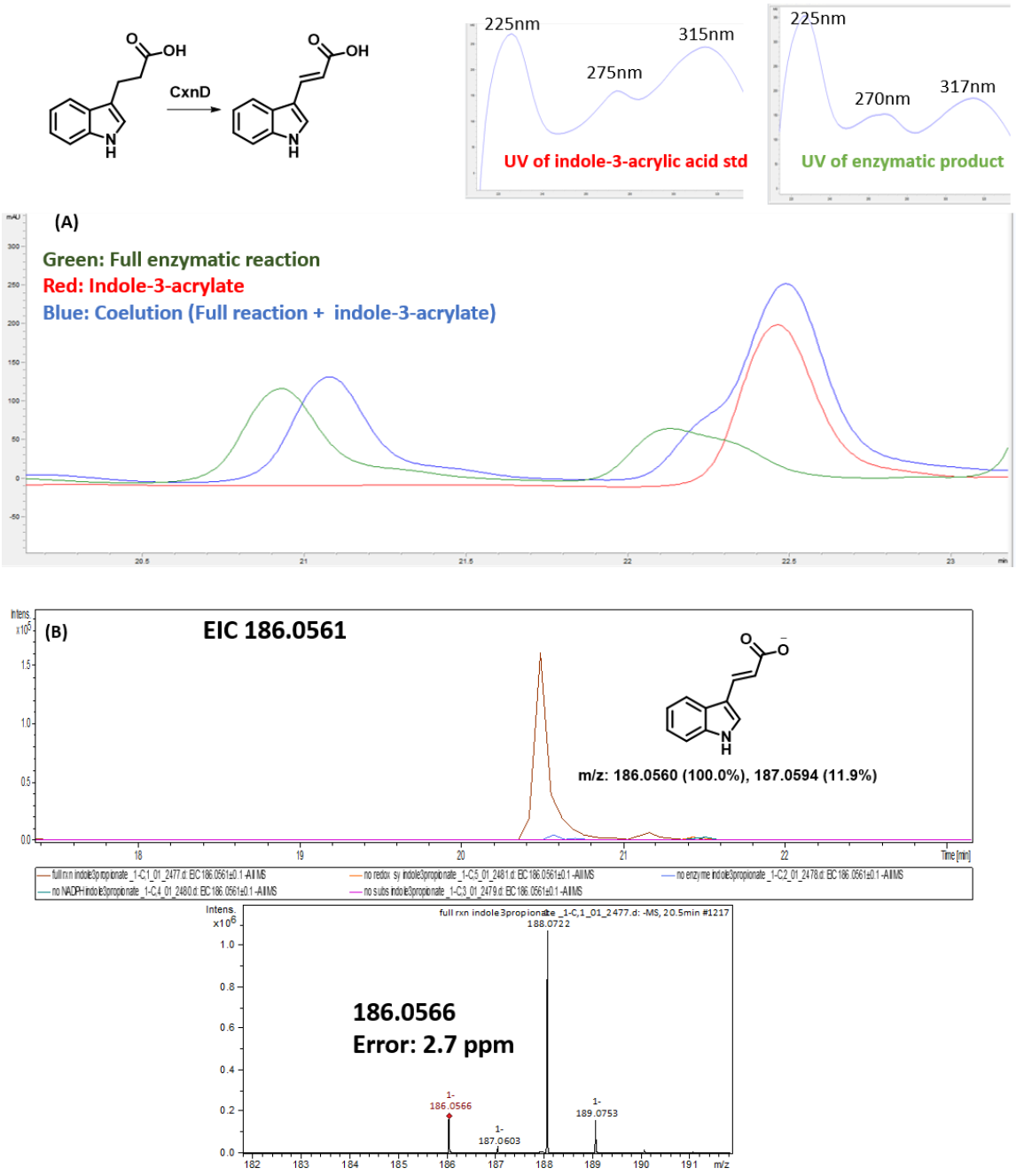

Figure VIII.12: Indole-3-acrylic acid standard coelutes with the enzymatic reaction peak. The distinct UV-vis spectra further confirm the assignment. (B) A mass corresponding to indole-3-acrylic acid is only detected in the CxnD catalyzed full reaction.

Co-elution of 4-(2-formamidophenyl)-4-oxobutanoic acid, 118

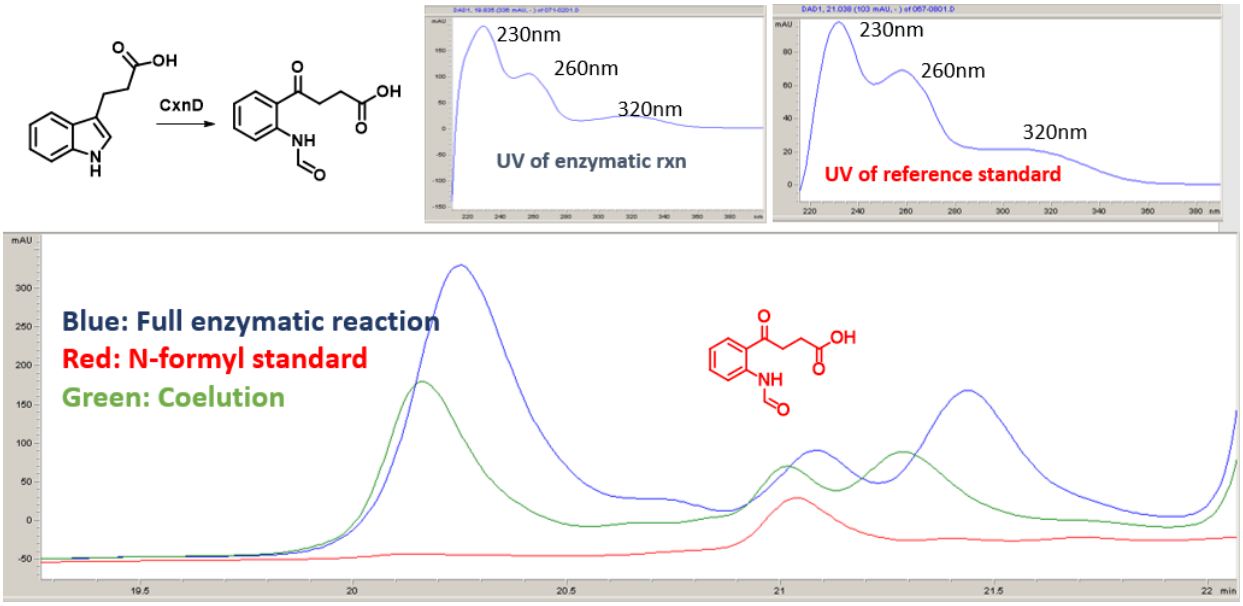

Figure VIII.13: 4-(2-formamidophenyl)-4-oxobutanoic acid standard coelutes with the enzyme reaction peak at 21 minutes. The UV-vis spectra and LC-MS further support the assignment.

Synthesis of 3-(1H-indol-3-yl)-2-mercaptopropanoic acid, 102

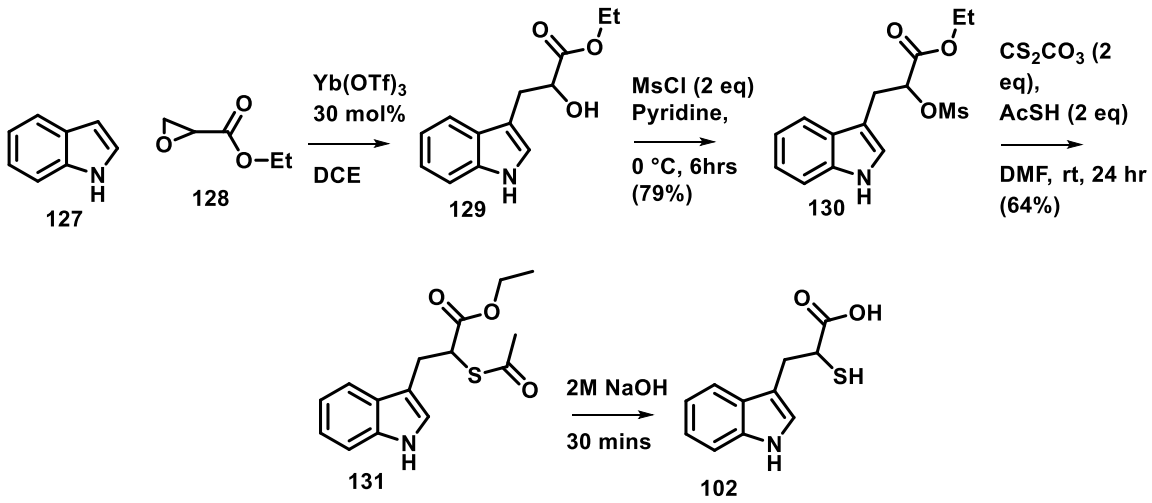

Preparation of methyl 2-hydroxy-3-(1H-indol-3-yl)propanoate, 129

The procedure of K. M. Snyder et al./Tetrahedron Letters 54 (2013) 192–194193 was followed. Indole (2 equivalent, 2 grams, 17.2 mmol) and ethyl-(3,3)-epoxypropanoate (1 equivalent, 8.61 mmol) is added to 1,2-dichloroethane (20 mL) and Ytterbium(III) trifluoromethanesulfonate (30% catalyst, 1.34 grams, 2.58 mmol) at room temperature under argon. The mixture is warmed to 80 °C and stirred for 75 minutes, and then cooled to room temperature.

The reaction was quenched with saturated aqueous sodium carbonate (25 mL), followed by 1N HCl (70 mL). The mixture was extracted with DCM, and the combined organic layer was washed with brine and dried by sodium sulfate anhydrous. The concentrated residue was purified by flash chromatography using ethyl acetate and hexane as a medium.

Preparation of methyl 3-(1H-indol-3-yl)-2-((methylsulfonyl)oxy)propanoate, 130

The procedure of Peng lab, Organic Letters, 2013, 15, 3, 550-553 was followed. To the stirred solution of alcohol (250mg, 1.14 mmol) in pyridine was added MsCl (2 equivalent, 2.3 mmol, 262.2 mg) dropwise at 0 °C. The reaction mixture was stirred for 6 hours in the ice bath, diluted with ethyl ether, washed with 10% aqueous HCl, water, brine, and then dried over anhydrous sodium sulfate. The resulting concentrated crude was crystallized from petroleum ether and used in the subsequent reaction.

Preparation of methyl 2-(acetylthio)-3-(1H-indol-3-yl)propanoate, 131

The procedure of Peng lab, Organic Letters, 2013, 15, 3, 550-553 was followed. To a stirred solution of cesium carbonate, Cs_2CO_3 (2 equivalent, 0.75 grams, 2028 mmol), in DMF (2 mL) under argon was added thioacetic acid (2 equivalent, 2.28 mmol, 0.16 mL) dropwise a room temperature. After 30 minutes, the solution of methyl 3-(1H-indol-3-yl)-2-((methylsulfonyl)oxy)propanoate (1 equivalent, 1.14 mmol) in DMF (2 mL) was added dropwise, and the resulting mixture was stirred for 24 hours at room temperature. The reaction was quenched by water then extracted with ethyl acetate. The organic layer was washed with water, brine and then dried over anhydrous sodium sulfate. The resulting crude was purified by flash chromatography using ethyl acetate and hexane as the solvent medium.

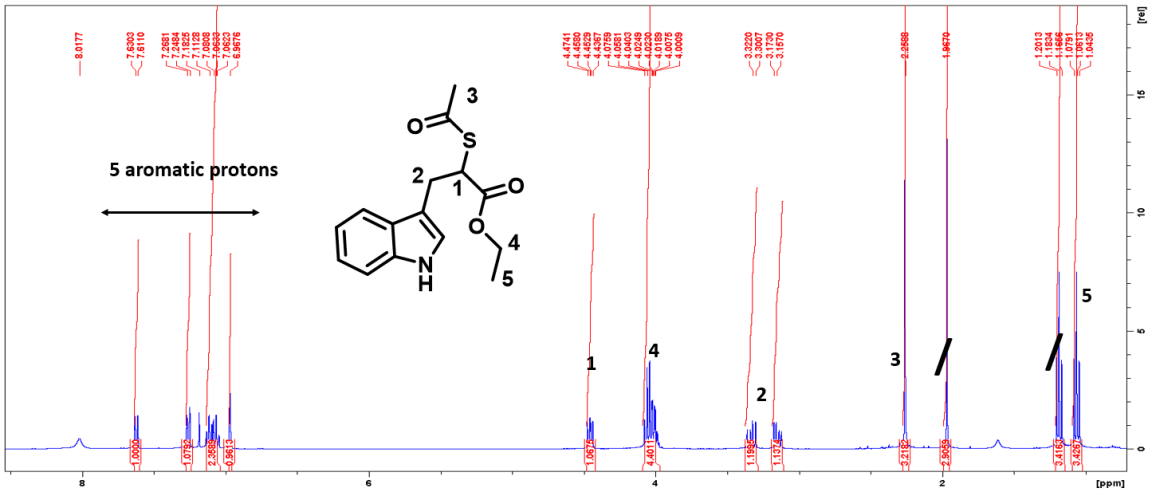

Preparation of 3-(1H-indol-3-yl)-2-mercaptopropanoic acid, 102

The deprotection is done *in situ* before setting up the enzymatic reaction. Aliquots of methyl 2-(acetylthio)-3-(1H-indol-3-yl)propanoate in methanol were prepared in

eppendorf. ~0.1 mL of 2M NaOH is added and mixed for 30 minutes on the reaction day. The solution is acidified to ~pH 7 and added into an enzymatic reaction.

Synthesis of 3-(4-iodo-1H-indol-3-yl)-2-mercaptopropanoic acid, 137

A procedure similar to the synthesis of 3-(1H-indol-3-yl)-2-mercaptopropanoic acid is followed.

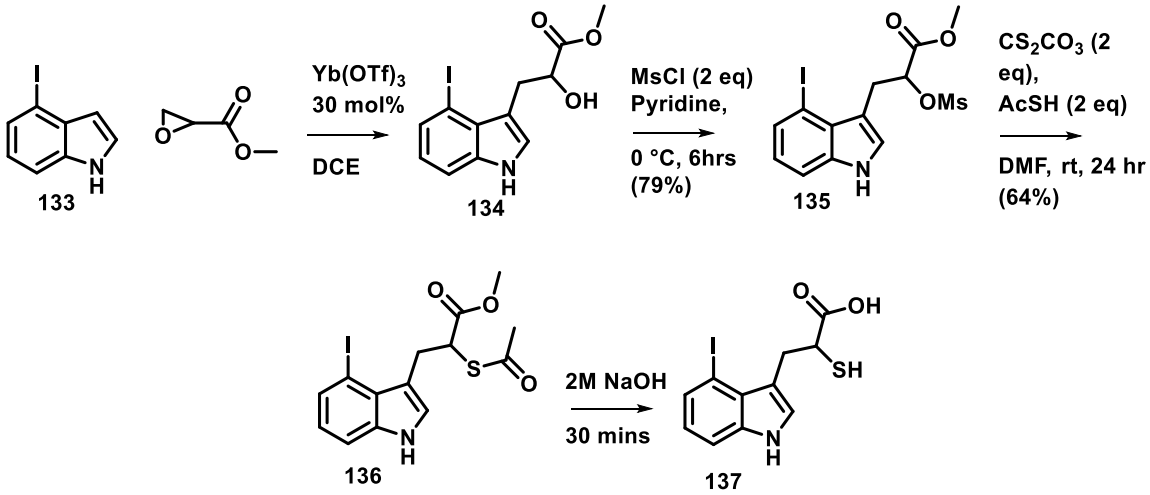

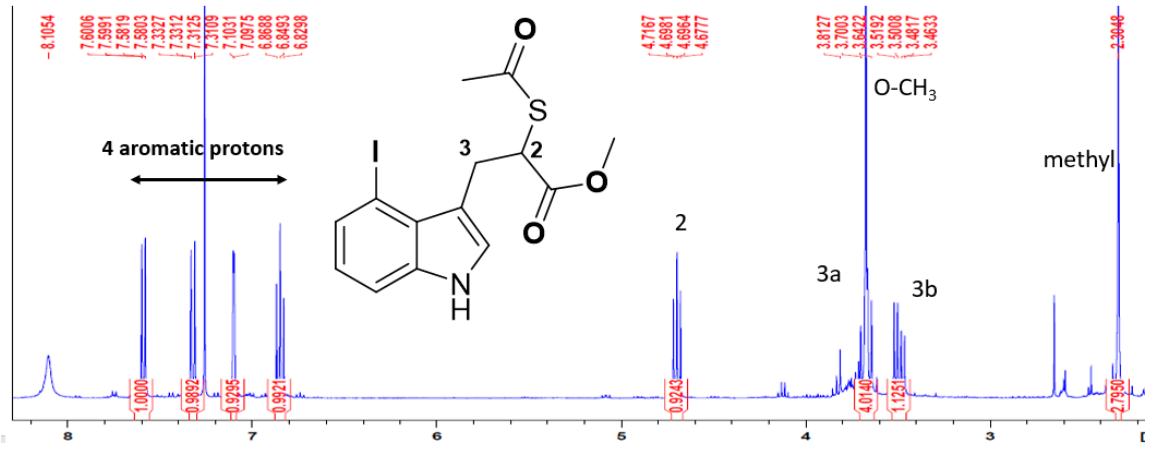

Synthesis of 3-(4-bromo-1H-indol-3-yl)-2-mercaptopropanoic acid, 138

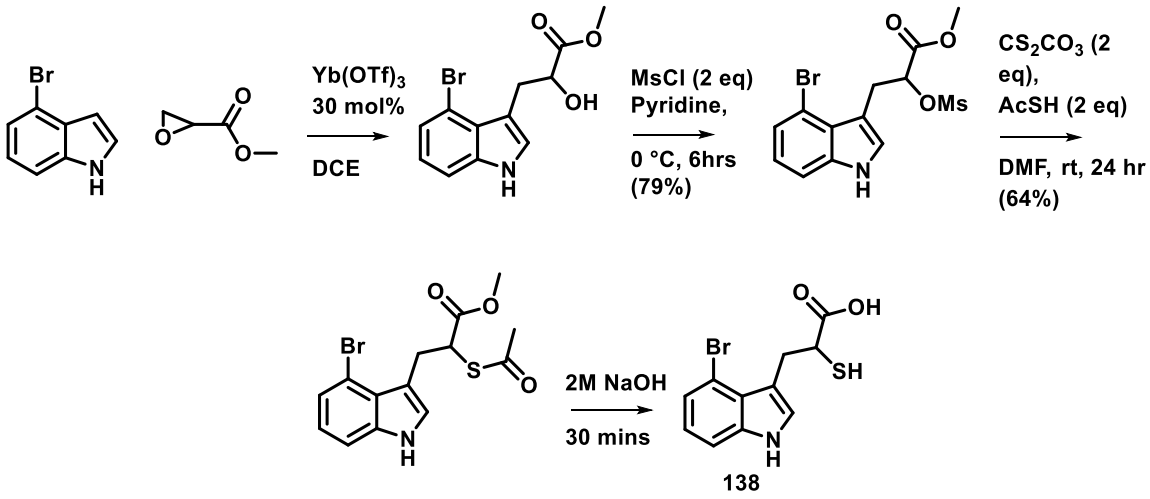

A procedure similar to the synthesis of 3-(1H-indol-3-yl)-2-mercaptopropanoic acid is followed.

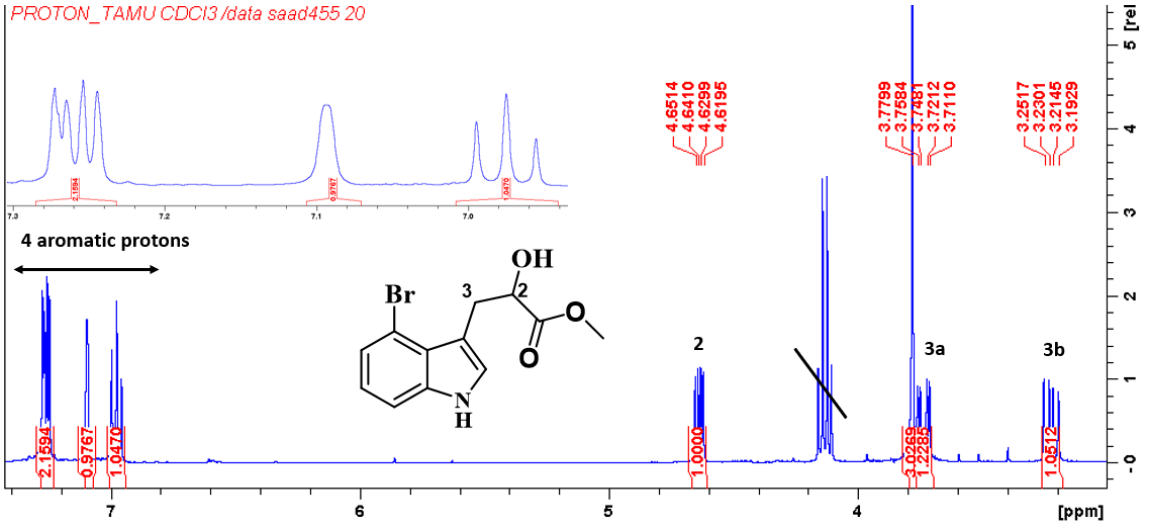

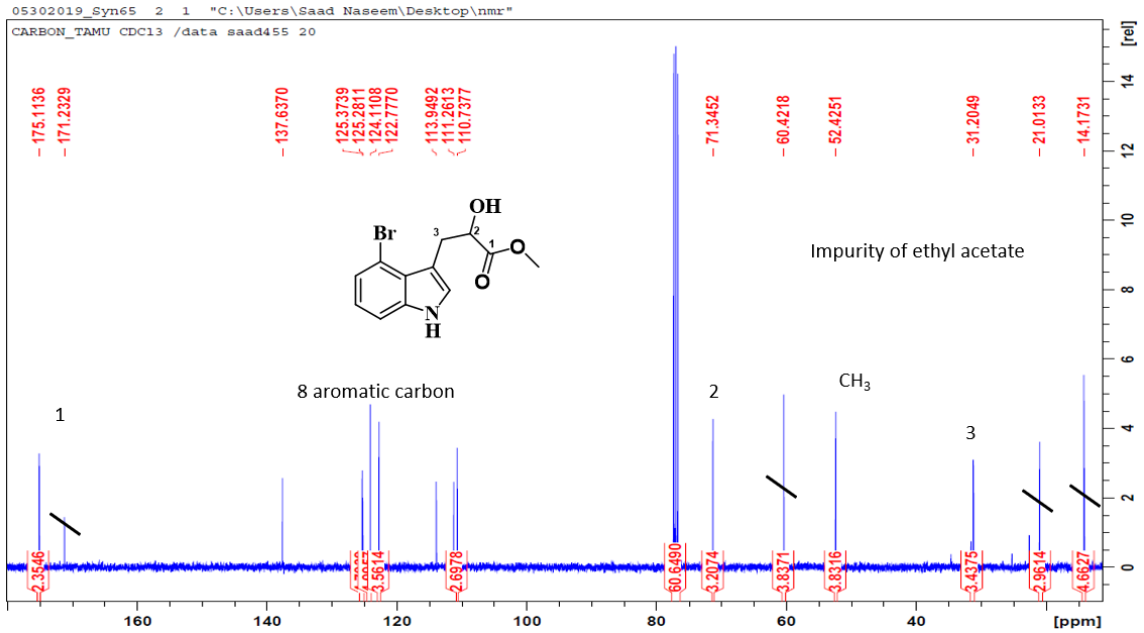
05302019_Syn65 2 1 "C:\Users\Saad Naseem\Desktop\nmr"
CARBON_TAMU CDCl3 /data saad455 20
Impurity of ethyl acetate
8 aromatic carbon
1
2
CH3
3
[ppm]

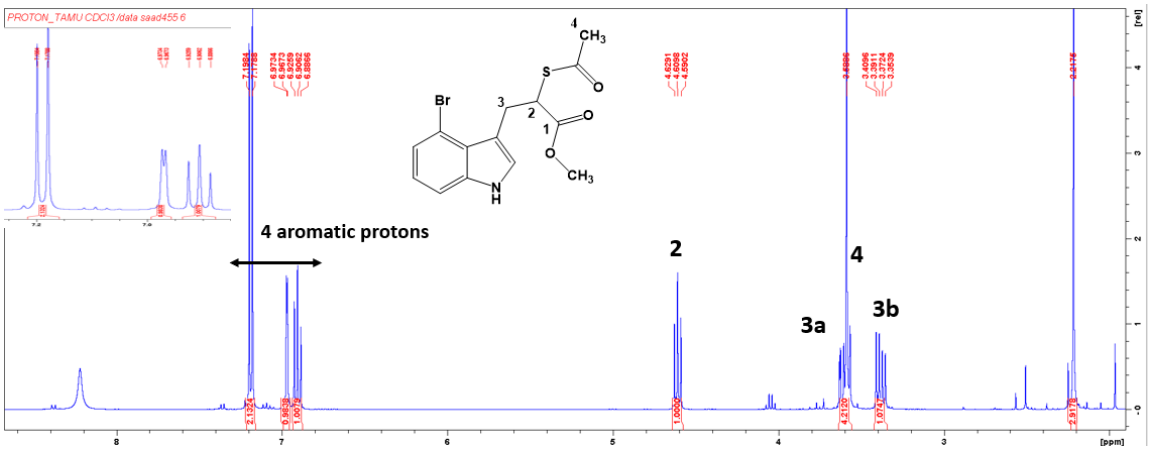
PROTON_TAMU CDCl3 /data saad455 6
4 aromatic protons
2
4
3a
3b
[ppm]

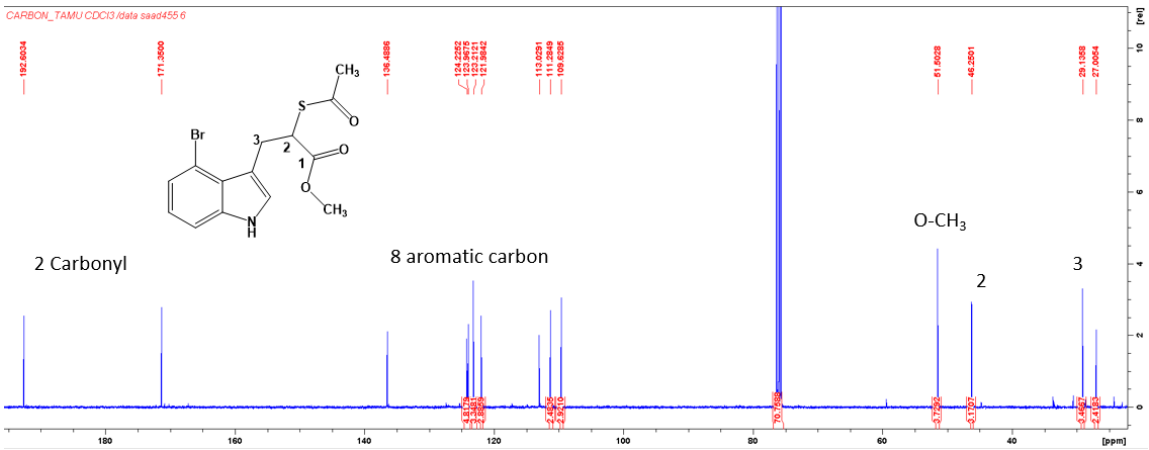
CARBON_TAMU CDCl3 /data saad455 6
2 Carbonyl
8 aromatic carbon
O-CH3
2
3
[ppm]

Synthesis of 3-(5-bromo-1H-indol-3-yl)-2-mercaptopropanoic acid, 143

A procedure similar to the synthesis of 3-(1H-indol-3-yl)-2-mercaptopropanoic acid is followed.

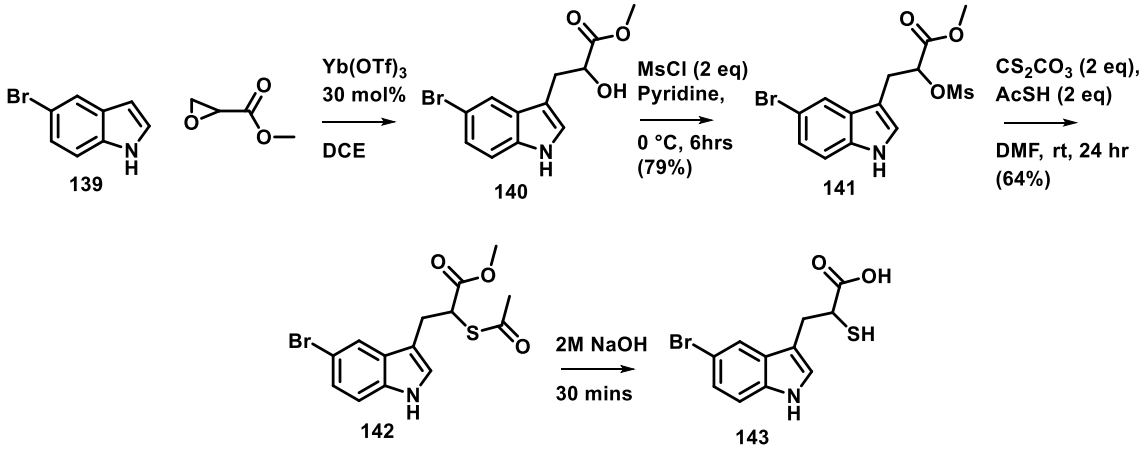

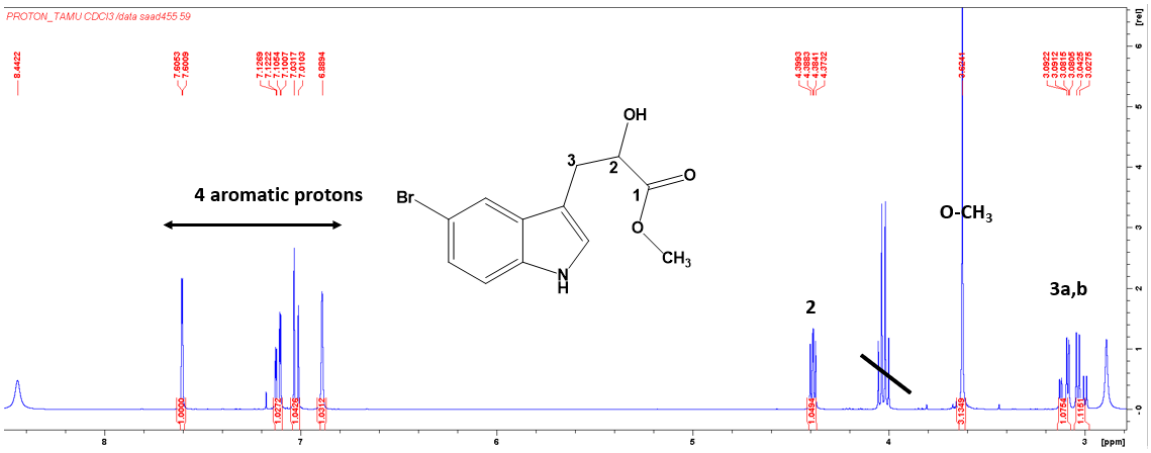

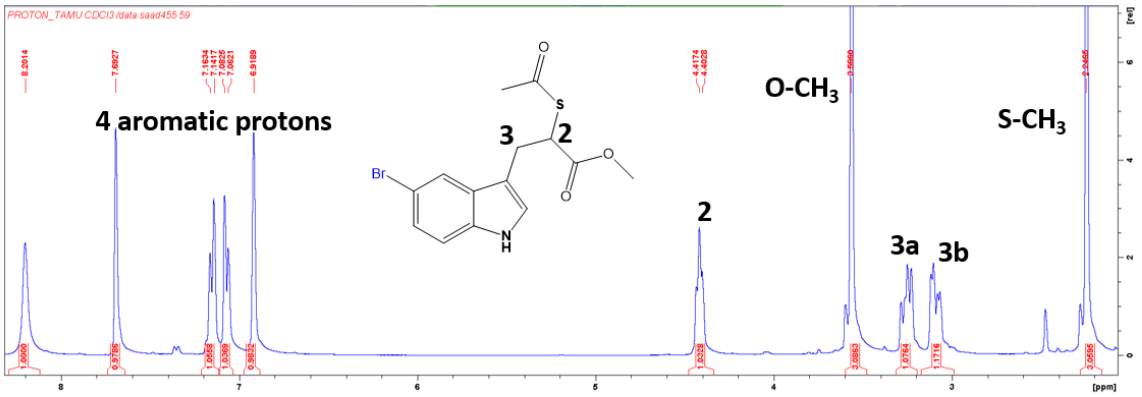

Synthesis of 3-(6-bromo-1H-indol-3-yl)-2-mercaptopropanoic acid, 112

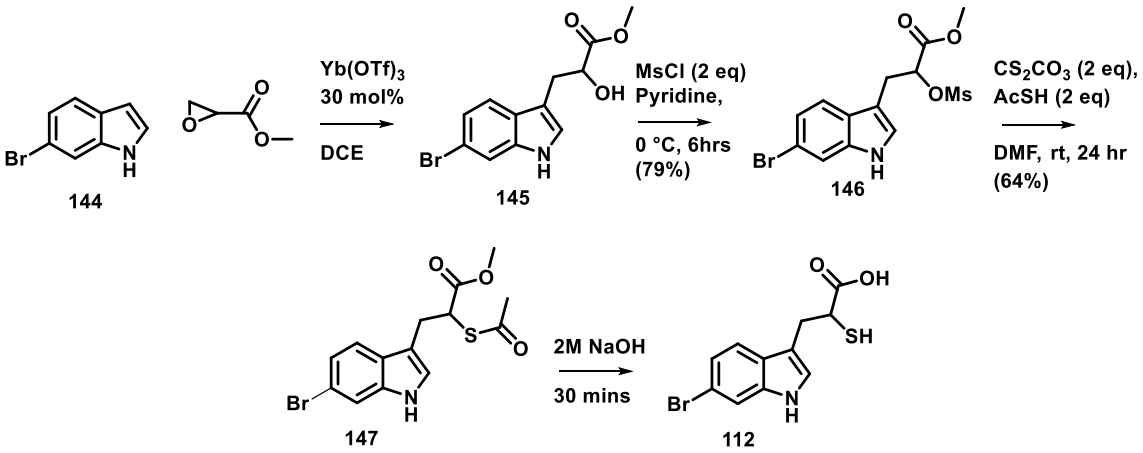

A procedure similar to the synthesis of 3-(1H-indol-3-yl)-2-mercaptopropanoic acid is followed.

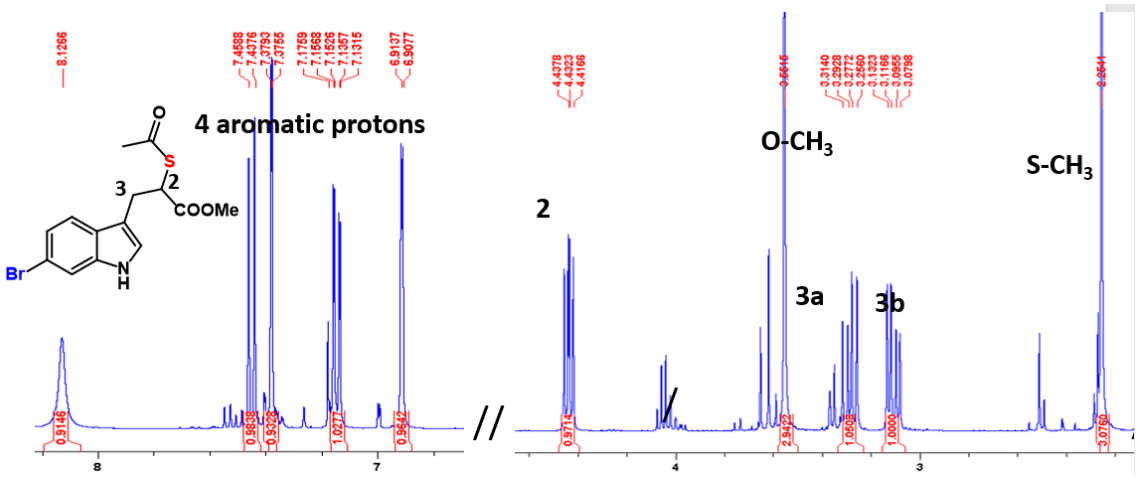

Synthesis of 3-(7-bromo-1H-indol-3-yl)-2-mercaptopropanoic acid, 153

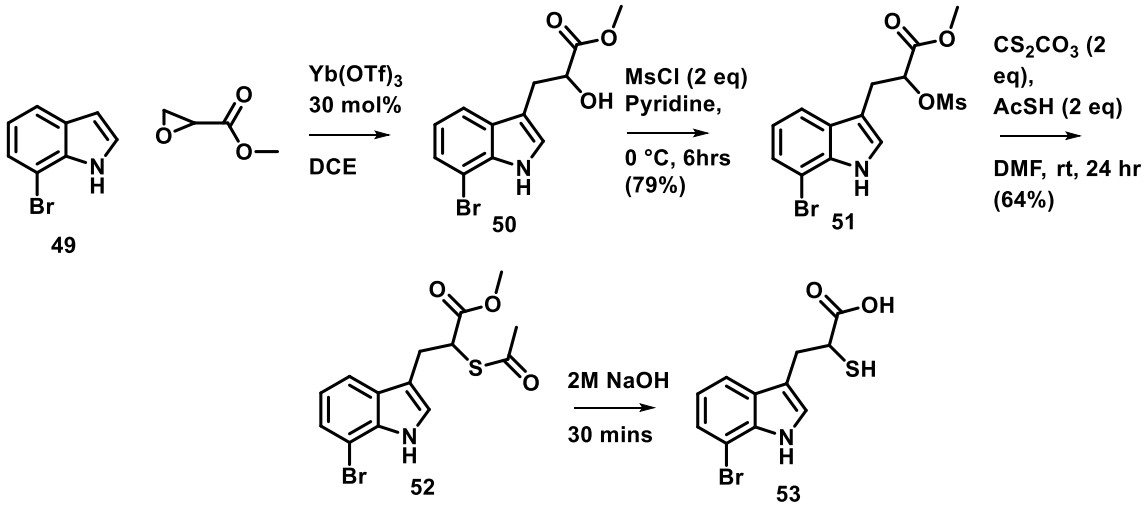

A procedure similar to the synthesis of 3-(1H-indol-3-yl)-2-mercaptopropanoic acid is followed.

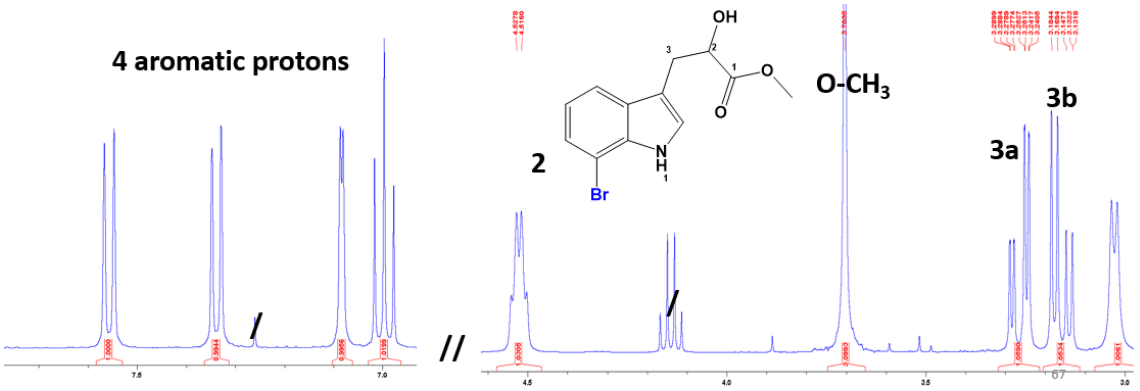
4 aromatic protons
OH
O
O
N
H
Br
2
O-CH3
3b
3a

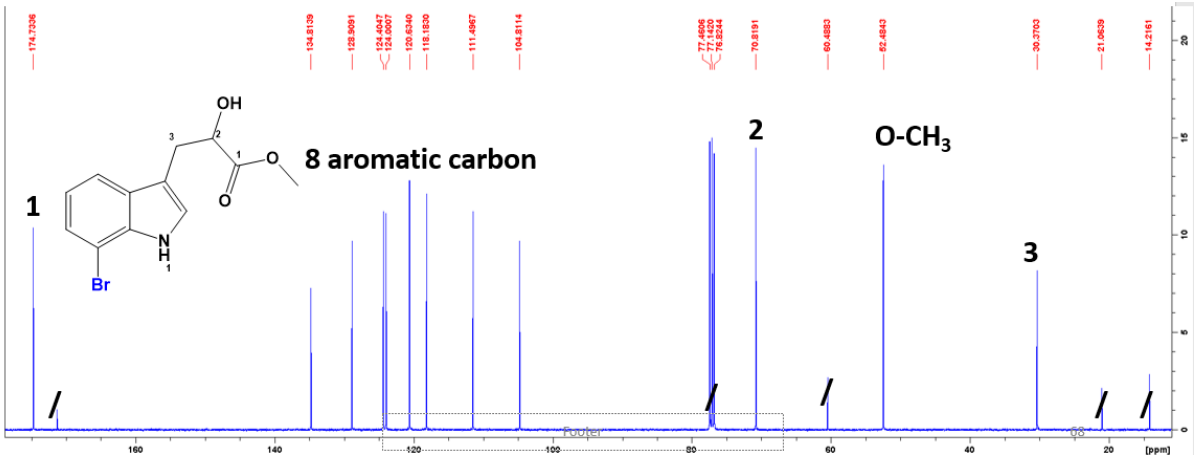
OH
O
O
N
H
Br
1
8 aromatic carbon
2
O-CH3
3

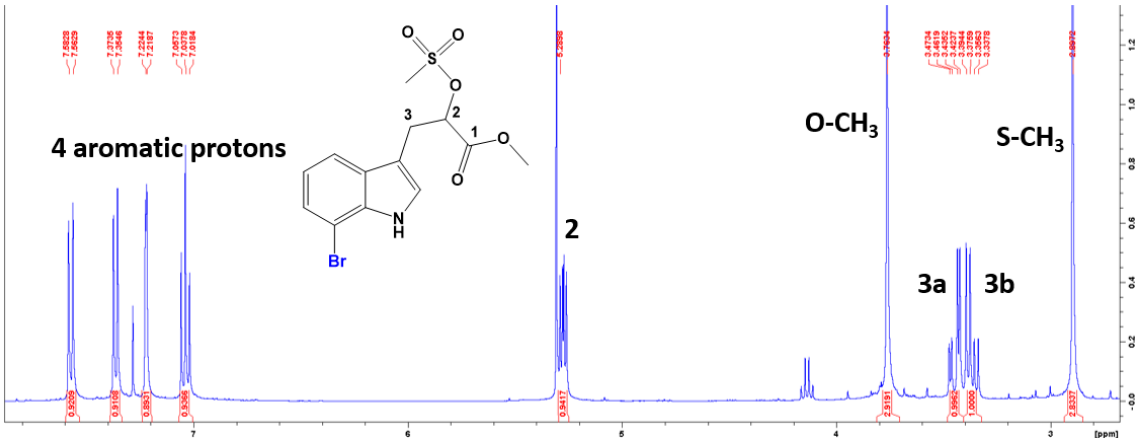
4 aromatic protons
O
S
O
O
N
H
Br
2
O-CH3
S-CH3
3a
3b

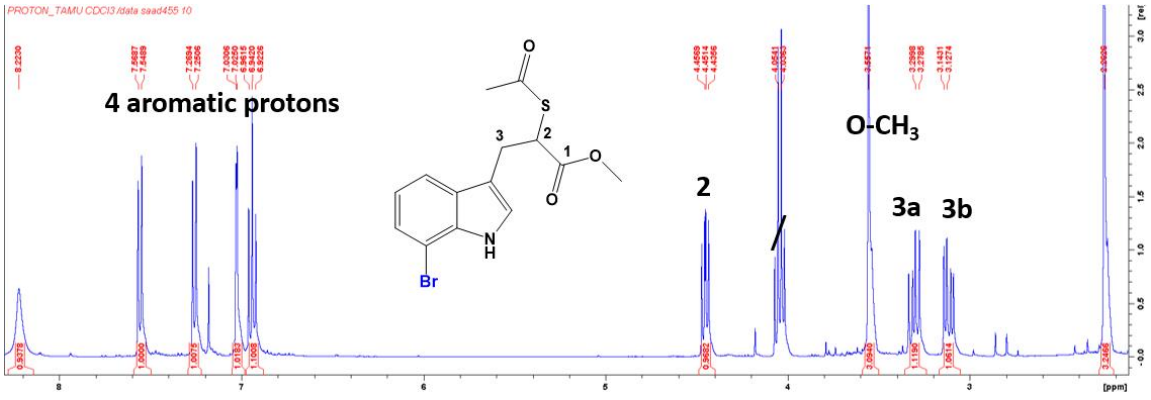

Synthesis of (4-hydroxy-1H-indol-3-yl)-propanoic acid, 115

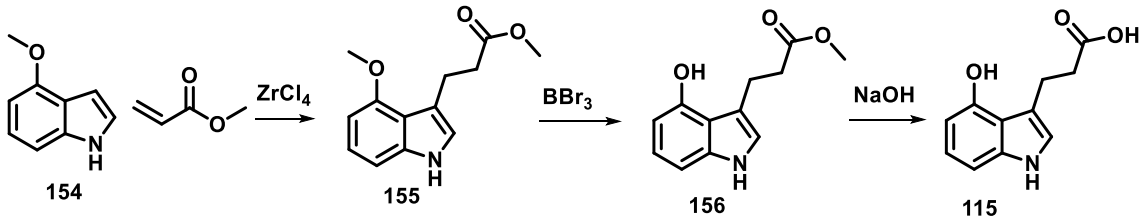

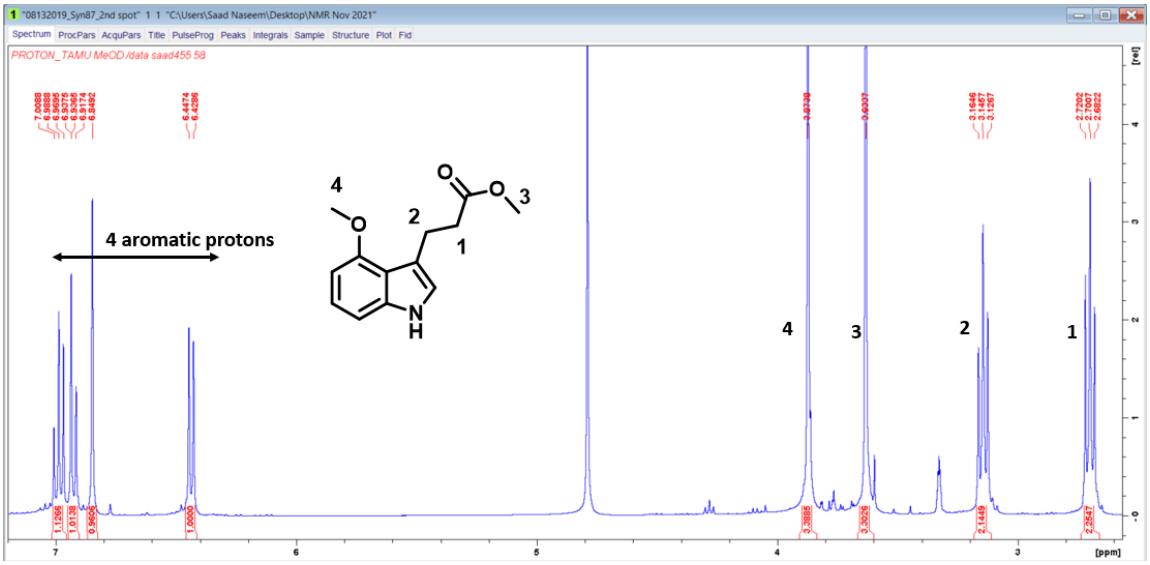

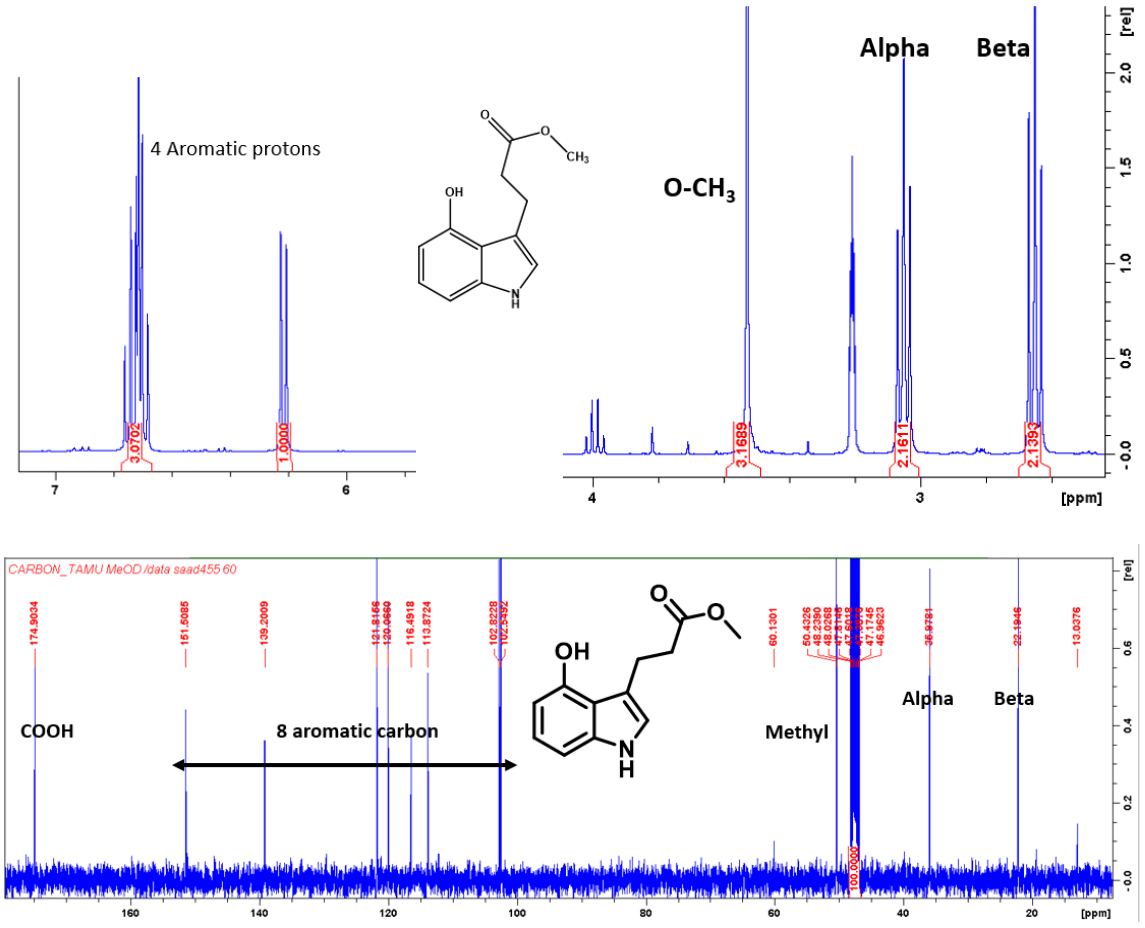

Synthesis of (5-hydroxy-1H-indol-3-yl)-propanoic acid, 161

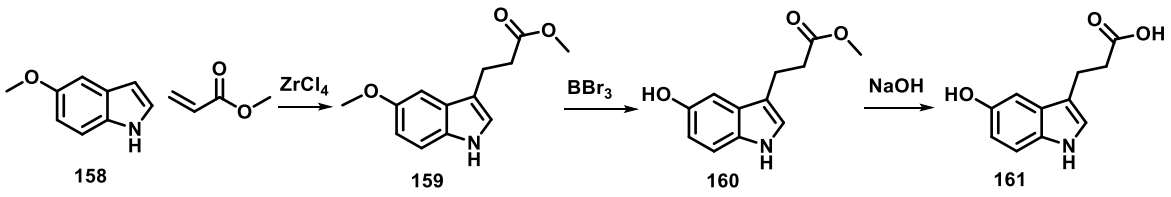

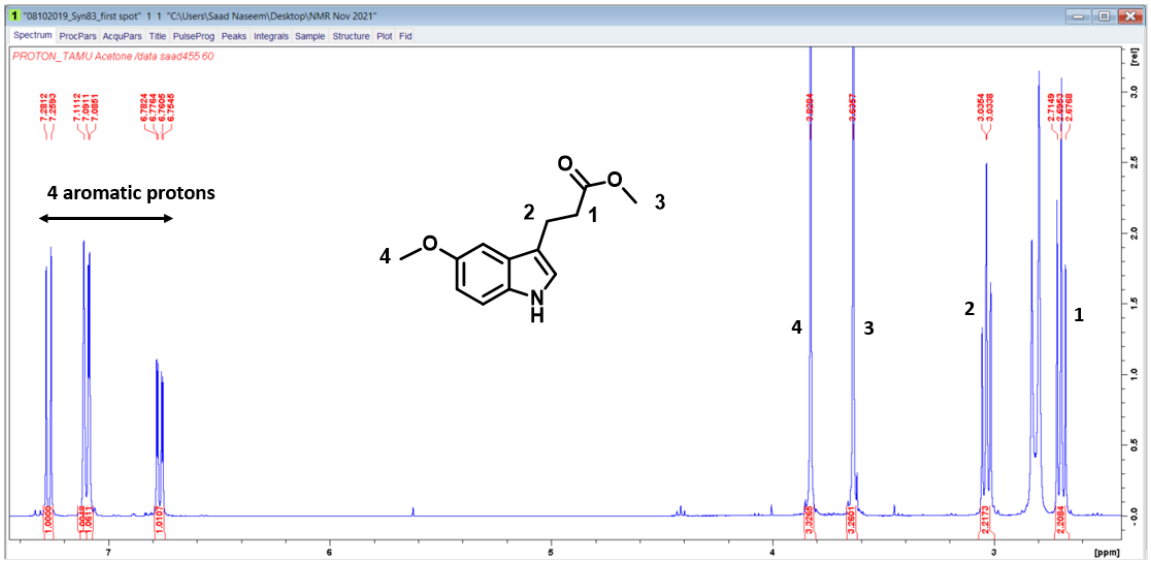
4 aromatic protons
4
3
2
1
[ppm]

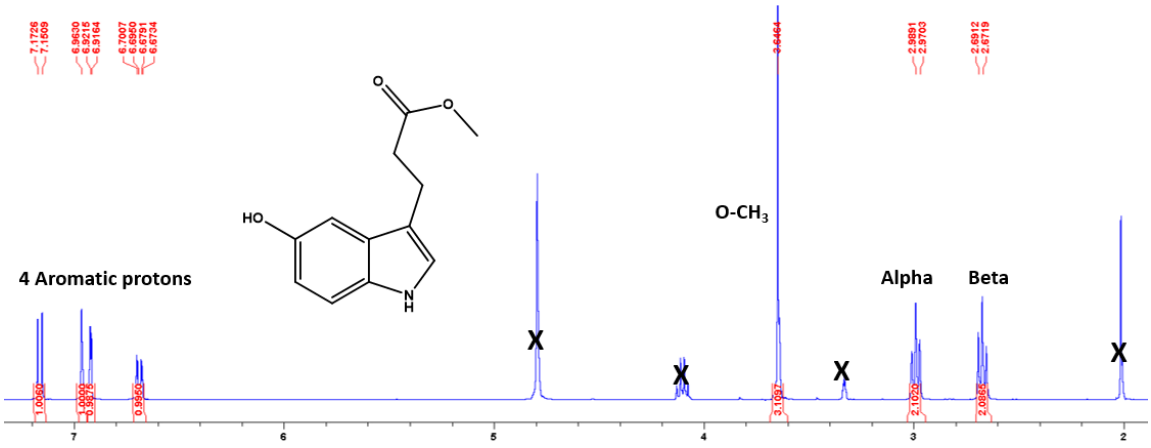
4 Aromatic protons
O-CH3
Alpha
Beta
X

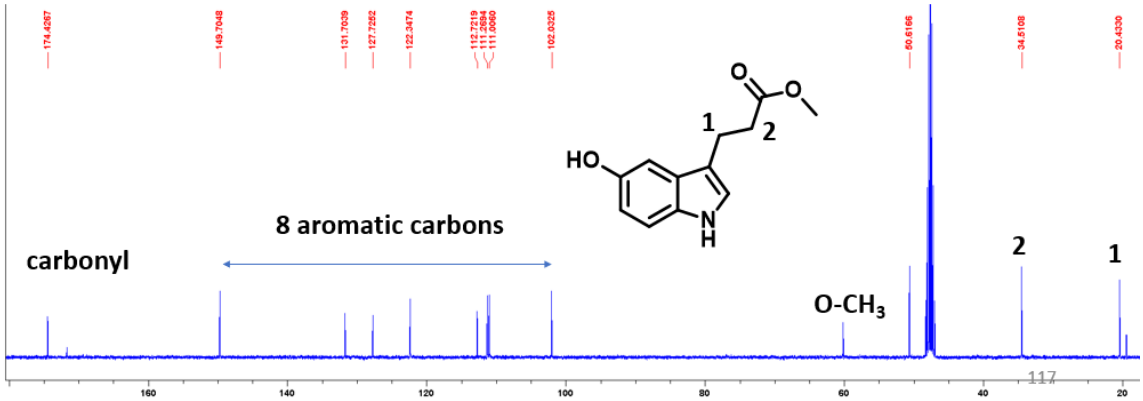
carbonyl
8 aromatic carbons
O-CH3
2
1

Synthesis of (6-hydroxy-1H-indol-3-yl)-propanoic acid, 165

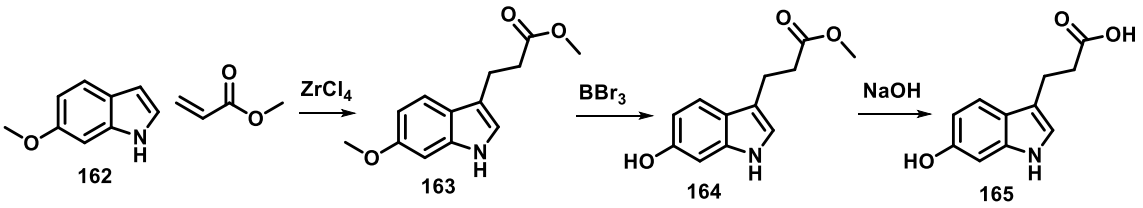

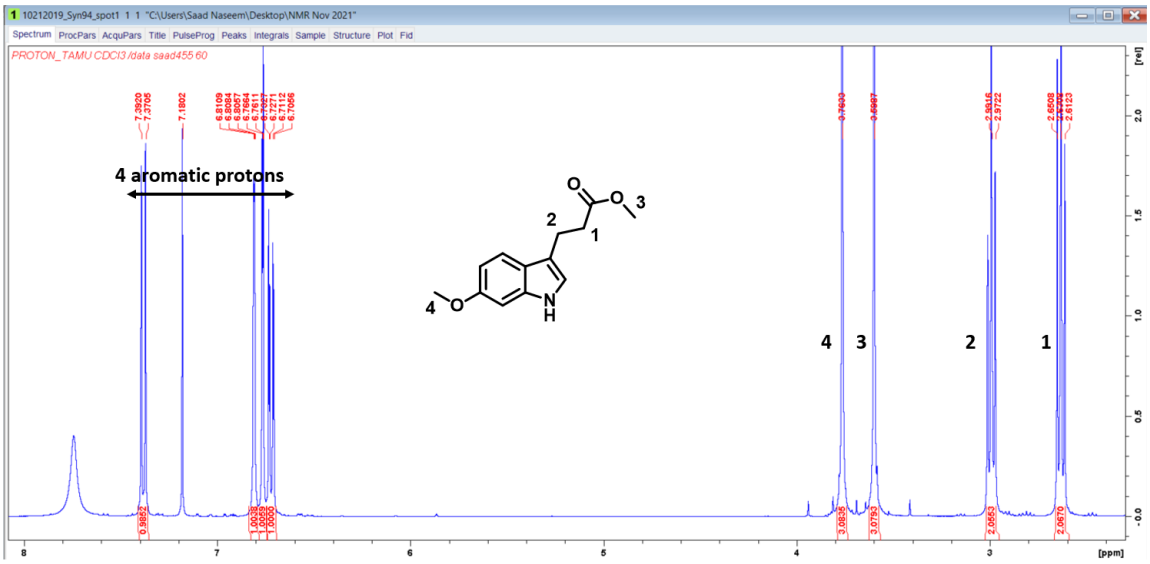

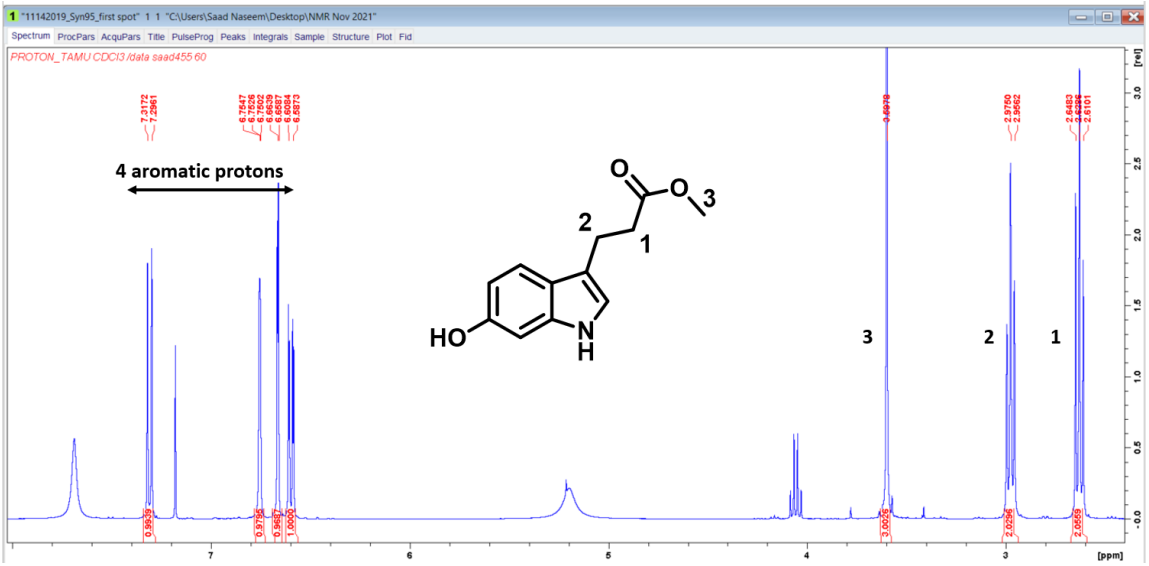

Synthesis of (7-hydroxy-1H-indol-3-yl)-propanoic acid, 169

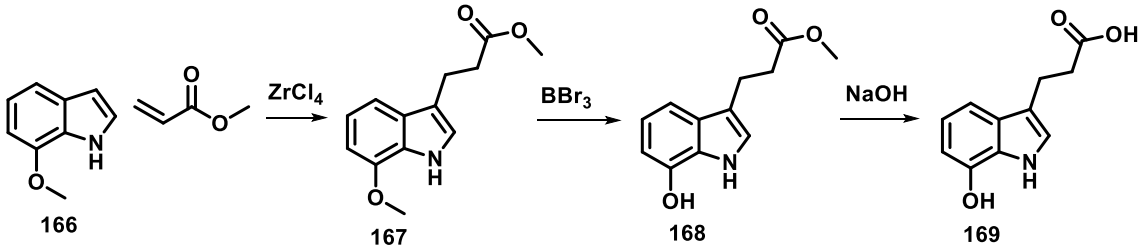

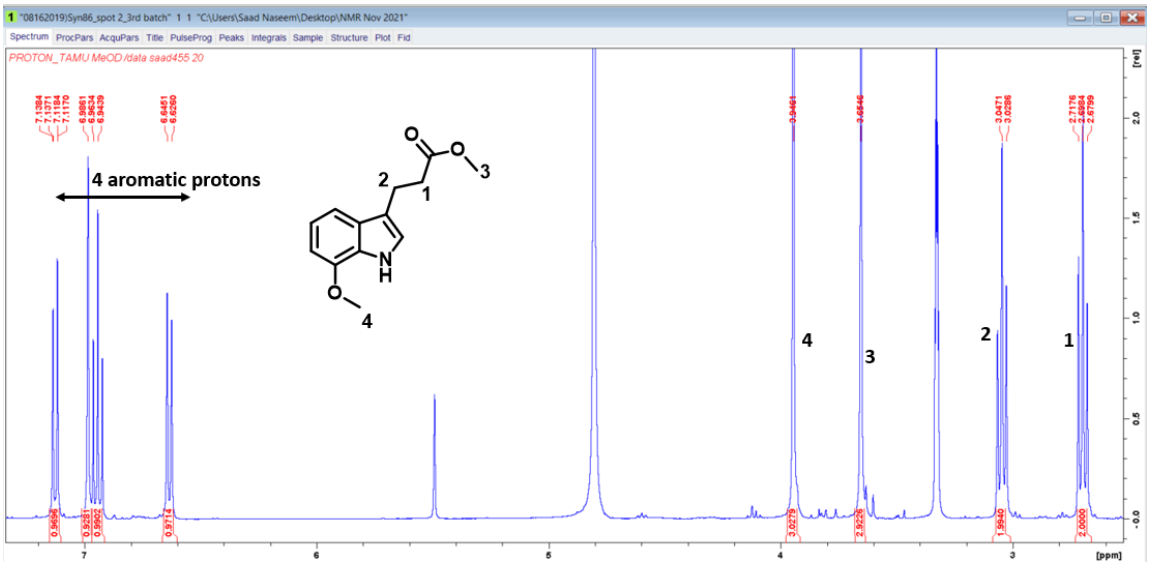

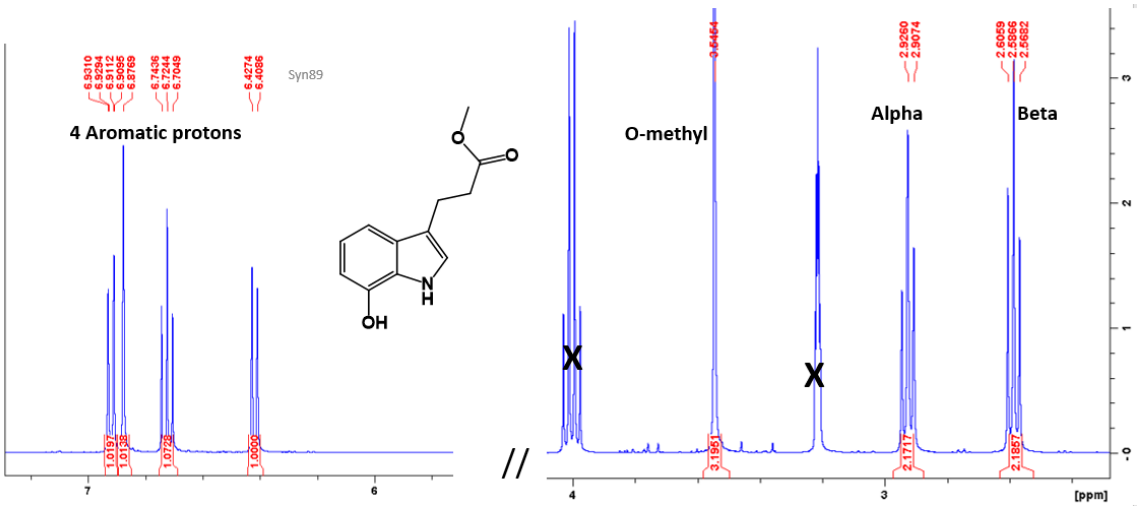

Synthesis of 3-(1-oxidobenzo[b]thiophen-3-yl)propanoic acid, 171

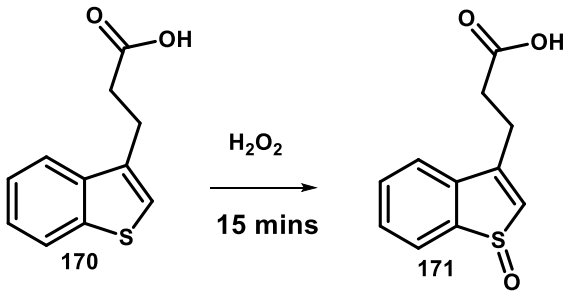

A mixture of 3-(benzo[b]thiophen-3-yl)propanoic acid (70 mg, 0.34 mmol) and hydrogen peroxide (1.1 equivalent, 0.37 mmol) in TFA (0.5 mL) was stirred for 15 minutes. The reaction was quenched with saturated acq. $NaHCO_3$ at 0 °C and then acidified. Then the acq. phase was extracted with DCM, and the combined organic layers were dried with anhydrous sodium sulfate and concentrated. The crude was purified by flash chromatography to give a pure compound.

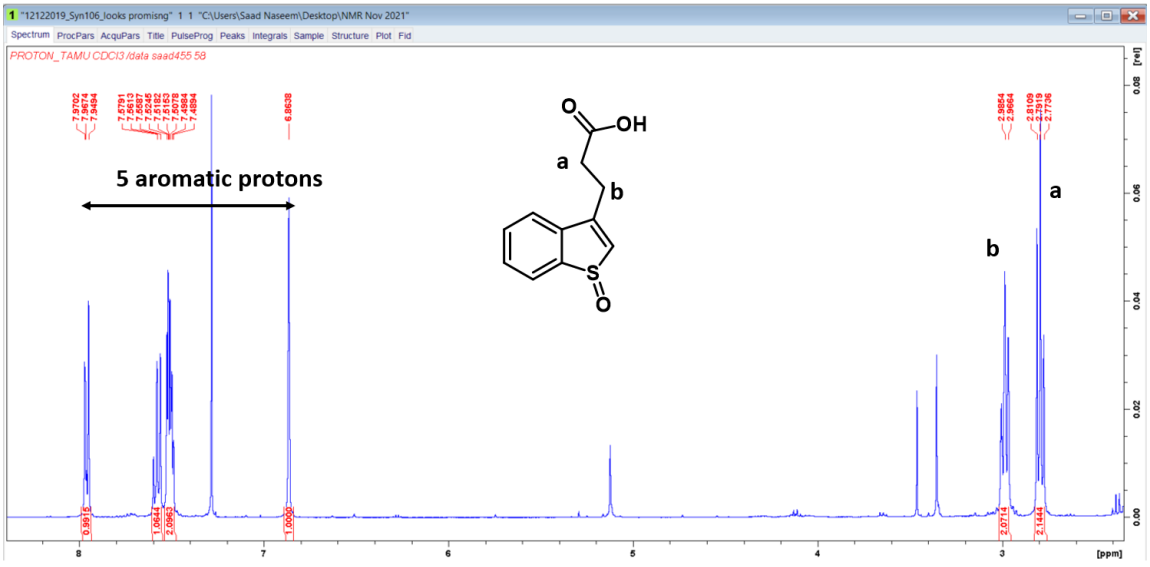

Synthesis of 3-(1-methyl-1H-indol-3-yl)propanoic acid, 172

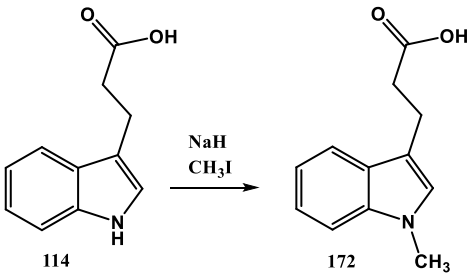

A stirred suspension of sodium hydride (5 equivalent, 120 mg, 2.7 mmol) in THF (10 mL) was cooled to 0 °C in an ice bath. A solution of indole-3-propanoic acid (100 mg, 0.5 mmol) in THF was added dropwise. After stirring for 30 minutes, a solution of iodomethane (3.3 equivalent, 1.7 mmol) in THF was added dropwise. The mixture was allowed to warm to room temperature and stirred overnight. Methanol and then water was slowly added to quench the reaction. The aqueous layer was acidified to pH 2 using 6M acqueous HCl and extracted with DCM. The combined organic phase was dried and concentrated. The crude solid was recrystallized from ethyl acetate and hexane to give the desired product.

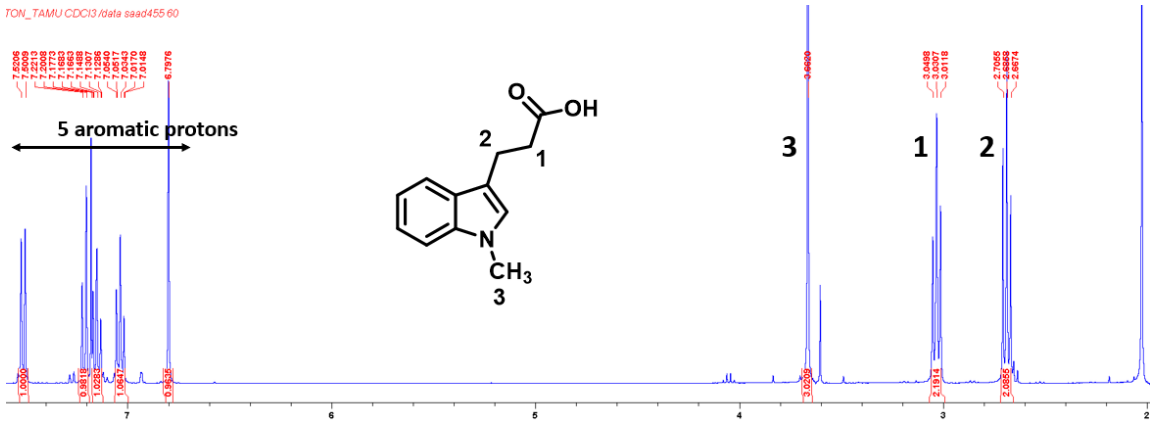

Synthesis of 3-(1-(hydroxymethyl)-1H-indol-3-yl)propanoic acid, 177

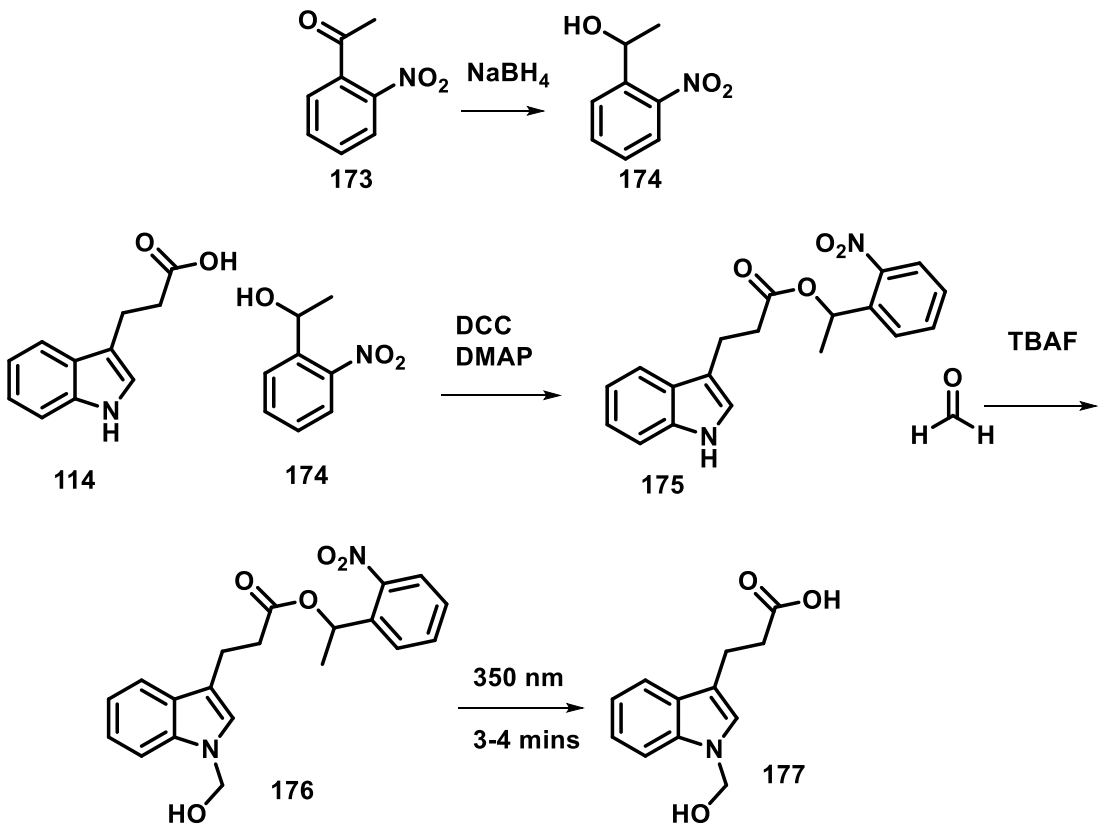

Preparation of 1-(2-nitrophenyl)ethan-1-ol

1-(2-nitrophenyl)ethan-1-one (3 grams, 18 mmol) was dissolved in methanol:1,4-dioxane (1:2), followed by sodium borohydride (2 equivalent, 1.4 grams, 36 mmol) portionwise. The reaction was run for 3 hours and quenched with 1M HCl. The product was purified by column using ethyl acetate and hexane as a solvent system.

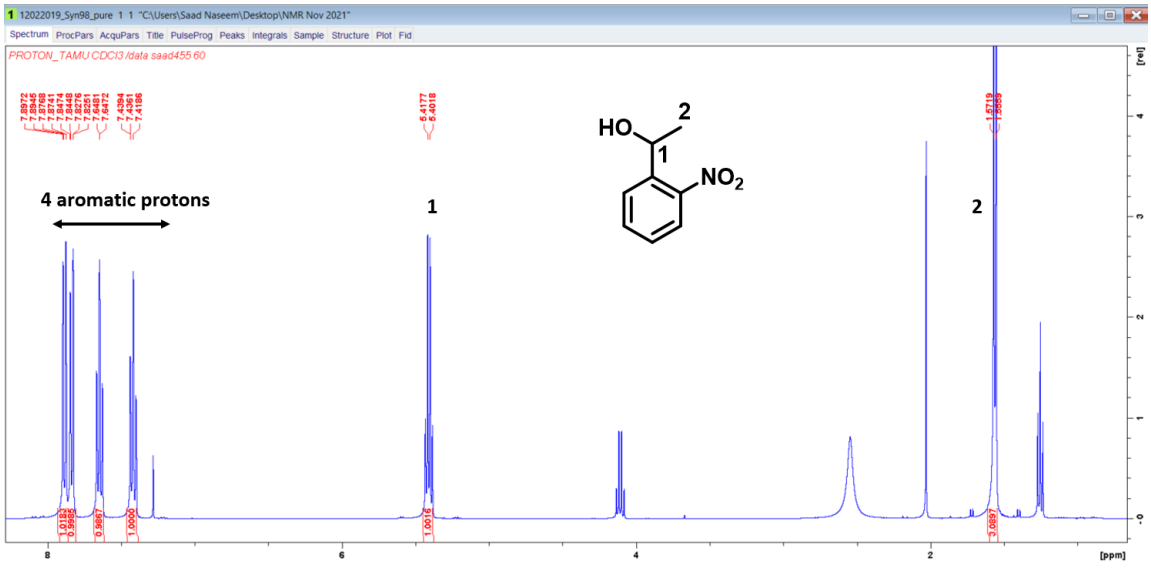

Preparation of 1-(2-nitrophenyl)ethyl 3-(1H-indol-3-yl)propanoate

A modified procedure of Kusaka *el al.* ChemBioChem, 2009, 10, 2195 – 2202 was followed. Indole-3-propanoic acid (200 mg, 1.058 mmol) and N,N'-dicyclohexylcarbodiimide (1.3 equivalent, 283 mg, 1.38 mmol) was added to the solution of 1-(2-nitrophenyl)ethan-1-ol (2 equivalent, 351 mg, 2.11 mmol) and 4-dimethylaminopyridine (1.3 equivalent, 170 mg, 1.38 mmol) in dry THF (3 mL), and then stirred for 6 h at room temperature. The reaction mixture was poured into the saturated ammonium chloride solution (10 mL) and then extracted with ethyl acetate. The organic layer was washed with brine and dried over anhydrous sodium sulfate, filtrated, and concentrated. This residue was purified by a flash column using ethyl acetate and hexane as a solvent system.

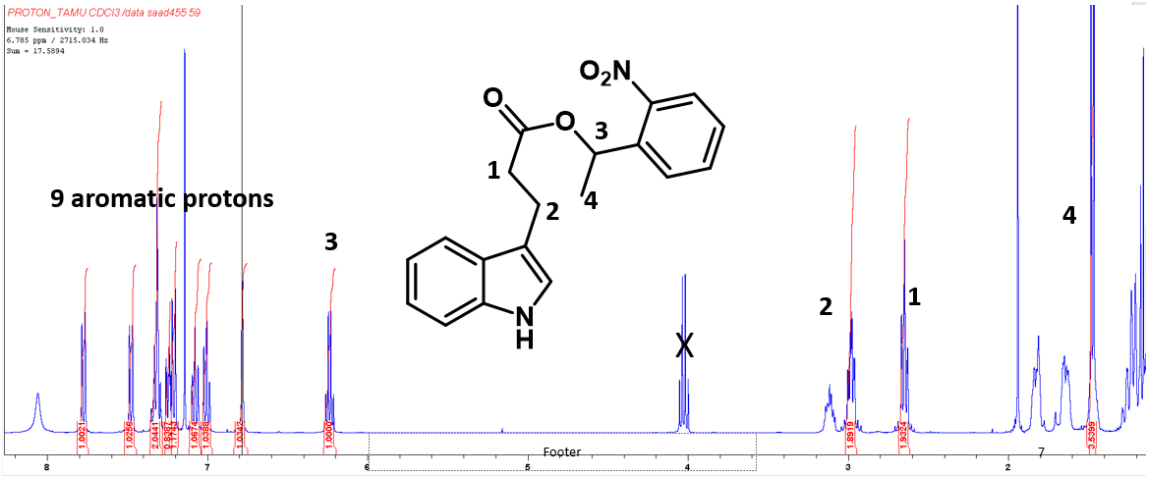

Preparation of 1-(2-nitrophenyl)ethyl 3-(1-(hydroxymethyl)-1H-indol-3-yl)propanoate

A modified protocol of Harshadas et al. Green Chemistry Letters and Reviews, 2013, 6:1, 95-100, was followed. A mixture of 1-(2-nitrophenyl)ethyl 3-(1H-indol-3-yl)propanoate and formaldehyde were combined with 5 mL THF in a round bottom flask. Tetrabutylammonium fluoride was added to the reaction mixture and stirred for 2 hours. The reaction mixture was extracted with ethyl acetate, and the organic layer was washed with brine and dried over anhydrous sodium sulfate, and concentrated. The crude product had some slight impurities, but the NMR showed a clean new peak at 5.5 ppm corresponding to hemiaminal. The presence of the product was confirmed by mass.

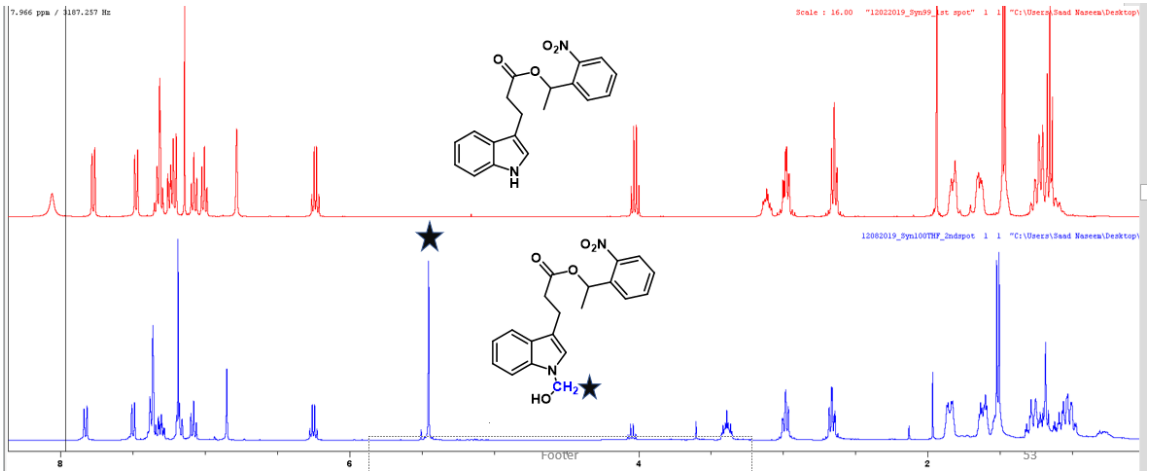

Preparation of 3-(1-(hydroxymethyl)-1H-indol-3-yl)propanoic acid

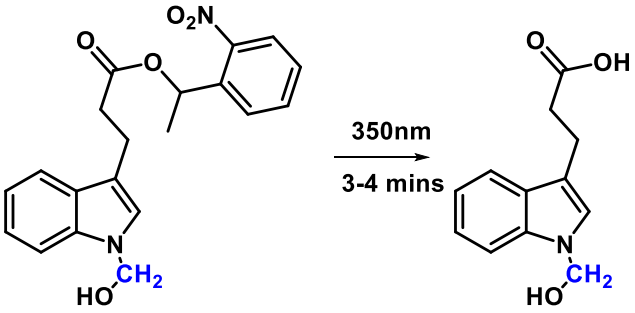

The sample of 1-(2-nitrophenyl)ethyl 3-(1-(hydroxymethyl)-1H-indol-3-yl)propanoate was prepared in methanol and shown at 350 nm for 3-4 minutes. Complete deprotection was observed using HPLC.

CHAPTER IX

CONCLUSIONS

Summary

Lumichrome catabolism

Riboflavin catabolism is an unwritten chapter in riboflavin enzymology. The identification of the genes involved in riboflavin catabolism is an essential contribution to cofactor literature.

Our lab has isolated *Pimelobacter simplex* that uses lumichrome as a carbon and nitrogen source for growth. We were able to identify the genes involved in the degradation of lumichrome to small metabolites and energy.

In this thesis, I report the discovery of the lumichrome monooxygenase involved in the oxidation of lumichrome to 7-hydroxymethyl-lumichrome (**85**) (Figure IX.1). NDMA-dependent hydroxymethyl-lumichrome oxidase further oxidizes 7-hydroxymethyllumichrome to 7-carboxylumichrome (**86**). This strategy increases the solubility and availability of the compound for biodegradation. A coupled assay of 7-carboxylumichrome with carboxy-lumichrome hydantoinase, Ureidoquinoxaline amidase, and aminoquinoxaline amidinase demonstrate the relevance of the carboxy group in the pathway.

Quinoxaline oxidase was successfully expressed and purified in *E.coli* TP1000 cells. Quinoxaline oxidase does nucleophilic oxidation at the most electropositive carbon center of the quinoxaline heterocycle (**70**).

Quinoxaline monooxygenase was a bottleneck in the progress of this project. I discovered that the NCBI and Uniprot databases have incorrect Open Reading Frames (ORF) of the genes. Later, I demonstrated the activity of quinoxaline monooxygenase with the carboxylated-quinoxaline-diamide (**43**). The product of quinoxaline monooxygenase (**49**) was found to be the substrate of amidocatechol dioxygenase. The discovery of the carboxylated substrate of quinoxaline monooxygenase led me in search of enzymes responsible for the oxidation of the methyl of lumichrome.

Briefly, I was able to functionally characterize 9 enzymes in the lumichrome catabolic pathway.

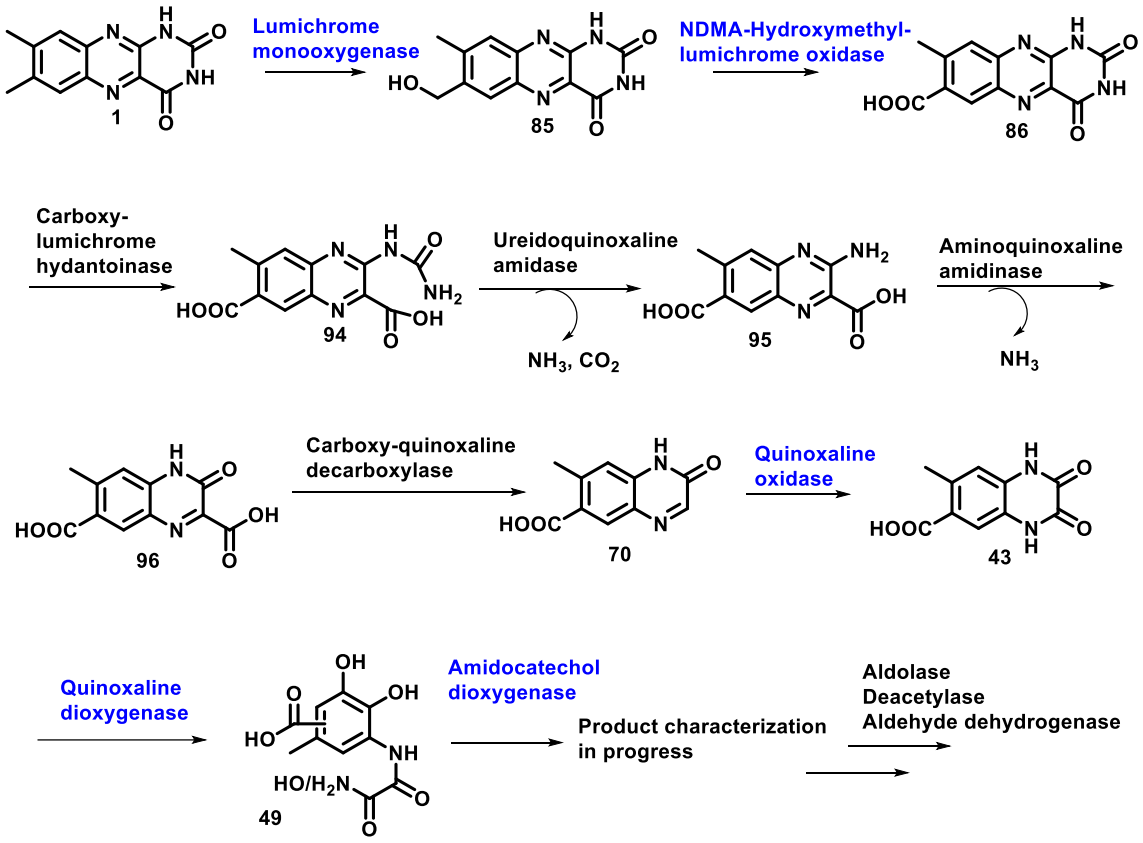

Figure IX.1: Current proposal of lumichrome catabolic pathway in *Pimelobacter simplex*.

Carbon-sulfur bond formation via (2-3)-epoxide intermediate in Chuangxinmycin biosynthesis

Carbon-sulfur bond formation in natural product biosynthesis has intrigued researchers for many years[18]. The method of the incorporation of sulfur into secondary metabolites remains poorly understood.

Chuangxinmycin (**104**), an indole alkaloid, was found to be effective against gram-positive and gram-negative bacteria as a tryptophanyl tRNA synthetase inhibitor[19]. The biosynthesis of chuangxinmycin requires the formation of two carbon-sulfur bonds using different strategies. The first bond is made using a sulfur carrier protein (SCP), CxnE[22],

similar to ThiS in thiamin biosynthesis; the second by CxnD, a cytochrome P450 enzyme[23].

We were interested in the mechanistic studies of aryl-carbon and sulfur bond formation by a cytochrome P450, CxnD. We proposed two plausible mechanisms for carbon-sulfur bond formation i) aryl radical anion intermediate ii) (2-3)-epoxyindole intermediate. To investigate the mechanism several substrate analogs were tested with CxnD. Bromo-substituted substrate analogs ruled out the carbon-sulfur bond formation via aryl radical anion intermediate. Indole-3-propanoic acid as a substrate analog of CxnD released multiple products that provide evidence for epoxyindole intermediate formation.

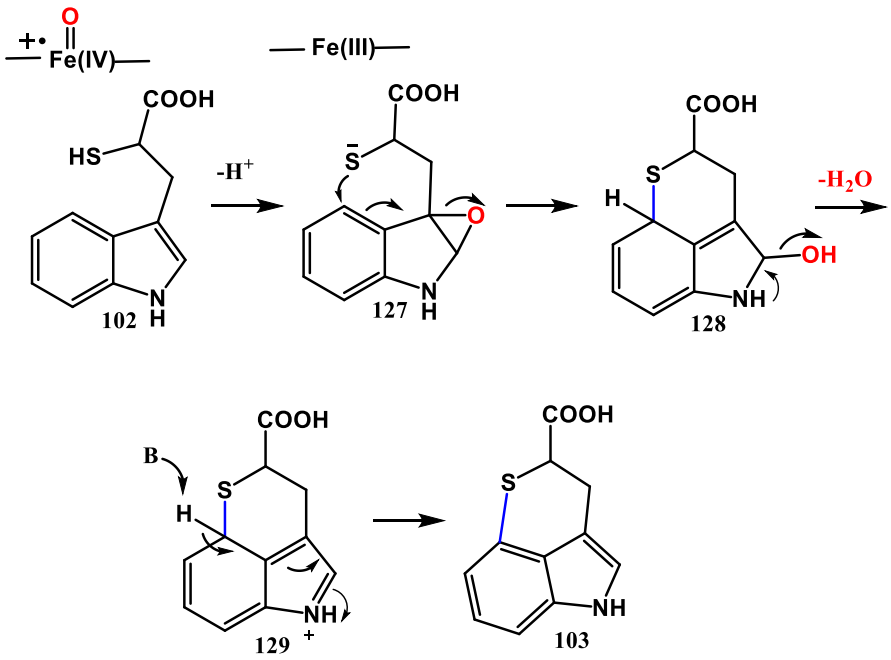

Figure IX.2: Proposed mechanism of aryl carbon-sulfur bond formation catalyzed by CxnD.

REFERENCES

1. Foster, J. W., Microbiological Aspects of Riboflavin: III. Oxidation Studies with Pseudomonas riboflavina. *J Bacteriol* **1944,** *48* (1), 97-111.

2. Foster, J. W., Microbiological Aspects of Riboflavin: I. Introduction. II. Bacterial Oxidation of Riboflavin to Lumichrome. *J Bacteriol* **1944,** *47* (1), 27-41.

3. Harkness, D. R.; Stadtman, E. R., Bacterial degradation of riboflavin. VI. Enzymatic conversion of riboflavin to 1-ribityl-2,3-diketo-1,2,3,4-tetrahydro-6, 7-dimethylquinoxaline, urea, and carbon dioxide. *J Biol Chem* **1965,** *240* (10), 4089-96.

4. Harkness, D. R.; Tsai, L.; Stadtman, E. R., Bacterial Degradation of Riboflavin. V. Stoichiometry of Riboflavin Degradation to Oxamide and Other Products, Oxidation of C14-Labeled Intermediates and Isolation of the Pseudomonad Effecting These Transformations. *Arch Biochem Biophys* **1964,** *108*, 323-33.

5. Xu, H.; Chakrabarty, Y.; Philmus, B.; Mehta, A. P.; Bhandari, D.; Hohmann, H. P.; Begley, T. P., Identification of the First Riboflavin Catabolic Gene Cluster Isolated from Microbacterium maritypicum G10. *J Biol Chem* **2016,** *291* (45), 23506-23515.

6. Wang, Y.; Li, J.; Liu, A., Oxygen activation by mononuclear nonheme iron dioxygenases involved in the degradation of aromatics. *J Biol Inorg Chem* **2017,** *22* (2-3), 395-405.

7. Perry, C.; de Los Santos, E. L. C.; Alkhalaf, L. M.; Challis, G. L., Rieske non-heme iron-dependent oxygenases catalyse diverse reactions in natural product biosynthesis. *Nat Prod Rep* **2018,** *35* (7), 622-632.

8. Saibu, S.; Adebusoye, S. A.; Oyetibo, G. O., Aerobic bacterial transformation and biodegradation of dioxins: a review. *Bioresour Bioprocess* **2020,** *7* (1).

9. Jaiswal, P. K.; Kohli, S.; Gopal, M.; Thakur, I. S., Isolation and characterization of alkalotolerant Pseudomonas sp. strain ISTDF1 for degradation of dibenzofuran. *J Ind Microbiol Biotechnol* **2011,** *38* (4), 503-11.

10. Barry, S. M.; Challis, G. L., Mechanism and Catalytic Diversity of Rieske Non-Heme Iron-Dependent Oxygenases. *ACS Catal* **2013,** *3* (10).

11. Hille, R.; Hall, J.; Basu, P., The mononuclear molybdenum enzymes. *Chem Rev* **2014,** *114* (7), 3963-4038.

12. Mintmier, B.; Nassif, S.; Stolz, J. F.; Basu, P., Functional mononuclear molybdenum enzymes: challenges and triumphs in molecular cloning, expression, and isolation. *J Biol Inorg Chem* **2020,** *25* (4), 547-569.

13. Correddu, D.; Di Nardo, G.; Gilardi, G., Self-Sufficient Class VII Cytochromes P450: From Full-Length Structure to Synthetic Biology Applications. *Trends Biotechnol* **2021,** *39* (11), 1184-1207.

14. Zhang, L.; Xie, Z.; Liu, Z.; Zhou, S.; Ma, L.; Liu, W.; Huang, J. W.; Ko, T. P.; Li, X.; Hu, Y.; Min, J.; Yu, X.; Guo, R. T.; Chen, C. C., Structural insight into the electron transfer pathway of a self-sufficient P450 monooxygenase. *Nat Commun* **2020,** *11* (1), 2676.

15. Haft, D. H.; Pierce, P. G.; Mayclin, S. J.; Sullivan, A.; Gardberg, A. S.; Abendroth, J.; Begley, D. W.; Phan, I. Q.; Staker, B. L.; Myler, P. J.; Marathias, V. M.; Lorimer, D.

D.; Edwards, T. E., Mycofactocin-associated mycobacterial dehydrogenases with non-exchangeable NAD cofactors. *Sci Rep* **2017,** *7*, 41074.

16. Haft, D. H., Bioinformatic evidence for a widely distributed, ribosomally produced electron carrier precursor, its maturation proteins, and its nicotinoprotein redox partners. *BMC Genomics* **2011,** *12*, 21.

17. Khaliullin, B.; Aggarwal, P.; Bubas, M.; Eaton, G. R.; Eaton, S. S.; Latham, J. A., Mycofactocin biosynthesis: modification of the peptide MftA by the radical S-adenosylmethionine protein MftC. *FEBS Lett* **2016,** *590* (16), 2538-48.

18. Dunbar, K. L.; Scharf, D. H.; Litomska, A.; Hertweck, C., Enzymatic Carbon-Sulfur Bond Formation in Natural Product Biosynthesis. *Chem Rev* **2017,** *117* (8), 5521-5577.

19. Brown, M. J.; Carter, P. S.; Fenwick, A. S.; Fosberry, A. P.; Hamprecht, D. W.; Hibbs, M. J.; Jarvest, R. L.; Mensah, L.; Milner, P. H.; O'Hanlon, P. J.; Pope, A. J.; Richardson, C. M.; West, A.; Witty, D. R., The antimicrobial natural product chuangxinmycin and some synthetic analogues are potent and selective inhibitors of bacterial tryptophanyl tRNA synthetase. *Bioorg Med Chem Lett* **2002,** *12* (21), 3171-4.

20. Shi, Y.; Jiang, Z.; Li, X.; Zuo, L.; Lei, X.; Yu, L.; Wu, L.; Jiang, J.; Hong, B., Biosynthesis of antibiotic chuangxinmycin from Actinoplanes tsinanensis. *Acta Pharm Sin B* **2018,** *8* (2), 283-294.

21. Xu, X.; Zhou, H.; Liu, Y.; Liu, X.; Fu, J.; Li, A.; Li, Y. Z.; Shen, Y.; Bian, X.; Zhang, Y., Heterologous Expression Guides Identification of the Biosynthetic Gene

Cluster of Chuangxinmycin, an Indole Alkaloid Antibiotic. *J Nat Prod* **2018,** *81* (4), 1060-1064.

22. Zhang, X.; Xu, X.; You, C.; Yang, C.; Guo, J.; Sang, M.; Geng, C.; Cheng, F.; Du, L.; Shen, Y.; Wang, S.; Lan, H.; Yang, F.; Li, Y.; Tang, Y. J.; Zhang, Y.; Bian, X.; Li, S.; Zhang, W., Biosynthesis of Chuangxinmycin Featuring a Deubiquitinase-like Sulfurtransferase. *Angew Chem Int Ed Engl* **2021,** *60* (46), 24418-24423.

23. Shi, Y.; Jiang, Z.; Hu, X.; Hu, X.; Gu, R.; Jiang, B.; Zuo, L.; Li, X.; Sun, H.; Zhang, C.; Wang, L.; Wu, L.; Hong, B., The cytochrome P450 catalyzing C-S bond formation in S-heterocyclization of chuangxinmycin biosynthesis. *Angew Chem Int Ed Engl* **2021**.

24. Barr, I.; Guo, F., Pyridine Hemochromagen Assay for Determining the Concentration of Heme in Purified Protein Solutions. *Bio Protoc* **2015,** *5* (18).

25. Xu, X. B.; Liu, J.; Zhang, J. J.; Wang, Y. W.; Peng, Y., Nickel-mediated inter- and intramolecular C-S coupling of thiols and thioacetates with aryl iodides at room temperature. *Org Lett* **2013,** *15* (3), 550-3.

26. Joshi, S.; Mahanta, N.; Fedoseyenko, D.; Williams, H.; Begley, T. P., Aminofutalosine Synthase: Evidence for Captodative and Aryl Radical Intermediates Using beta-Scission and SRN1 Trapping Reactions. *J Am Chem Soc* **2017,** *139* (32), 10952-10955.

27. Zhang, Y.; Zou, Y.; Brock, N. L.; Huang, T.; Lan, Y.; Wang, X.; Deng, Z.; Tang, Y.; Lin, S., Characterization of 2-Oxindole Forming Heme Enzyme MarE, Expanding the Functional Diversity of the Tryptophan Dioxygenase Superfamily. *J Am Chem Soc* **2017,** *139* (34), 11887-11894.

28. Geng, J.; Weitz, A. C.; Dornevil, K.; Hendrich, M. P.; Liu, A., Kinetic and Spectroscopic Characterization of the Catalytic Ternary Complex of Tryptophan 2,3-Dioxygenase. *Biochemistry* **2020,** *59* (30), 2813-2822.

29. Lin, Z.; Ji, J.; Zhou, S.; Zhang, F.; Wu, J.; Guo, Y.; Liu, W., Processing 2-Methyl-l-Tryptophan through Tandem Transamination and Selective Oxygenation Initiates Indole Ring Expansion in the Biosynthesis of Thiostrepton. *J Am Chem Soc* **2017,** *139* (35), 12105-12108.

30. Xu, J.; Liang, L.; Zheng, H.; Chi, Y. R.; Tong, R., Green oxidation of indoles using halide catalysis. *Nat Commun* **2019,** *10* (1), 4754.